Robust Fractional Order LQI Controller Design for Quadruple Tank Process and its Feasibility Study in Bond Graph Domain - An Optimisation Approach

A thesis submitted

in partial fulfillment for the award of the degree of

Doctor of Philosophy

by

R S Mohankumar

Department of Avionics

Indian Institute of Space Science and Technology

Thiruvananthapuram, India

January 2025

Certificate

This is to certify that the thesis titled ***Robust Fractional Order LQI Controller Design for Quadruple Tank Process and its Feasibility Study in Bond Graph Domain - An Optimisation Approach*** submitted by **R S Mohankumar**, to the Indian Institute of Space Science and Technology, Thiruvananthapuram, in partial fulfillment for the award of the degree of **Doctor of Philosophy** is a bonafide record of the original work carried out by him under my supervision. The contents of this thesis, in full or in parts, have not been submitted to any other Institute or University for the award of any degree or diploma.

Name of the Co-Supervisor
Dr. M. Jayakumar
Project Director, PSLV,
VSSC, ISRO.

Name of the Supervisor
Dr. N. Selvaganesan
Professor and Head,
Department of Avionics, IIST.

Place: Thiruvananthapuram
Date: January 2025

Declaration

I declare that this thesis titled ***Robust Fractional Order LQI Controller Design for Quadruple Tank Process and its Feasibility Study in Bond Graph Domain - An Optimisation Approach*** submitted in partial fulfillment for the award of the degree of **Doctor of Philosophy** is a record of the original work carried out by me under the supervision of **Dr. N. Selvaganesan**, and has not formed the basis for the award of any degree, diploma, associateship, fellowship, or other titles in this or any other Institution or University of higher learning. In keeping with the ethical practice in reporting scientific information, due acknowledgments have been made wherever the findings of others have been cited.

Place: Thiruvananthapuram R S Mohankumar

Date: January 2025 (SC14D008)

This thesis is dedicated to the Almighty, whose blessings and guidance have been a constant source of strength and inspiration throughout this journey.

Acknowledgements

The work presented in this thesis was only possible with my close association with many people. I take this opportunity to extend my sincere gratitude and appreciation to all those who made this Ph.D thesis possible.

First and foremost, I would like to extend the sincere gratitude to my beloved mentors ***Dr. A. Rajeswari,*** Principal, Coimbatore Iistitute of Technology (CIT), Coimbatore, ***Dr. V. Selladurai***, Former principal, CIT, ***Dr. N. Rajam Ramasamy***, HOD, Department of Mechanical Engineering, CIT and the ***Management*** of CIT along with ***AICTE-INAE*** for facilitating the research fellowship at ***ISRO and IIST*** for conducting research and guidance.

I want to render my sincere gratitude to my research supervisor ***Dr. N. Selvaganesan***, Professor for introducing me to this exciting field of optimisation in fractional controllers and for his dedicated help, guidance, advice, inspiration, encouragement, continuous support and patience throughout my Ph.D. His continuous motivation has greatly changed me as a person in this society. His technical and editorial advice is essential for the completion of this thesis. I am really happy to be associated with a mentor like him.

I gratefully acknowledge my research co-supervisor ***Dr. M. Jayakumar,*** Project director, PSLV, VSSC, ISRO and doctoral committee chairman, ***Dr. H. Priyadarshan***, Professor, IIST. I sincerely thank the other doctoral committee members ***Dr. K. Kurian Issac***, Senior Professor, IIST, ***Dr. Krishna Vasudevan***, Professor, IIT Madras, ***Dr. V. R. Lalithamika***, Former Director, Human Spaceflight Programme, VSSC, ISRO, ***Dr. I. R. Praveen Krishna***, Associate Professor, IIST for their periodic assessments during my research period at IIST.

I am also thankful to my institute, especially **Department of Avionics**, for providing good research facilities and an excellent research environment. I would like to express my sincere gratitude to our Director **Dr. S. Unnikrishnan Nair** and our former directors as well for their encouragement and continuous support.

I make a special wishes to my co-research scholar ***Dr. P. Sathishkumar*** who gave constant and valuable support for my research and I also thank my wife, parents, family members and friends for their unconditional love and support.

-R S Mohankumar

Abstract

The Quadruple Tank Process (QTP) is a classical control problem often used in control theory and practical research. This process is a valuable testbed for studying and implementing control algorithms, allowing researchers/engineers to explore the various design process such as feedback control in the presence of uncertainties and optimisation in a practical context. The main objective of the problem is to maintain the desired levels in the bottom two tanks under (i) nonlinearity due to the interconnected dynamics (ii) potential coupling between the tanks and (iii) disturbance and uncertainty conditions. Interestingly, QTP exhibits its operation under both minimum and non-minimum phase modes. In specific, designing a controller for a non-minimum phase system requires more attention due to its inherent complexities and challenges involved.

The Linear Quadratic Integrator (LQI) controller, a widely acclaimed control design technique combines both feedback control i.e Linear Quadratic Regulator (LQR) and feedforward integral control strategy. The integral action of the LQI controller plays an important role in the system's performance by integrating the error signal between the actual and desired states over time, hence it eliminates the steady state error which drives the system towards the desired setpoint. The optimisation problem leads to minimise the cost function that combines quadratic penalties on state deviations, input deviations and integrated error signals along with constraints on control inputs and states.

The initial phase of the research work proposes robust Fractional Order LQI (FOLQI) controller design for QTP in the presence of disturbance and uncertainty conditions. This approach involves utilising fractional calculus concepts in designing the controller which allows more flexibility and adaptability in handling complex dynamics. By incorporating fractionality in the integrator part of the LQI controller, the FOLQI controller can capture more intricate system behaviours and effectively improve the system performance. The controller parameters of FOLQI is obtained by minimising control effort in the presence of load disturbance conditions along with time domain constraints such as overshoot, settling time and steady state error.

The optimal tuning of FOLQI controller parameters are obtained by solving the proposed constrained optimisation problem using (i) deterministic approach and (ii) heuristic approach. Deterministic optimisation methods aim to find the optimal solution by systematically exploring the entire solution space or using mathematical algorithms to determine

the best solution. These methods guarantee convergence to the global optimum (if such a solution exists) under certain conditions. It utilises the fmincon function from MATLAB which uses the Sequential Quadratic Programming (SQP) algorithm as a solver. The superior time response characteristics obtained from FOLQI controller are compared with responses obtained from the existing Integer Order LQI (IOLQI) and Linear Active Disturbance Rejection (LADR) controllers.

To enhance the performance, heuristic optimisation methods such as Cuckoo Search (CS), Accelerated Particle Swarm Optimisation (APSO) and FireFly (FF) are used to solve the proposed constrained optimisation problem. These methods are beneficial for complex problems where deterministic optimisation techniques may need more computational complexity or ample solution space that provides the solution within a reasonable time frame. The superior performance of these algorithms are shown by conducting simulations in the presence of disturbance along with parameter uncertainty conditions and the results are compared with the existing IOLQI controller.

In the second phase of the research work, the Bond Graph (BG) based QTP model along with FOLQI controller is proposed. BG serve as a graphical modelling technique, offering a unified framework for representing the dynamics of interconnected physical systems. The closed loop configuration of the QTP and FOLQI controller are modelled using BG technique. A unconstrained optimisation problem is proposed to tune the FOLQI controller parameters using various optimisation algorithms such as Newton Raphson, Davidon–Fletcher–Powell, Steepest Descent Method and Broyden–Fletcher–Goldfarb–Shanno. The obtained results using FOLQI controller are compared with the existing IOLQI controller.

Contents

List of Figures **xv**

List of Tables **xix**

Abbreviations **xxi**

Nomenclature **xxiii**

1 Introduction **1**

1.1 Literature Survey and Motivation 2

1.1.1 QTP 2

1.1.2 Controllers for QTP 3

1.1.3 Fractional Order Controller 5

1.1.4 FOC for QTP 6

1.1.5 LQI Controllers 7

1.1.6 Heuristic Optimisation based Controllers 7

1.1.7 LADR Controllers 9

1.1.8 Controller Implementation using BG 10

1.2 Motivation and Research Contribution 10

1.2.1 Motivation 10

1.2.2 Research Contribution 12

1.3 Organisation of Thesis 12

2 Quadruple Tank Process **15**

2.1 Introduction 15

2.2 Schematic Representation and Physical Construction 16

2.3 Mathematical Modelling 17

2.3.1 Nonlinear Model and its Equilibrium Points 18

2.3.2 Taylor Series Expansion 20
2.3.3 State Space Representation of Linearised Model 20
2.4 Operating conditions of QTP 24
2.5 Summary 25

3 Fractional Order LQI Controller **27**
3.1 Preliminaries of Fractional Calculus 27
3.1.1 Introduction 27
3.1.2 Fractional Order Transfer Functions 28
3.1.3 Oustaloup Approximation Method in Continuous Domain 28
3.2 Linear Quadratic Integral Controllers 29
3.2.1 Linear Quadratic Regulator Controller 29
3.2.2 Integer Order Linear Quadratic Integral Controller 31
3.3 Fractional Order Linear Quadratic Integral Controller 31
3.3.1 FOLQI Design 31
3.3.2 Proposed Optimisation Problem 33
3.4 Summary 34

4 Tuning of FOLQI Controller using Deterministic Approach **35**
4.1 Introduction 35
4.2 Sequential Quadratic Programming 36
4.3 Optimisation Specifications 38
4.4 Results and Discussions 42
4.4.1 Performance under Disturbance Condition 42
4.4.2 Performance under Disturbance and Parameter Uncertainty 45
4.4.3 Stability Analysis 51
4.5 Summary 53

5 Tuning of FOLQI Controller using Heuristic Approach **55**
5.1 Introduction 55
5.2 Heuristic Algorithms 56
5.2.1 CS Algorithm 56
5.2.2 APSO Algorithm 58
5.2.3 FF Algorithm 60
5.3 Optimisation and its Specifications 62
5.4 Results and Discussion 68

5.4.1 Performance under Disturbance Condition 68
5.4.2 Performance under Disturbance and Parameter Uncertainty 74
5.4.3 Stability Analysis 84
5.5 Summary 86

6 Tuning of FOLQI Controller using BG Approach 87
6.1 Introduction to BG 87
6.2 BG Elements 88
6.2.1 Element Description 90
6.2.2 Representation of BG Variables and its Causal Relations 93
6.3 BG Model 95
6.3.1 BG Model of QTP 95
6.3.2 BG Model of FOLQI Controller 96
6.3.3 BG Model of QTP and FOLQI Controller in Closed Loop 97
6.4 Optimisation and its Specifications 98
6.4.1 Optimisation Algorithms 98
6.5 Results and Discussions 100
6.6 Summary 105

7 Conclusions and Future Scope 107

Bibliography 108

Appendices 123

A Linear Active Disturbance Rejection Controller 123

List of Publications 127

List of Figures

2.1 Schematic illustration of the QTP 16

3.1 Closed loop representation of MIMO system with LQR controller 30
3.2 Closed loop representation of MIMO system with FOLQI controller 32
3.3 QTP with FOLQI controller 33

4.1 Flow chart representing sequence of steps for fmincon function 37
4.2 Load disturbance signal 42
4.3 Output and controller responses for minimum phase condition under $d(t)$. 43
4.4 Output and controller responses for non-minimum phase condition under $d(t)$ 43
4.5 Output responses under $d(t)$ and parameter variations for minimum phase condition 46
4.6 Output responses under $d(t)$ and parameter variations for non-minimum phase condition 47
4.7 Controller responses under $d(t)$ and parameter variations for minimum phase condition 48
4.8 Controller responses under $d(t)$ and parameter variations for non-minimum phase condition 49
4.9 Bode response of FOLQI controller for minimum phase condition 51
4.10 Bode response of FOLQI controller for non-minimum phase condition . . . 52

5.1 Flowchart and process sequence of CS algorithm 57
5.2 Flowchart and process sequence of APSO algorithm 59
5.3 Flowchart and process sequence of FF algorithm 61
5.4 Convergence response of CS, APSO and FF algorithms for IOLQI Controller 65
5.5 Convergence response of CS, APSO and FF algorithms for FOLQI Controller 66

5.6 Output $h_1(t)$ and controller $u_1(t)$ responses for minimum phase condition of QTP with IOLQI controller 70
5.7 Output $h_2(t)$ and controller $u_2(t)$ responses for minimum phase condition of QTP with IOLQI controller 70
5.8 Output $h_1(t)$ and controller $u_1(t)$ responses for non-minimum phase condition of QTP with IOLQI controller 71
5.9 Output $h_2(t)$ and controller $u_2(t)$ responses for non-minimum phase condition of QTP with IOLQI controller 71
5.10 Output $h_1(t)$ and controller $u_1(t)$ responses for minimum phase condition of QTP with FOLQI controller 72
5.11 Output $h_2(t)$ and controller $u_2(t)$ responses for minimum phase condition of QTP with FOLQI controller 72
5.12 Output $h_1(t)$ and controller $u_1(t)$ responses for non-minimum phase condition of QTP with FOLQI controller 73
5.13 Output $h_2(t)$ and controller $u_2(t)$ responses for non-minimum phase condition of QTP with FOLQI controller 73
5.14 Output responses ($h_1(t)$ and $h_2(t)$) for minimum phase operating condition of QTP with IOLQI controller using CS algorithm 78
5.15 Output responses ($h_1(t)$ and $h_2(t)$) for non-minimum phase operating condition of QTP with IOLQI controller using CS algorithm 78
5.16 Output responses ($h_1(t)$ and $h_2(t)$) for minimum phase operating condition of QTP with FOLQI controller using CS algorithm 79
5.17 Output responses ($h_1(t)$ and $h_2(t)$) for non-minimum phase operating condition of QTP with FOLQI controller using CS algorithm 79
5.18 Output responses ($h_1(t)$ and $h_2(t)$) for minimum phase operating condition of QTP with IOLQI controller using APSO algorithm 80
5.19 Output responses ($h_1(t)$ and $h_2(t)$) for non-minimum phase operating condition of QTP with IOLQI controller using APSO algorithm 80
5.20 Output responses ($h_1(t)$ and $h_2(t)$) for minimum phase operating condition of QTP with FOLQI controller using APSO algorithm 81
5.21 Output responses ($h_1(t)$ and $h_2(t)$) for non-minimum phase operating condition of QTP with FOLQI controller using APSO algorithm 81
5.22 Output responses ($h_1(t)$ and $h_2(t)$) for minimum phase operating condition of QTP with IOLQI controller using FF algorithm 82

5.23 Output responses ($h_1(t)$ and $h_2(t)$) for non-minimum phase operating condition of QTP with IOLQI controller using FF algorithm 82
5.24 Output responses ($h_1(t)$ and $h_2(t)$) for minimum phase operating condition of QTP with FOLQI controller using FF algorithm 83
5.25 Output responses ($h_1(t)$ and $h_2(t)$) for non-minimum phase operating condition of QTP with FOLQI controller using FF algorithm 83

6.1 Representation of bond in BG 88
6.2 BG model of QTP 95
6.3 BG model of FOLQI controller 96
6.4 Closed loop BG representation of QTP with FOLQI controller 97

A.1 Closed loop representation of LADR Controller with plant 123

List of Tables

2.1 Symbols and descriptions of QTP 17

4.1 QTP parameters and its equilibrium points 38
4.2 Random initial guesses of FOLQI controller parameters for minimum phase system 39
4.3 Converged values of FOLQI controller parameters for minimum phase system 40
4.4 Random initial guesses of FOLQI controller parameters for non-minimum phase system 40
4.5 Converged values of FOLQI controller parameters for non-minimum phase system 40
4.6 IOLQI controller parameters from the set of converged values resulting minimal controller effort 41
4.7 LADR controller parameters from the set of converged values resulting minimal controller effort 41
4.8 Time domain performance metrices under $d(t)$ condition for minimum and non-minimum phase systems 44
4.9 Time domain performance metrices under $d(t)$ and parameter uncertainty for minimum phase condition 50
4.10 Time domain performance metrices under $d(t)$ and parameter uncertainty for non-minimum phase condition 50
4.11 Stability analysis of FOLQI controller for minimum and non-minimum phase condition 52
4.12 Controller performance of IOLQI and FOLQI controller under $d(t)$ and parameter uncertainty conditions 53

5.1 Parameters of CS, APSO and FF algorithms 63
5.2 Converged controller parameters of IOLQI and FOLQI controllers 64

5.3 Convergence epochs and statistical indices of CS, APSO and FF algorithms 67
5.4 Performance characteristics for IOLQI and FOLQI controllers of QTP under $d(t)$ condition 69
5.5 Performance characteristics for IOLQI and FOLQI controllers of QTP under $d(t)$ and parameter uncertainty conditions using CS algorithm 75
5.6 Performance characteristics for IOLQI and FOLQI controllers of QTP under $d(t)$ and parameter uncertainty conditions using APSO algorithm 76
5.7 Performance characteristics for IOLQI and FOLQI controllers of QTP under $d(t)$ and parameter uncertainty conditions using FF algorithm 77
5.8 Stability analysis of controllers tuned using CS algorithm 84
5.9 Stability analysis of controllers tuned using APSO algorithm 85
5.10 Stability analysis of controllers tuned using FF algorithm 85

6.1 Effort and Flow representation in various domain 93
6.2 Casual relationship of BG elements 94
6.3 Converged parameters of IOLQI and FOLQI controllers obtained using NR and DFP methods 102
6.4 Converged parameters of IOLQI and FOLQI controllers obtained using SD and BFGS methods 103
6.5 Controller effort of IOLQI and FOLQI controller under d(t) and parameter uncertainty conditions 104

Abbreviations

ACO	Ant Colony Optimisation
ADR	Active Disturbance Rejection
AIEN	Adaptive Inverse Evolutionary Neural
APPC	Adaptive Pole Placement Controller
APSO	Accelerated Particle Swarm Optimisation
ASMC	Adaptive Sliding Mode Controller
BA	Bat Algorithm
BFO	Bacterial Foraging Optimisation
BG	Bond Graph
BLT	Bounded Linear Time Invariant
BVS	Baseline Variable Structure
CS	Cuckoo Search
DOIB	Disturbance Observer-based Integral Backstepping
EWT	Empirical Wavelet Transform
FC	Fractional Calculus
FF	FireFly
FOC	Fractional Order Controller
FOLQI	Fractional Order Linear Quadratic Integrator
FPO	Flower Pollination Optimisation
GA	Genetic Algorithm

GWO	Grey Wolf Optimisation
HHO	Harris Hawks Optimisation
IAE	Integral Absolute Error
IMC	Internal Model Control
IMF	Intrinsic Mode Function
ISE	Integral Square Error
ITAE	Integral Time Absolute Error
LMI	Linear Matrix Inequality
LQG	Linear Quadratic Gaussian
LQGR	Linear Quadratic Gaussian Regulator
LQI	Linear Quadratic Integrator
LQR	Linear Quadratic Regulator
LSTM	Long Short Term Memory
LTV	Linear Time Variant
MPC	Model Predictive Controller
MIMO	Multi Input Multi Output
OPT	Objective Performance Index
PSO	Particle Swarm Optimisation
QFT	Quantitative Feedback Theory
QTP	Quadruple Tank Process
RGA	Relative Gain Array
SA	Simulated Annealing
SMC	Sliding Mode Controller
SQP	Sequential Quadratic Programming
TD	Track Differentiator
TF	Transfer Function
TLBO	Teaching-Learning-Based Optimisation

Nomenclature

A_i	Area of Cross Section of Tank T_i
a_i	Area of Cross Section of Orifice
C	Capacitance
$d(t)$	Disturbance
J	Effective Control Effort
e	Effort
S_e	Effort Source
f	Flow
γ	Flow Control coefficients between Tanks
S_f	Flow Source
g	Gravitational Constant
GY	Gyrator
h_i	Height of Water Level in Tank T_i
I	Inertance
$Total_{inflowrate}$	Inflow Rate to the Tank
u_i	Input Voltage to Pump p_i
LT_i	Level Transmitter in Tank T_i
T	No of Iterations

$F_{Oustaloup}(s)$	Oustaloup Approximation of F(s)
$Total_{outflowrate}$	Outflow Rate from the Tank
$\%M_p$	Percentage Maximum Overshoot
p_a	Probability Function
p_i	Pump i
k_i	Pump Constant for Pump p_i
P_i	Pressure in Tank i
R	Resistance
$\mathbb{Z}$	Set of Integer Numbers
$\mathbb{N}$	Set of Natural Numbers
$\mathbb{R}$	Set of Positive Real Numbers
e_{ss}	Steady State Error
t_s	Settling Time
T_i	Tank i
TF	Transformer

Chapter 1

Introduction

In many industrial processes, particularly in process control and chemical engineering, multiple variable must be controlled simultaneously to ensure optimal performance. These variables can include temperature, pressure, flow rates and concentrations. The Quadruple Tank Process (QTP) with its four interconnected tanks representing different variables provides a platform for studying and implementing multivariable control strategies. Engineers/researchers can develop control algorithms considering the interactions between these variables and nonlinearities which allow for more efficient and precise control. The QTP is a complex system with various operating modes including minimum and non-minimum phase conditions. Understanding and effectively controlling such a system requires advanced control system design techniques with the ability to handle nonlinearities, interactions and complex transfer matrix configurations.

This thesis presents the tuning of Fractional Order (FO) Linear Quadraic Integrator (LQI) controller parameters to meet the required time domain specifications such as overshoot, settling time and steady state error using constrained optimisation problem with minimum control effort. The optimisation problem is solved using the fmincon function which uses Sequential Quadratic Programming (SQP) algorithm for obtaining the solution. Further, various heuristic optimisation algorithms such as CS, APSO and FF are used to tune the parameters of FOLQI controller in the presence of load disturbance conditions in addition to meet the desired specifications. The obtained results are compared with existing controllers such as Integer Order (IO) LQI and LADR. Further, the feasibility of tuning FOLQI controller parameters in the Bond Graph (BG) domain is explored without considering the constraints on the time domain requirements. This methodology offers valuable insight into alternative method for representing QTP and tuning of controller parameters in BG.

1.1 Literature Survey and Motivation

In recent industrial and engineering applications, most systems are inherently nonlinear, highly coupled and Multiple Input Multiple Output (MIMO) system. These systems can operate in minimum and non-minimum phase modes which presents specific characteristics and challenges. Unlike minimum phase systems, non-minimum phase systems exhibit a delay between change in input and its output response. This delay is due to zeros placed in (i) right half of the s-plane in case of continuous time systems and (ii) outside the unit circle in case of discrete time systems [1]. A detailed analysis of non-minimum phase systems and control synthesis techniques providing essential theoretical background for engineering practitioners are given in [2]. This exhibits internal dynamics that can lead to instabilities or undesirable transient behaviours. Control system design for the circuit system with different configurations exhibiting non-minimum phase characteristics is presented in [3]. The benchmark provides a practical and theoretical foundation for testing and developing control strategies modified to address the complexities associated with non-minimum phase dynamics. A few such practical systems widely used for control applications are twin-rotor system [4], AC/HVDC interconnected system [5], Rosenbrock's system and Wood-Berry's binary distillation column [6], Shaker setup of an aeronautical structure [7] and QTP [1]. These systems typically exhibit inherent interaction effects among the process variables which makes complex in system analysis and controller design. These interaction effect requires a comprehensive review of various decoupling principles as discussed in [8].

1.1.1 QTP

To meet these challenges, the process industries consider QTP as a benchmark process for analysing, detailing its configuration, mathematical modeling, and the concept of adjustable zeros, making it a key reference for understanding the non-minimum phase behavior for designing controllers [9], [10] and [11]. The QTP presents with multivariable control challenges which require coordinated regulation of multiple inputs to achieve the desired outputs. To regulate the characteristics of QTP in the presence of disturbance/uncertainty, the design of controller is crucial. Many researchers investigated different control techniques like PID control, adaptive control, Model Predictive Control (MPC) and advanced optimisation algorithms to achieve precise set point tracking, disturbance rejection and optimal control of QTP.

In 1985, authors introduced the concept of process modelling and feedback control

using Kalman filter in two tank system in the presence of disturbance and measurement error. This experimentation consist of PI and PID control, modelling and parameter fitting, auto-tuning, selector control, anti-windup, state feedback and output feedback [12]. This leads to establish QTP as a classic example in the field of process control and system dynamic [13].

In [9] and [10] authors introduced the updated model of QTP, demonstrating the non-linear dynamics, interaction effect and the complex nature of the non-minimum phase operating modes. In [11], the effect of non-minimum phase behaviours such as reduction in bandwidth, unstable dynamics for simpler control methods and extended computational time issues are explored and found that Linear Quadratic Gaussian (LQG) controller augmented with integrator provides better disturbance rejection capability than the existing H∞, loop-shaping, feedback linearisation and MPC for non-minimum phase operating condition.

1.1.2 Controllers for QTP

In [14], an effective method for designing and tuning decentralised PI controllers of stable MIMO systems is presented. The approach uses the direct Nyquist array technique to shape the Gershgorin bands individually for each control loop, intersecting a predefined point corresponding to a specified phase margin specification and found to provide better results than Ziegler–Nichols tuning of controller. In [15], implementation of decentralised PI controller by analysing the severity of the interaction using the Relative Gain Array (RGA) principle and the performance comparison of the step response plots show that non-minimum phase condition has nearly 10 times lower bandwidth than minimum phase operating condition. The robust decentralised PID controller has been designed in frequency and time domain using Linear Matrix Inequality (LMI) and inverse dynamic approach [16]. The results show that (i) LMI based design of static output feedback controller provides better performance for minimum phase configuration and (ii) non-minimum phase system prefers the inverse dynamics approach.

Control design methodologies like decentralised PI, multivariable Internal Model Controller (IMC) and μ analysis based H∞ controllers are employed in [17]. These controllers are evaluated for stability, performance in set point tracking and disturbance rejection using robustness metrices. The results show that IMC and H∞ controllers provide better performance than the decentralised PI controller. In [18], gain and phase margin specifications are used to tune the decentralised PI/PID controller. The evaluated performance measures

such as Integral Absolute Error (IAE), Integral Square Error (ISE), Integral Time Absolute Error (ITAE), peak overshoot and rise time show that the proposed method has better performance than other controllers like IMC-PI and Bounded Linear Time invariant (BLT)-PI. In [19], QTP operates with a nonlinear zero dynamic attack in non-minimum phase conditions. The attack utilises Byrness-Isidori standard representation and employs Lyapunov analysis to ensure stealthiness in the presence of uncertainties and parameter variations. The attack remains undetectable until certain tanks reach overflow or depletion conditions, exploiting the system's nonlinear dynamics for stealthy intrusion. Experimental results demonstrate the effectiveness and stealthiness of the proposed attack strategy, highlighting its potential threat to the security and robustness of QTP control systems.

The design of a robust H∞ observer based controller for Takagi-Sugeno (TS) fuzzy systems, equivalent to QTP with time varying delays, parameter uncertainties and external disturbances are presented [20]. The Lyapunov-Krasovskii function is employed to guarantee the asymptotic stability of the proposed controller. Experimental results demonstrate the effectiveness of the controller to achieve robust control performance and minimising the effect of uncertainties and disturbances in TS fuzzy systems with time varying delays. In [21], a Disturbance Observer based Integral Backstepping (DOIB) controller for a two tank system is presented in the presence of external disturbances. The comparative performance analysis is conducted with a Sliding Mode Controller (SMC) to evaluate the effectiveness of the proposed DOIB controller. Experimental results demonstrate that the DOIB controller outperforms SMC by avoiding chattering, reducing steady state error, and enhancing disturbance suppression characteristics which highlights its superiority for control applications in dynamic systems subjected to external disturbances. In [22], design and comparative analysis of two control laws for rejecting disturbances and handling parameter uncertainty in dynamic systems are presented. These control laws have been designed to address set point tracking problems while accounting for disturbances, uncertain parameters, measurement errors and neglected dynamics. The comparative analysis provide the strength and limitations of each control law for the given conditions.

In [23], design and comparative performance analysis of an Adaptive Inverse Evolutionary Neural (AIEN) controller under the disturbance and uncertainty conditions against a conventional PID controller designed using error criteria is presented. The performance of both the controllers are evaluated based on error criteria such as ISE, IAE and ITAE. In this work, AIEN controller outperforms the conventional PID controller across various error criteria, highlighting its effectiveness in achieving superior control performance. In [24], testing of two adaptive control strategies, namely Adaptive Pole Placement Con-

troller (APPC) and Robust Adaptive Sliding Mode Controller (ASMC) are presented to achieve high performance control of a minimum phase QTP. The controllers are evaluated based on their robustness to set point variations, parametric uncertainties and rejection of disturbance inputs. Simulation results demonstrate that the proposed adaptive control configurations outperform PID controller due to lower performance indices and faster settling times. ASMC also demonstrates superior performance compared to APPC across various input variations and regulation scenarios due to the inherent robustness of SMC against uncertainties and disturbances.

In [25], a single variable synthesis method, the balanced tuning and the desired model approach based optimal controller is designed. The RGA tool obtains the optimal control pairs to minimise integral performance indices and ensure robust disturbance rejection. Comparative performance analysis is conducted with conventional controllers to evaluate the effectiveness of the proposed optimal controller in terms of set point tracking accuracy and disturbance rejection. Experimental results demonstrate that the optimal controller outperforms conventional controllers in terms of ITSE and ITAE under disturbance conditions. An adaptive decentralised neuro-fuzzy inference system based controller provides better performances in terms of accurate level tracking for QTP with less computational time [26]. The SMC structured with an optimal integral sliding surface, is designed to outperform conventional LQI setup by minimising integral absolute error under disturbance and uncertainty conditions [27]. In [28], robust optimal decentralised PID controller based on nonlinear optimisation provides improved bandwidth for specified stability margins and robustness against parameter uncertainty compared to existing adaptive decentralised PI controller.

1.1.3 Fractional Order Controller

Researchers have developed novel control strategies based on Fractional Calculus (FC) called FO Controller (FOC) [29] to address the challenges in control systems like (i) to capture the complex dynamics more effectively [30] (ii) handle the nonlinearities more efficiently [31], [32] and (iii) making them suitable for a wide range of control applications [33]. These include adaptive, robust and distributed FOC which provide improved performance, robustness and scalability compared to traditional Integer Order (IO) controllers [34]. A notable contribution by various researchers presented in the literature are summarised and given below.

The authors of [30] present the tuning of FOPI controller using the kissing circle method

which relies on a frequency domain approach that provides 6% decrease in power consumption and better robustness characteristics compared to IOPI controller. This method does not require model dynamics and controller parameters are obtained through frequency domain identification method. The design of FOPID controller to minimise IAE, ISE, ITAE and control effort is proposed in [33]. The unconstrained optimisation problem is solved using fmincon function in Matlab which shows better performance than the IO controller. Implementation of FOC like PI^{α} and $[PI]^{\alpha}$ for limit cycle suppression of system with backlash found to produce better performance than conventional PID controller [31], [32] and [35]. In [36], unified expressions for FO and fractional complex order controllers to regulate systems with complex coefficients and dead time are proposed to meet the Wang et al. specifications. The FOC design with adaptive laws for the process with variable time delay provides better performances than conventional controllers [37]. In [38] and [39], numerical methods for optimising the parameters of FOC's and the practical guidance on implementing controllers using MATLAB are presented.

1.1.4 FOC for QTP

FOC presented for QTP are given below. In [40], a dual-mode adaptive FOPI controller and an adaptive feed-forward controller using a variable parameter transfer function model are presented for QTP. This research concludes that the proposed model performs better than other controllers like decentralised PI, multivariable Quantitative Feedback Theory (QFT) and SMC. FOPI controller and conventional feed-forward controller are designed in [41] using frequency domain approach and found better performances than PI/PID/2DOF-PI/3DOF-PI with feed-forward controller. In [42], an optimal FOPID controller based on a Genetic Algorithm (GA) is presented for a system with time delay and found to have better ITAE performance than a conventional controller.

The design of FO predictive controller for QTP with dead time is presented in [43] and the performance characteristics like settling time, rise time, peak time, overshoot and ISE are evaluated. The results indicates that gain shaping method of tuning controller provides better performance than Hagglund, amigo and Z-N techniques. In [44], FO-SMC controller is proposed to dealt with plant uncertainties which ensure the finite time convergence and provide better performance than conventional SMC.

1.1.5 LQI Controllers

The LQI controller is a robust and flexible tool in control theory, offering a comprehensive approach to regulating dynamical systems addressing both transient and steady state performance. It is a fusion of LQR and integral control action. This combines the benefits of both methodologies aiming to optimise system performance across a broad spectrum of applications. The Q and R matrices are the key components in formulating the control law that maintains the desired state trajectory and control signal respectively [45], [46] and [47].

Few researchers have recently developed LQI controllers that produces better performance than conventional controllers. Variable structured LQI controller presented in [46] for underactuated rotary pendulum system equipped with adaptive weighting mechanism performs better in terms of disturbance rejection, stability and minimum control effort compared to SMC and Baseline Variable Structure (BVS) LQI controller. The complicated nonlinear and coupled twin rotor MIMO system introduced with LQI controller found to have better set point tracking performances than the existing LQG and SMC controllers [47]. In [48], GA and cross entropy optimisation methods are employed to obtain the control parameters of LQR controller and found better time characteristics in terms of minimum error and control effort. In [49], various optimal controllers like LQR, LQG Regulator (LQGR), H_∞ and H_2 controllers are presented for QTP under disturbance conditions and noted that the performance of LQR controller is better in terms of settling time.

1.1.6 Heuristic Optimisation based Controllers

Heuristic based tuning of controller parameters are often more robust to system uncertainties and nonlinearities than controllers tuned using deterministic approaches [50]. Heuristic controllers have been successfully applied to various optimisation problems including scheduling, routing, resource allocation, machine learning and engineering design [51], [52], [53] and [54]. Their ability to effectively explore complex solution space, handle uncertainties and achieve optimal solution in less time make these methods as a valuable tools for handling complex problems.

A few contributions of the researchers towards controller design using heuristic methods are as follows. In [55], authors presented the tuning of PID controllers using heuristic algorithms like GA, Ant Colony Optimisation (ACO), Artificial Bee Colony (ABC) optimisation, Teaching-Learning-Based Optimisation (TLBO), Bat Algorithm (BA), Bacterial Foraging Optimisation (BFO), Particle Swarm Optimisation (PSO), Cuckkoo Search (CS), Simulated Annealing (SA), Grey Wolf Optimisation (GWO), Krill herd and Whale optimi-

sation algorithms. In [56], researchers used GWO and PSO methods to reduce the annual energy consumption of an industrial building under Seattle's weather conditions. The result shows that GWO performs better than PSO in terms of convergence rate and the required number of building simulations.

PSO and GA based heuristic methods are adopted to minimise annual cooling energy consumption for a residential building prototype situated in a hot and dry region of India, found PSO provides more economical design compared to GA based optimisation [57]. In [58], authors have developed a new hybrid forecasting framework to enhance the forecasting performance of digital currencies such as BTC, XRP, DASH and LTC by forecasting the nonlinear dynamical model. This model is developed by combining the Long Short Term Memory (LSTM) neural network method and Empirical Wavelet Transform (EWT) decomposition technique. The optimal estimated Intrinsic Mode Function (IMF) outputs obtained using CS algorithm captures the nonlinear characteristics more accurately than all considered models according to the statistical error criteria.

A novel hybrid wind speed forecasting model has been devised by integrating a long short term memory neural network decomposition method with GWO [59]. This combined approach effectively captures the nonlinear features inherent in wind speed time series data, result in enhancing the forecast accuracy significantly compared to individual forecasting models. In [60], authors investigated the design of PID controller parameters for attitude and altitude control of a quadrotor using both PSO and Harris Hawks Optimisation (HHO) algorithms under different geometric paths. The results indicate that HHO based controller offers superior performance characterised by its simplicity, flexibility and capability to explore the search space randomly, thereby obtaining local optimal solution. In [61], a combination of Hybrid HHO and GWO based algorithms are utilised for optimal path planning and tracking in executing the payload hold release mission of UAVs during obstacle avoidance. This approach demonstrates superior performance compared to controllers tuned using PSO and GWO.

The PID controller parameters obtained through an enhanced CS algorithm yield superior outcome in terms of peak time, overshoot and settling time in contrast to the controller tuned using conventional CS and PSO methods [62]. In [63], PID controller is designed for an automatic voltage regulator system tuned using CS demonstrates superior performance compared to PSO and ABC algorithms in terms of overshoot, settling time and steady state error. In [64], an integration of PSO and CS algorithm is utilised to tune the PID controller parameters for a quadrotor system to demonstrate with an improved efficiency compared to conventional CS and classical reference models in terms of ISE error. The implementation

of FF algorithm to optimise the membership function within a fuzzy controller is presented in [65] which improves the actuation function of autonomous mobile robots. In [66], tuning of PID controllers for QTP using GA yields superior performances in terms of rise time, settling time and steady state error compared to PI/PID controllers tuned using IMC, PSO and BFO algorithms.

Implementation of heuristic based algorithms for optimising controller parameters in LQI controller provide better performances. The optimal tuning of the LQI controller for Z-source inverters in the presence of parameter variations, unmodeled dynamics and load disturbances are performed by selecting the optimal weighting matrices Q and R through BA for better time domain characteristics and robustness compared to existing PI and state feedback controllers [49]. Utilising GA for tuning Q and R matrices of the LQI controller in speed control applications provides superior performance in terms of overshoot and settling time compared to conventional LQI and PID controllers [67].

1.1.7 LADR Controllers

Linear Active Disturbance Rejection (LADR) controllers specifically address disturbance rejection problems which improve the performance in the presence of plant uncertainties and disturbances. Unlike traditional control methods, LADR controllers actively estimate and eliminate the disturbances in real time systems that provides more precise control [68] and [69]. A proposed optimisation based approach for tuning the parameters of LADR controller using Bacterial Foraging Optimisation-Flower Pollination Algorithm (BFO-FPA) offers enhanced trajectory tracking and disturbance rejection capabilities compared to ADR and PID controllers for the unmanned helicopter system [70]. An improved LADR controller proposed in [71] provides superior attenuation of input disturbances compared to the conventional LADR controller for wheeled robots operating on soft terrains.

In [72], LADR controller designed for QTP shows its superior performance in disturbance rejection and position tracking compared to PID and ADR controllers. In [73], ADR controller is presented with nonlinear PD control and the Track Differentiator (TD) to serve as a nonlinear state error feedback. In feedback loop, a sliding mode extended state observer is introduced to estimate both the system's state and overall disturbance. The proposed controller provides better performance in terms of disturbance rejection, output tracking, ITAE and Objective Performance Index (OPI) compared to conventional linear and nonlinear ADR controllers. The proposed centralised FOLQI controller is tuned using SQP optimisation under continuous load disturbance and parameter uncertainty condi-

tions [74]. The controller outperforms LADR controller in terms of steady state error and control effort.

1.1.8 Controller Implementation using BG

Recent study in BG reveals that the better performance characteristics and fault diagnosis are achieved by representing the system and controller in BG domain using power variables (ie. effort and flow). This method offers several advantages like unified representation, causal representation, energy based modelling, hierarchical structure, graphical representation and model based control design.

Basic BG elements and its modelling aspects in various domains like electrical, mechanical and hydraulic are presented in [75] and [76]. In [77], synthesising the decoupling law for a Linear Time Varying (LTV) system using BG provides a simplified approach with less computing time compared to the conventional decoupling methods. In [78], heuristic approach based controller for swing up phase and PI controller for stabilisation phase are designed for inverted pendulum that overcomes the characteristics of pendulum nonlinearity and its instability.

Modelling industrial back support exoskeleton platform with Kalman filter observer and LQR controller using BG provides a simple representation compared to the conventional model [79]. The experimental results indicate that both BG and conventional models provide similar responses. In [80], BG based controller is designed using an inversion of the system through their causal input/output for trajectory tracking problem. The simulation results show that this method is effective and robust against the parameter uncertainties. On the other hand, the power and energy shaping principle is used in the BG approach to synthesise the control law for QTP which produce efficient output regulation and better fault tolerance [81].

1.2 Motivation and Research Contribution

1.2.1 Motivation

In [14] - [16], tuning of decentralised controllers are presented for QTP without disturbance conditions. In contrast, an observer based controller is presented under disturbance and parameter uncertainty conditions [20]. The results indicate that this approach required more than $100\ sec$ to reach the steady state value. The APPC/AMSC is presented for

minimum phase QTP with disturbance and parameter uncertainty conditions. It is noted that the parameter variations are limited only to the area of cross section of tank [24]. A decentralised PI controller based on nonlinear constraint optimisation is presented which provides better closed loop frequency domain performances limited to (i) overshoot as a constraint and (ii) $\pm$ 10% of parameter variation [28]. In [72], tuning of LADR controller for QTP provides better steady state and disturbance rejection performance compared to conventional PID and ADR controllers.

LQI controller helps to eliminate steady state error with enhanced tracking performance and disturbance rejection condition [82] and [83]. Introduction of integral action in LQ controller improves a controller ability to handle setpoint changes and disturbances in specific, system is subjected to steady state error [84]. This ensures better disturbance rejection and zero steady state error in closed loop design [85]. In general, FC supports the design of FOC by enhancing controller flexibility which allow to reduce controller effort [86]. The additional degrees of freedom in FOC's enable fine tuning of control performance, reducing the magnitude of control efforts while maintaining system stability [87] compared to conventional PID controller performance [88].

FOC's also perform well in time delay systems due to their flexibility in tuning with improved system performance [89]. The ability to control both phase and magnitude across a broad frequency range enables FOC's to perform better in time delay systems than IO controllers [90] and are more robust than conventional PID controllers with extra tuning parameters that improve control of phase lag caused by delays which enhance the stability and transient performance [91] and [92]. Comparative analysis shows that FOPID controllers are more effective than traditional PID controllers in mitigating time delay effects which leads to provide an improved transient response and stability margins [93]. On the other hand, stability bounds derived for delayed FO systems demonstrate that FO controllers are better suited for managing time delays due to their flexibility in controlling system dynamics [94] and [95].

Many literature indicate that FOC provide better performances than their respective integer order controllers [37] - [44]. Linear quadratic controllers provide better performances than other controllers [45] - [47] as they try to penalise the change in state and control by adapting the weights individually. On the other hand, obtaining the values of Q and R matrices in LQR through optimisation provides better performance than conventionally assigned Q and R matrices [48] and [49] .

Due to lack of performance in the presence of disturbance and parameter uncertainties, it is mandate to develop a new controller that provides better performance with less control

effort. This motivate to propose (i) FOLQI controller by introducing fractionality in the integral part of the conventional LQR controller with optimal selection of Q and R matrices and (ii) an energy based method using BG to model QTP and FOLQI controller.

1.2.2 Research Contribution

As stated in previous sections, the thesis aims to propose a constrained optimisation problem to tune the FOLQI controller parameters of QTP in the presence of disturbance condition. The contributions of this thesis are summarised as follows:

(i) The basic schematic representation with the nonlinear dynamical equations and its linearised state space model of QTP are presented.

(ii) Centralised optimal FOLQI controller is proposed for rejecting continuous load disturbances in both minimum and non-minimum phase operating conditions of QTP.

(iii) A constrained optimisation problem is framed for tuning the parameters of the proposed FOLQI controller to effectively suppress the load disturbances and meet the required time domain specifications with minimum control effort.

(iv) The controller parameters for the proposed FOLQI controller are obtained by solving the constrained optimisation problem by using the SQP method and various heuristic algorithms such as CS, APSO and FF.

(v) Through detailed simulation and time domain analysis, the superiority of the proposed FOLQI controller for QTP is effectively demonstrated under disturbances and uncertainty conditions by showcasing its improved performance compared to conventional IOLQI and LADR controllers.

(vi) Implementation of FOLQI controller for QTP in BG domain is explored for an unconstrained optimisation problem. The simulation results show that the effective control effort is less compared with an optimally tuned IOLQI controller.

1.3 Organisation of Thesis

- Chapter 2 details the schematic representation and construction of QTP which includes the dynamics of both nonlinear and linear. These models are useful to understand the dynamical behaviour of QTP which makes the analysis and controller design systematically facilitating the future analysis.

- Chapter 3 explores the introduction of FC includes transfer function representation and approximation methods in continuous domain in specific Oustaloop method. It also outlines the mathematical framework of LQI controller and further extended to the proposed FOLQI controller. This chapter also explains the proposed optimisation problem which includes objective function and related time domain constraints.

- In Chapter 4, the system parameters with required assumptions are outlined along with the disturbance signal used in the simulation. The proposed optimisation method explained in Chapter 3 is used to tune FOLQI controller parameters using SQP method. The results are discussed in detail which includes how the controller parameters impact the system's performance in the presence of disturbance and parameter uncertainty conditions. The superior performance of the FOLQI controller is compared with existing IOLQI and LADR controllers.

- Chapter 5 presents the various heuristic algorithms for tuning FOLQI controller and the performance of different algorithms are compared. Also, the performance of the proposed FOLQI controller is compared with optimally tuned IOLQI controller.

- In chapter 6, the BG method of modelling QTP along with FOLQI controller is presented with unconstrained optimisation problem. The controller parameters are optimised by using various optimisation methods and the results are compared with optimally tuned IOLQI controller.

- Chapter 7 provides the conclusion and future direction of this research work.

Chapter 2

Quadruple Tank Process

2.1 Introduction

The QTP represents a benchmark dynamic system utilised in control theory and practise by researchers and engineers. The primary objective of the QTP is to manipulate the fluid levels within the tanks by adjusting the flow rates of incoming and outgoing streams, thereby facilitating control system analysis and experimentation. Due to its inherent complexity and multivariable nature, QTP is an ideal testbed for investigating various control strategies. The experiments provide valuable insights into the dynamics of interconnected systems, disturbance rejection and parameter estimation techniques. Hence, QTP is considered as a benchmark problem to test the advanced controllers in industrial environments.

The QTP is a nonlinear and highly interacted MIMO system. The setup includes four interconnected tanks made of transparent material and allow for easy visualisation of fluid levels and interactions. Each tank has inlet and outlet valves which enable precise control over fluid flow. The arrangement of interconnections between tank can vary depending on the specific experiment or applications with various configurations such as series, parallel and hybrid to mimic different real world process. In addition, (i) sensors are crucial for QTP providing real time fluid levels, pressure or weight data and (ii) actuators such as valves or pumps respond to sensor feedback to adjust flow rates and maintain desired set points. These configurations influence the complex behaviour of the system dynamics which allow the control practitioners to design and apply various control strategies.

In general, the controllers for QTP is implemented using PLCs, microcontrollers or other programmable devices. Control algorithms such as PID control, cascade control and MPC etc., are programmed to regulate fluid levels in addition to obtain the optimal system performance. It is a scalable platform for simulating and optimising the complex processes in chemical engineering, water treatment and manufacturing industries. The

QTP offers a comprehensive approach to study process dynamics and control theory. Researchers/engineers can experiment with different control strategies and parameter tuning to achieve desired outcomes. Its modular design and advanced control algorithms enable in depth learning experiences and practical insights into other real world applications.

2.2 Schematic Representation and Physical Construction

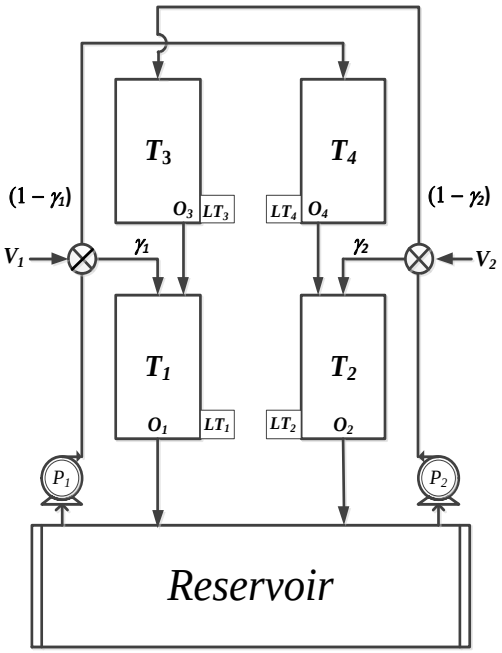

Figure 2.1: Schematic illustration of the QTP

The schematic diagram of QTP shown in Fig. 2.1 consists of various components which includes four tanks with orifices, reservoir, two pumps, two directional control valves and four Level Transmitters (LT). The reservoir delivers the input through two channels (i) pump p_1 supplies fluid to tanks T_1 and T_4 by maintaining proportional flows of γ_1 and $(1-\gamma_1)$ respectively controlled by directional control valve V_1 and (ii) pump p_2 feeds fluid to tanks T_2 and T_3 by maintaining proportional flows of γ_2 and $(1-\gamma_2)$ respectively regulated by directional control valve V_2. The discharge through pumps p_1 and p_2 is regulated by their corresponding input voltages u_1 and u_2. Each tank T_i is equipped with orifice O_i (where i ranges from 1 to 4). Orifices O_1 of T_1 and O_2 of T_2 direct the flow to the reservoir, while

orifices O_3 of T_3 and O_4 of T_4 divert the flow to T_1 and T_2 respectively. Their respective LT measures the liquid level in the tanks.

The construction of QTP emphasises precision and consistency to ensure reliable experimental results. Tank dimensions such as height, width and cross sectional area are carefully measured and controlled to maintain uniformity across all tanks. The valves are calibrated to accurately control the flow rates of fluid which makes precise manipulation of the system dynamics during experiments. Table 2.1 provides symbols and its represention of QTP.

Table 2.1: Symbols and descriptions of QTP

Symbols	Descriptions
A_i, $i = 1$ to 4	Area of cross section of tank T_i in cm^2
a_i, $i = 1$ to 4	Area of cross section of orifice O_i in cm^2
h_i, $i = 1$ to 4	Height of liquid level in tank T_i in cm
LT_i, $i = 1$ to 4	Level transmitter in tank T_i
u_i, $i = 1, 2$	Input voltage to pump p_i in $volts$
k_i, $i = 1, 2$	Pump constant for p_i
γ_i, $i = 1, 2$	Flow control coefficients between two tanks
g	Gravitational constant in cm/sec^2

2.3 Mathematical Modelling

The QTP model typically involved in solving a system representing either Ordinary Differential Equations (ODE) or Partial Differential Equations (PDE) to capture the dynamics of the liquid levels. The resulting model allows to analyse the system characteristics and designing control strategies to regulate the liquid levels effectively. Through simulation and experimentation, the researchers can validate the accuracy of the model and explore the possible control techniques to optimise the performance of QTP in hardware-inloop configuration.

The QTP model obtained using classical approach involves applying a mass balance equation for individual tanks. This principle states that the rate of change of mass within a control volume equals the net rate of mass flow into the control volume minus the net rate of mass flow out of the control volume. Here, the liquid height in each tank is denoted as h_i, where $'i'$ spans from 1 to 4.

The generalised mass balance equation for each tank can be formulated and as follows [96]:

$$\frac{d}{dt}(h_i A_i) = (Total_{inflowrate}) - (Total_{outflowrate}) \tag{2.1}$$

where, $Total_{inflowrate}$ is the inflow rate to the tank (i) and $Total_{outflowrate}$ is the outflow rate from the tank (i).

The flow rate through the orifice O_i can be expressed as the function of valve position and height of the liquid in tank i. This is expressed as $a_i\sqrt{2gh_i}$. Based on (2.1), mass balance equation for each tank is formulated and as follows [97]:

$$Tank\ 1 : \frac{dh_1}{dt} = \frac{q_{\text{in}} + q_{31} - q_{out}}{A_1} \tag{2.2}$$

$$Tank\ 2 : \frac{dh_2}{dt} = \frac{q_{\text{in}} + q_{42} - q_{out}}{A_2} \tag{2.3}$$

$$Tank\ 3 : \frac{dh_3}{dt} = \frac{q_{\text{in}} - q_{31}}{A_3} \tag{2.4}$$

$$Tank\ 4 : \frac{dh_4}{dt} = \frac{q_{\text{in}} - q_{42}}{A_4} \tag{2.5}$$

where,

$$For\ tank\ 1\ and\ 2 : q_{in} = u_i k_i \gamma_i\ (i \in 1, 2)$$
$$For\ tank\ 3\ and\ 4 : q_{in} = u_i k_i (1 - \gamma_i)\ (i \in 2, 1)$$

$$q_{out} = a_i\sqrt{2gh_i}\ (i \in 1, 2)$$
$$q_{31} = a_i\sqrt{2gh_3}$$
$$q_{42} = a_i\sqrt{2gh_4}$$

2.3.1 Nonlinear Model and its Equilibrium Points

From (2.2) - (2.5), the nonlinear differential equations of QTP are obtained [1] and as follows:

$$\frac{dh_1}{dt} = -\frac{a_1}{A_1}\sqrt{2gh_1} + \frac{a_3}{A_1}\sqrt{2gh_3} + \frac{\gamma_1 k_1}{A_1}u_1 \tag{2.6}$$

$$\frac{dh_2}{dt} = -\frac{a_2}{A_2}\sqrt{2gh_2} + \frac{a_4}{A_2}\sqrt{2gh_4} + \frac{\gamma_2 k_2}{A_2}u_2 \tag{2.7}$$

$$\frac{dh_3}{dt} = -\frac{a_3}{A_3}\sqrt{2gh_3} + \frac{(1-\gamma_2)k_2}{A_3}u_2 \tag{2.8}$$

$$\frac{dh_4}{dt} = -\frac{a_4}{A_4}\sqrt{2gh_4} + \frac{(1-\gamma_1)k_1}{A_4}u_1 \tag{2.9}$$

The inputs to the system are control voltages (u_1 and u_2) and states are height of the liquid in tanks (h_1 - h_4).

Mathematically, an equilibrium point of QTP can be interpreted as a combination of state variables and input variables, where the fluid level variations result in a static condition. This indicates the attainment of a stable equilibrium point when inflow and outflow rates in each tank are equal. The process of identifying the equilibrium points are important for solving the differential equations and this involves setting the time derivatives of the state variables to zero such that one can determine the corresponding equilibrium value of state and input variables. This process simplify the QTP model to understand the dynamical characteristics in the presence of disturbance and parameter uncertainty conditions. Using this procedure, initially the equilibrium levels (h_{30} and h_{40}) are obtained and as follows:

By equating $\frac{dh_3}{dt} = 0$ provides

$$\begin{aligned} &-\frac{a_3}{A_3}\sqrt{2gh_3} + \frac{(1-\gamma_2)k_2}{A_3}u_2 = 0 \implies \frac{a_3}{A_3}\sqrt{2gh_{30}} = \frac{(1-\gamma_2 k_2)}{A_3}u_{20} \\ &\sqrt{2gh_{30}} = \frac{(1-\gamma_2)k_2}{a_3}u_{20} \implies h_{30} = \frac{1}{2g}\frac{(1-\gamma_2)^2 k_2^2}{a_3^2}u_{20}^2 \end{aligned} \tag{2.10}$$

By equating $\frac{dh_4}{dt} = 0$ provides

$$\begin{aligned} &-\frac{a_4}{A_4}\sqrt{2gh_4} + \frac{(1-\gamma_1)k_1}{A_4}u_1 = 0 \implies \frac{a_4}{A_4}\sqrt{2gh_{40}} = \frac{(1-\gamma_1)k_1}{A_4}u_{10} \\ &\sqrt{2gh_{40}} = \frac{(1-\gamma_1)k_1}{a_4}u_{10} \implies h_{40} = \frac{1}{2g}\frac{(1-\gamma_1)^2 k_1^2}{a_4^2}u_{10}^2 \end{aligned} \tag{2.11}$$

The equilibrium points h_{30} and h_{40} obtained from (2.10) and (2.11) are used to find h_{10} and h_{20}. By equating $\frac{dh_1}{dt} = 0$ provides

$$\begin{aligned} &-\frac{a_1}{A_1}\sqrt{2gh_1} + \frac{a_3}{A_1}\sqrt{2gh_3} + \frac{\gamma_1 k_1}{A_1}u_1 = 0 \implies \frac{a_1}{A_1}\sqrt{2gh_{10}} = \frac{a_3}{A_1}\sqrt{2gh_{30}} + \frac{\gamma_1 k_1}{A_1}u_{10} \\ &\sqrt{2gh_{10}} = \frac{a_3\sqrt{2gh_{30}} + \gamma_1 k_1 u_{10}}{a_1} \implies \sqrt{2gh_{10}} = \frac{a_3\sqrt{2g\frac{1}{2g}\frac{(1-\gamma_2^2)k_2^2}{a_3^2}u_{20}^2} + \gamma_1 k_1 u_{10}}{a_1} \\ &\sqrt{2gh_{10}} = \frac{\sqrt{(1-\gamma_2)^2 k_2^2 u_{20}^2} + \gamma_1 k_1 u_{10}}{a_1} \implies h_{10} = \left(\frac{1}{2g}\right)\left(\frac{(1-\gamma_2)k_2 u_{20} + \gamma_1 k_1 u_{10}}{a_1}\right)^2 \end{aligned} \tag{2.12}$$

By equating $\frac{dh_2}{dt} = 0$ provides

$$\implies -\frac{a_2}{A_2}\sqrt{2gh_{20}} + \frac{a_4}{A_2}\sqrt{2gh_{40}} + \frac{\gamma_2 k_2}{A_2}u_{20} = 0 \implies \frac{a_2}{A_2}\sqrt{2gh_{20}} = \frac{a_4}{A_2}\sqrt{2gh_{40}} + \frac{\gamma_2 k_2}{A_2}u_{20}$$

$$\sqrt{2gh_{20}} = \frac{a_4\sqrt{2gh_{40}} + \gamma_2 k_2 u_{20}}{a_2} \implies \sqrt{2gh_{20}} = \frac{a_4\sqrt{2g\frac{1}{2g}\frac{(1-\gamma_1^2)k_1^2}{a_2^2}u_{10}^2} + \gamma_2 k_2 u_{20}}{a_2}$$

$$\sqrt{2gh_{20}} = \frac{\sqrt{(1-\gamma_1)^2 k_1^2 u_{10}^2} + \gamma_2 k_2 u_{20}}{a_2} \implies h_{20} = \left(\frac{1}{2g}\right)\left(\frac{(1-\gamma_1)k_1 u_{10} + \gamma_2 k_2 u_{20}}{a_2}\right)^2 \tag{2.13}$$

2.3.2 Taylor Series Expansion

Nonlinear dynamical equations of QTP are linearised using Taylor series expansion. An equilibrium point of a dynamical system is a state at which all state variables and their derivatives are independent of time. In general, state space equations and equilibrium points are described as $\dot{x} = f(x, u)$ and (x_e, u_e) respectively to satisfy $f(x_e, u_e) = 0$. The Taylor series expansion is a mathematical method to approximate a function near a point using a series of derivatives of the function. For a single variable function $f(x)$, the Taylor series expansion about a point $x = a$ is given by:

$$f(x) \approx f(a) + \frac{f'(a)}{1!}(x-a) + \frac{f''(a)}{2!}(x-a)^2 + \cdots$$

For a multivariable function, $f(x_1, x_2, \ldots, x_n)$, the expansion is extended to multiple dimensions.

The linearised system is expressed in terms of perturbations from the equilibrium point. For example, if $x = x_e + \Delta x$ and $u = u_e + \Delta u$, where Δx and Δu represent small deviations from the equilibrium point. Hence, the linearised system can be written as:

$$\Delta\dot{x} = A\Delta x + B\Delta u$$

where, A and B are matrices obtained from the derivatives of the system dynamics at the equilibrium point.

2.3.3 State Space Representation of Linearised Model

The state space representation of the QTP involves describing the system dynamics in terms of state, input and output variables. Let $h = [h_1, h_2, h_3, h_4]^T$ is the state variable denoting state vector representing the liquid levels in tanks 1 to 4 respectively. The input vector $u = [u_1, u_2]$ is the pump voltage. The dynamics of QTP can be described by a state and

output equations: $\frac{dh}{dt} = Ah + Bu$ and $y = Ch + Du$, where A, B, C and D are state, input, output and feed forward matrix respectively. The nonlinear dynamical equations represented in (2.6) - (2.9) are linearised around the equilibrium points specified in (2.10) - (2.13) using Taylor series expansion and as follows:

$$\begin{aligned} f(h_1, h_2, h_3, h_4) \approx f(h_{10}, h_{20}, h_{30}, h_{40}) + \frac{\partial f}{\partial h_1}(h_{10}, h_{20}, h_{30}, h_{40})(h_1 - h_{10}) + \\ \frac{\partial f}{\partial h_2}(h_{10}, h_{20}, h_{30}, h_{40})(h_2 - h_{20}) + \frac{\partial f}{\partial h_3}(h_{10}, h_{20}, h_{30}, h_{40})(h_3 - h_{30}) + \\ \frac{\partial f}{\partial h_4}(h_{10}, h_{20}, h_{30}, h_{40})(h_4 - h_{40}) \end{aligned} \tag{2.14}$$

The linearised state equation for QTP is as follows:

$$\begin{bmatrix} \Delta\dot{h}_{10} \\ \Delta\dot{h}_{20} \\ \Delta\dot{h}_{30} \\ \Delta\dot{h}_{40} \end{bmatrix} = \begin{bmatrix} \frac{\partial f(h_1)}{\partial h_1} & \frac{\partial f(h_1)}{\partial h_2} & \frac{\partial f(h_1)}{\partial h_3} & \frac{\partial f(h_1)}{\partial h_4} \\ \frac{\partial f(h_2)}{\partial h_1} & \frac{\partial f(h_2)}{\partial h_2} & \frac{\partial f(h_2)}{\partial h_3} & \frac{\partial f(h_2)}{\partial h_4} \\ \frac{\partial f(h_3)}{\partial h_1} & \frac{\partial f(h_3)}{\partial h_2} & \frac{\partial f(h_3)}{\partial h_3} & \frac{\partial f(h_3)}{\partial h_4} \\ \frac{\partial f(h_4)}{\partial h_1} & \frac{\partial f(h_4)}{\partial h_2} & \frac{\partial f(h_4)}{\partial h_3} & \frac{\partial f(h_4)}{\partial h_4} \end{bmatrix} \begin{bmatrix} \Delta h_{10} \\ \Delta h_{20} \\ \Delta h_{30} \\ \Delta h_{40} \end{bmatrix} + \begin{bmatrix} \frac{\partial f(h_1)}{\partial u_1} & \frac{\partial f(h_1)}{\partial u_2} \\ \frac{\partial f(h_2)}{\partial u_1} & \frac{\partial f(h_2)}{\partial u_2} \\ \frac{\partial f(h_3)}{\partial u_1} & \frac{\partial f(h_3)}{\partial u_2} \\ \frac{\partial f(h_4)}{\partial u_1} & \frac{\partial f(h_4)}{\partial u_2} \end{bmatrix} \begin{bmatrix} \Delta u_{10} & \Delta u_{20} \end{bmatrix}$$

where, $f(h_1)$, $f(h_2)$, $f(h_3)$ and $f(h_4)$ are the functions representing the dynamics of each tank.

From (2.6), the function $f(h_1)$ is written as follows:

$$f(h_1) = -\frac{a_1}{A_1}\sqrt{2gh_1} + \frac{a_3}{A_1}\sqrt{2gh_3} + \frac{\gamma_1 k_1}{A_1}u_1$$

Using linearisation,

$$\begin{aligned}
\frac{\partial f(h_1)}{\partial h_1} &\implies -\frac{a_1\sqrt{2g}}{A_1}\frac{1}{2\sqrt{h_1}} \implies -\frac{1}{T_1} \\
\frac{\partial f(h_1)}{\partial h_2} &\implies 0 \\
\frac{\partial f(h_1)}{\partial h_3} &\implies \frac{a_3\sqrt{2g}}{A_1}\frac{1}{2\sqrt{h_3}} \implies \frac{A_3}{A_1.T_3} \\
\frac{\partial f(h_1)}{\partial h_4} &\implies 0 \\
\frac{\partial f(h_1)}{\partial u_1} &\implies \frac{\gamma_1 k_1}{A_1} \\
\frac{\partial f(h_1)}{\partial u_2} &\implies 0
\end{aligned}$$

From (2.7), the function $f(h_2)$ is written as follows:

$$f(h_2) = -\frac{a_2}{A_2}\sqrt{2gh_2} + \frac{a_4}{A_2}\sqrt{2gh_4} + \frac{\gamma_2 k_2}{A_2}u_2$$

Using linearisation,

$$\begin{aligned}
\frac{\partial f(h_2)}{\partial h_1} &\implies 0 \\
\frac{\partial f(h_2)}{\partial h_2} &\implies -\frac{a_2\sqrt{2g}}{A_2}\frac{1}{2\sqrt{h_2}} \implies -\frac{1}{T_2} \\
\frac{\partial f(h_2)}{\partial h_3} &\implies 0 \\
\frac{\partial f(h_2)}{\partial h_4} &\implies \frac{a_4\sqrt{2g}}{A_2}\frac{1}{2\sqrt{h_4}} \implies \frac{A_4}{A_2.T_4} \\
\frac{\partial f(h_2)}{\partial u_1} &\implies 0 \\
\frac{\partial f(h_2)}{\partial u_2} &\implies \frac{\gamma_2 k_2}{A_2}
\end{aligned}$$

From (2.8), the function $f(h_3)$ is written as follows:

$$f(h_3) = -\frac{a_3}{A_3}\sqrt{2gh_3} + \frac{(1-\gamma_2)k_2}{A_3}u_2$$

Using linearisation,

$$\begin{aligned}
\frac{\partial f(h_3)}{\partial h_1} &\implies 0 \\
\frac{\partial f(h_3)}{\partial h_2} &\implies 0 \\
\frac{\partial f(h_3)}{\partial h_3} &\implies -\frac{a_3\sqrt{2g}}{A_3}\frac{1}{2\sqrt{h_3}} \implies -\frac{1}{T_3} \\
\frac{\partial f(h_3)}{\partial h_4} &\implies 0 \\
\frac{\partial f(h_3)}{\partial u_1} &\implies 0 \\
\frac{\partial f(h_3)}{\partial u_2} &\implies \frac{1-\gamma_2 k_2}{A_3}
\end{aligned}$$

From (2.9), the function $f(h_4)$ is written as follows:

$$f(h_4) = -\frac{a_4}{A_4}\sqrt{2gh_4} + \frac{(1-\gamma_1)k_1}{A_4}u_1$$

Using linearisation,

$$\begin{aligned}
\frac{\partial f(h_4)}{\partial h_1} &\implies 0 \\
\frac{\partial f(h_4)}{\partial h_2} &\implies 0 \\
\frac{\partial f(h_4)}{\partial h_3} &\implies 0 \\
\frac{\partial f(h_4)}{\partial h_4} &\implies -\frac{a_4\sqrt{2g}}{A_4}\frac{1}{2\sqrt{h_4}} \\
\frac{\partial f(h_4)}{\partial u_1} &\implies \frac{1-\gamma_1 k_1}{A_4} \\
\frac{\partial f(h_4)}{\partial u_2} &\implies 0
\end{aligned}$$

where, $T_i = \frac{A_i}{a_i} * \sqrt{\frac{2h_{io}}{g}}$, and i = 1 to 4.

Based on the above procedure, the dynamics of the QTP are obtained by linearising the

nonlinear equations given in (2.6) - (2.9). It is as follows:

$$\begin{bmatrix} \dot{\Delta h_1} \\ \dot{\Delta h_2} \\ \dot{\Delta h_3} \\ \dot{\Delta h_4} \end{bmatrix} = \begin{bmatrix} -\frac{1}{T1} & 0 & \frac{A_3}{A_1.T_3} & 0 \\ 0 & -\frac{1}{T_2} & 0 & \frac{A_4}{A_2.T_4} \\ 0 & 0 & -\frac{1}{T_3} & 0 \\ 0 & 0 & 0 & -\frac{1}{T_4} \end{bmatrix} \begin{bmatrix} \Delta h_1 \\ \Delta h_2 \\ \Delta h_3 \\ \Delta h_4 \end{bmatrix} + \begin{bmatrix} \frac{\gamma_1.k_1}{A_1} & 0 \\ 0 & \frac{\gamma_2.k_2}{A_2} \\ 0 & \frac{(1-\gamma_2).k_2}{A_3} \\ \frac{(1-\gamma_1).k_1}{A_4} & 0 \end{bmatrix} \begin{bmatrix} \Delta u_1 \\ \Delta u_2 \end{bmatrix} \tag{2.15}$$

$$\Delta \text{y} = \begin{bmatrix} 1 & 0 & 0 & 0 \\ 0 & 1 & 0 & 0 \end{bmatrix} \begin{bmatrix} \Delta h_1 \\ \Delta h_2 \\ \Delta h_3 \\ \Delta h_4 \end{bmatrix} \tag{2.16}$$

2.4 Operating conditions of QTP

The QTP can operate in both minimum and non-minimum phase conditions, depending on the configuration of the valves and how the pumps feed into the tanks. It refers to a system in minimum phase condition, where the initial response to a control input is in the same direction as the desired output and hence easier to control. On the other hand, non-minimum phase systems have initial response to a control input in the opposite direction of the desired output which makes the system more challenging to control. The critical parameters influencing the operating conditions are flow control coefficients γ_1 and γ_2 as shown in Fig. 2.1. Their corresponding flow control coefficients are given in the Table. 4.1.

In minimum phase condition, maximum water from p_1 flows to T_1, and p_2 flows to T_2. This happens when γ_1 and γ_2 are relatively large (γ_1 and $\gamma_2 \geq 0.5$). During this condition, (i) change in the input from p_1 results in a direct increase or decrease in the water level of T_1 and (ii) change in the input from p_2 directly affects the water level of T_2. During non-minimum phase condition, system shows an initial inverse response to control inputs, resulting an increase in the pump voltage might initially decrease the water level of the desired tank before it eventually increases. In this configuration, p_1 and p_2 feeds maximum water into T_4 and T_3 respectively. This condition occurs when γ_1 and γ_2 are small (γ_1 and $\gamma_2 \leq 0.5$). The flow from the pumps primarily feeds into the upper tanks (T_3 and T_4) which lead to an initial inverse response in the water levels of the lower tanks (T_1 and T_2). This makes more challenging to control the inverse response and hence, such systems requires advanced control techniques.

2.5 Summary

This chapter presented the schematic diagram of QTP along with its mathematical model representing a complex nonlinear differential equations. The nonlinear model is linearised about its equilibrium point using Taylor series expansion method. This model is useful to simulate QTP along with the controller to analyse the closed loop characteristics under disturbances and parameter uncertainty conditions.

Chapter 3

Fractional Order LQI Controller

3.1 Preliminaries of Fractional Calculus

3.1.1 Introduction

Like converting from integer exponents to fractional exponents, FC is a natural extension of conventional IO calculus. When dealing with an integer exponent, such as $x^4 = 1 \cdot x \cdot x \cdot x \cdot x$, its physical interpretation involves multiplying 1 by x four times. However, this direct interpretation becomes challenging for a fractional exponent, for an example $x^{2.53}$. This is difficult to form the notion of multiplying 1 by a fractional number of times by x. However, the expression $x^{2.53}$ holds a specific value for the given x and can be verified it through infinite series expansion.

Similarly, understanding derivatives and integrals of arbitrary orders presents a challenge unlike their IO counterparts [98]. However, within the domain of mathematics, these concepts exist. Their formulations naturally arise by extending the principles of IO calculus to incorporate arbitrary orders. Importantly, this extension can include orders that are real and or even complex.

Considering an infinite sequence comprising n-fold integrals and n-th order derivatives, illustrated as follows:

$$\ldots, \int_a^t d\tau_2 \int_a^{\tau_2} f(\tau_1) d\tau_1, \int_a^t f(\tau_1) d\tau_1, f(t), \frac{df(t)}{dt}, \frac{d^2 f(t)}{dt^2}, \ldots \tag{3.1}$$

The sequence in (3.1) can be made continuous by incorporating derivatives and integrals of arbitrary real orders.

3.1.2 Fractional Order Transfer Functions

FO differential and integral equations consist of FO derivatives and integrals. A set of such equations characterise the dynamics of FO system. Consider a Linear Time Invariant (LTI) FO system governed by the subsequent FO ordinary differential equation:

$$\begin{aligned} a_n D^{\alpha_n} y(t) + a_{n-1} D^{\alpha_{n-1}} y(t) + ... + a_0 D^{\alpha_0} y(t) = \\ b_m D^{\beta_m} u(t) + b_{m-1} D^{\beta_{m-1}} u(t) + ... + b_0 D^{\beta_0} u(t) \end{aligned} \tag{3.2}$$

where, $y(t)$ and $u(t)$ represents output and input signals respectively.

Also $a_i, \alpha_i (i = 0, 1, \ldots, n), b_k, \beta_k (k = 0, 1, \ldots, m) \in \mathbb{R}$; $n, m \in \mathbb{N}$. Assuming zero initial conditions and applying the Laplace transform to (3.2), the following Transfer Function (TF) is obtained:

$$\frac{Y(s)}{U(s)} = \frac{b_m s^{\beta_m} + b_{m-1} s^{\beta_{m-1}} + ... + b_0 s^{\beta_0}}{a_n s^{\alpha_n} + a_{n-1} s^{\alpha_{n-1}} + ... + a_0 s^{\alpha_0}} \tag{3.3}$$

where, $Y(s) = \mathcal{L}\{y(t)\}, U(s) = \mathcal{L}\{u(t)\}$

The TF given in (3.3) can represent either a *commensurate* or a *non-commensurate* order system. It qualifies as a *commensurate* order system if there exists a greatest common divisor $q \in \mathbb{R}$ such that $\alpha_i = qe_i, \beta_k = qf_k; e_i, f_k \in \mathbb{Z}$. In such instances, q denotes the commensurate order, which may be rational or irrational.

3.1.3 Oustaloup Approximation Method in Continuous Domain

The TF in FO systems often takes irrational forms, representing the ratio of pseudo polynomials, i.e. polynomials of arbitrary orders. Various methods have been suggested in the literature to approximate them using rational functions [87]. In this research work, Oustaloup approximation is used for approximating fractional functions.

The Oustaloup approximation $F_{Oustaloup}(s)$ for $F(s) = s^{\alpha}$ (where the expected fitting range $[\omega_b, \omega_h]$ is achieved) is obtained as follows:

$$F_{Oustaloup}(s) = K \prod_{k=-N}^{N} \frac{s + z_k}{s + p_k} \tag{3.4}$$

where,

$$z_k = \omega_b \left(\frac{\omega_h}{\omega_b} \right)^{\frac{k+N+\frac{1}{2}(1-\alpha)}{2N+1}}$$
$$p_k = \omega_b \left(\frac{\omega_h}{\omega_b} \right)^{\frac{k+N+\frac{1}{2}(1+\alpha)}{2N+1}}$$
$$K = \omega_h^{\alpha}$$

This method utilises an approximation order of $(2N + 1)$, where N is an odd integer $(N = 1, 2, \dots)$. The generalised Oustaloup method can be employed to derive the approximation $F_{GenOustaloup}(s)$ with an order of $N = 1, 2, \dots$.

$$F_{GenOustaloup}(s) = K \prod_{k=1}^{N} \frac{s + z_k}{s + p_k} \tag{3.5}$$

where,

$$z_k = \omega_b \left(\frac{\omega_h}{\omega_b} \right)^{\frac{2k-1-\alpha}{2N}}$$
$$p_k = \omega_b \left(\frac{\omega_h}{\omega_b} \right)^{\frac{2k-1+\alpha}{2N}}$$
$$K = \omega_h^{\alpha}$$

The Oustaloup method is frequently employed to achieve a satisfactory rational approximation of the FO TF within the selected frequency range, as noted in literature [99].

3.2 Linear Quadratic Integral Controllers

3.2.1 Linear Quadratic Regulator Controller

The LQR controller is a popular technique for designing optimal feedback controllers for linear dynamical systems. The main objective of the LQR controller is to minimise a quadratic cost function representing a trade off between control effort and system performance. The LQR controller requires a linear dynamic model of the system, typically represented by state space equations:

$$\dot{x} = Ax + Bu \tag{3.6}$$
$$y = Cx + Du$$

where, x represents the state vector, u is the control input and y is the output. The cost function to be minimised by the LQR controller is given by:

$$J = \int_0^\infty \left(x^T Q x + u^T R u\right) dt \tag{3.7}$$

where, Q and R are positive semi-definite weighting matrices penalising state deviations and control effort respectively. Continuous time algebraic Riccati equation is solved to obtain the optimal control law:

$$A^T P + PA - PBR^{-1}B^T P + Q = 0 \tag{3.8}$$

where, P is the solution matrix.

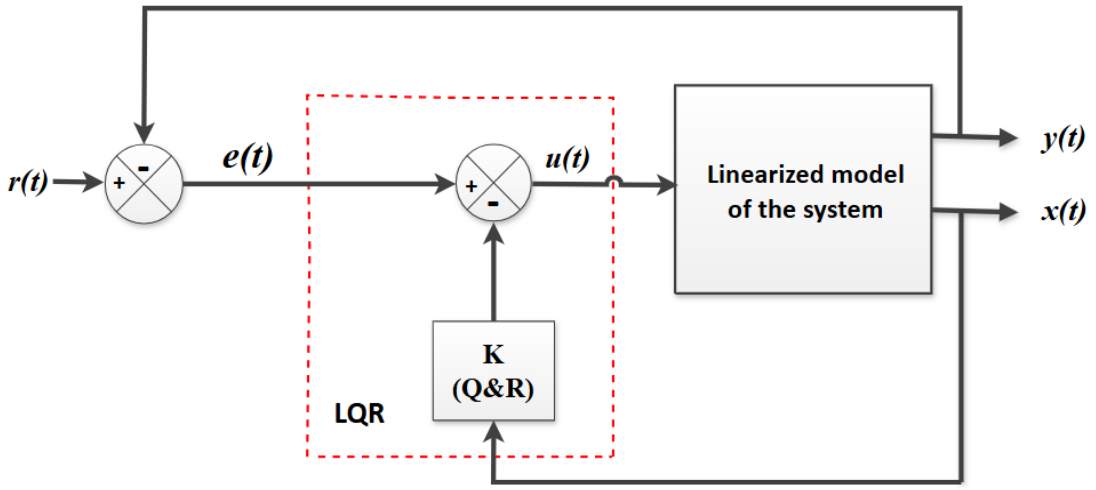

Figure 3.1: Closed loop representation of MIMO system with LQR controller

Fig. 3.1 represents the structure of linearised system with LQR controller in its closed loop configuration. The feedback gain matrix K is calculated as $K = R^{-1}B^T P$ and the control law is given by $u(t) = e(t) - Kx(t)$. The LQR controller provides guaranteed stability for the closed loop system under certain conditions and is inherently robust. Overall, the LQR controller is widely used in various engineering applications due to its simplicity, effectiveness and optimality in controlling linear dynamical systems.

The LQR controller computes the optimal feedback gain matrix based on the system's state space representation and a cost function. Applying this gain matrix to the system's state vector determines the control input that minimises the specified cost function over a

finite time horizon.

3.2.2 Integer Order Linear Quadratic Integral Controller

By combining LQR with integrator, Integer Order LQI (IOLQI) controller is developed. Essentially, IOLQI controller provides the improved system performance by minimising the quadratic cost function similar to the LQR controller and integral action eliminates the steady state error which is absent in the conventional LQR design.

The optimal control law, $u(t) = \frac{K_i}{s} \int e(t)\, dt$ - $Kx(t)$, is derived by solving the associated algebraic Riccati differential equation with an additional integral term. The IOLQI controller requires careful tuning of the weighting matrices Q and R to achieve desired performance specifications such as settling time, overshoot and steady state error.

This controller offers improved tracking performance and robustness to disturbances compared to the LQR controller by adding an integral term. In practical applications, IOLQI controller finds widespread use across diverse engineering disciplines including aerospace, automotive, robotics and industrial automation, where precise control of system dynamics and robust performance are critical. In specific, motion control systems, robotic manipulators and automotive control systems, the system demands precisely tracks the reference inputs. This controller delivers an improved stability, robustness and performance through an ideal integration, making it well suited for managing complex systems subjected to disturbances and uncertainties.

3.3 Fractional Order Linear Quadratic Integral Controller

3.3.1 FOLQI Design

By incorporating integral action, the LQI controller is capable of tracking setpoint changes and rejecting disturbances more effectively, particularly in systems with non-zero steady state error requirements. The integral term ensures that any steady state error is continuously corrected which leads to improve the system performance.

Fig. 3.2 represents the FOLQI controller along with linearised system in closed loop configuration. FOC provide greater flexibility in tuning the controller response due to their additional FO. This allows for better matching of the controller dynamics to the system dynamics resulting in improved performance, faster response times and reduced over-

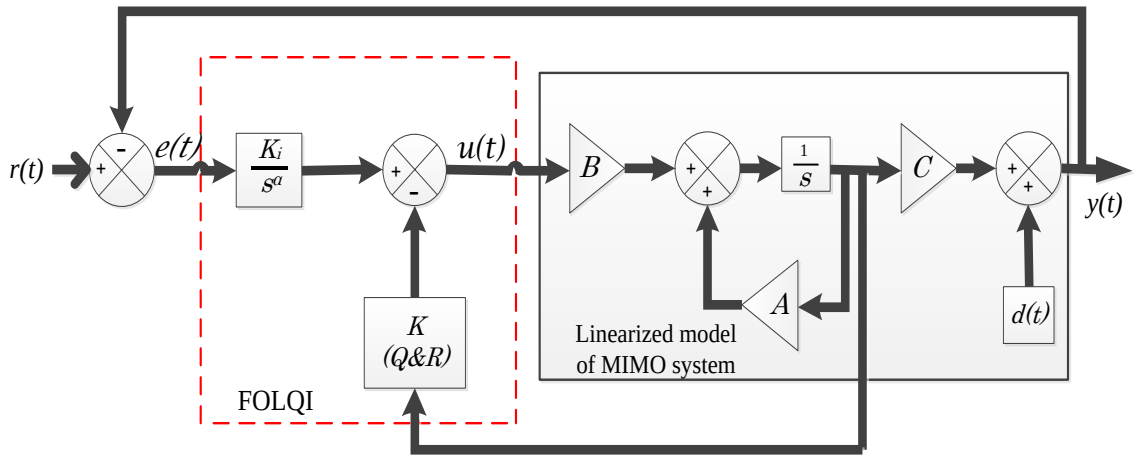

Figure 3.2: Closed loop representation of MIMO system with FOLQI controller

shoot [89]. This can effectively handle systems with time delay as FO introduces memory effects that can compensate the system delay. Time delay in control systems can introduce phase lag that reduce stability and responsiveness. These issues are increased in traditional LQI controllers, as the delay impacts the integrator's ability to correct errors in real time. A detailed study presented in [100] show that FC can manage such lags by providing a more comprehensive range of phase adjustment options. The robustness to time delay is particularly an advantage in control systems where delays are significant such as in networked control systems or systems with long transportation delays [101].

Many physical systems exhibit non integer order dynamics due to the presence of complex behaviours or nonlinearity. FOC offer a more accurate representation of these dynamics compared to traditional IO controllers allowing for better control performance and stability [102]. FOC also can improve system stability by damping out oscillations and resonances more effectively than IO controllers. This is especially beneficial in systems with complex dynamics or resonance phenomena such as flexible structures, electromechanical systems or biological systems [103]. FOC can be adapted and tuned more easily to accommodate changes in system dynamics or operating conditions. This adaptability makes them suitable for applications where the system parameters may vary over time [104]. FOC can potentially reduce energy consumption in control systems by optimising the controller response and limiting excess control action. This can lead to improved efficiency and reduced operating costs in energy intensive applications [105].

The closed loop representation of QTP with the proposed FOLQI controller can be realised as shown in Fig. 3.3. The additional control signal $\Delta u(t)$ required to reject the

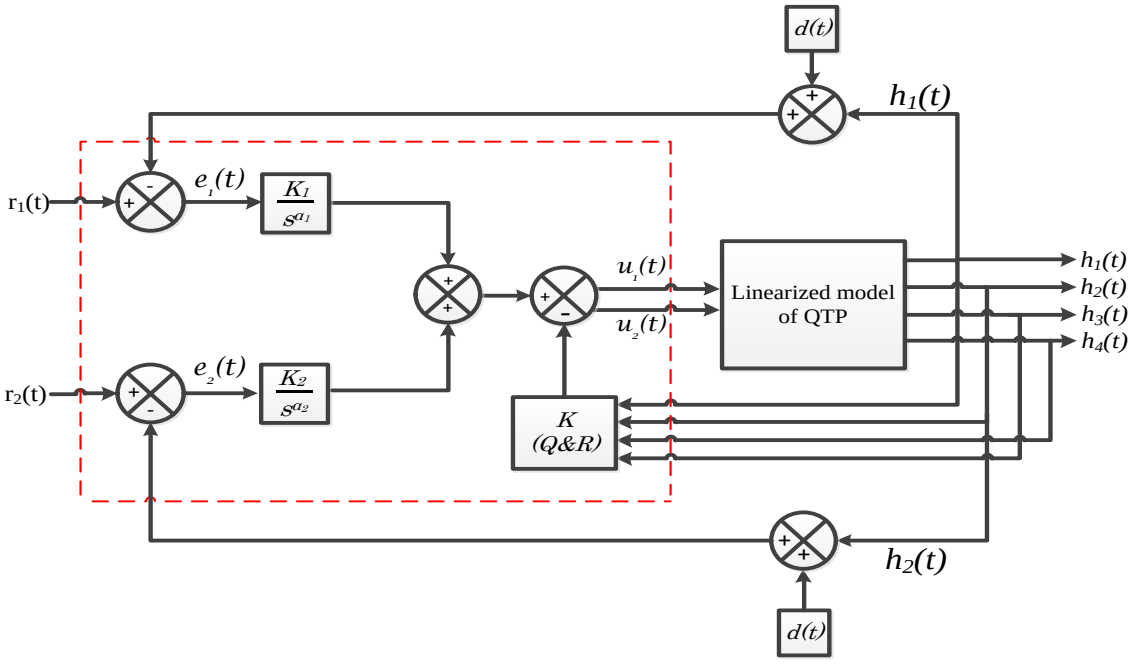

Figure 3.3: QTP with FOLQI controller

continuous load disturbance $d(t)$ is given as:

$$\begin{bmatrix} \Delta u_1 \\ \Delta u_2 \end{bmatrix} = - \begin{bmatrix} K_{11} & K_{12} & K_{13} & K_{14} \\ K_{21} & K_{22} & K_{23} & K_{24} \end{bmatrix} \begin{bmatrix} \Delta h_1 \\ \Delta h_2 \\ \Delta h_3 \\ \Delta h_4 \end{bmatrix} + \begin{bmatrix} \frac{K_{i1}}{s^{\alpha_1}} & 0 \\ 0 & \frac{K_{i2}}{s^{\alpha_2}} \end{bmatrix} \begin{bmatrix} \Delta e_1 \\ \Delta e_2 \end{bmatrix} \tag{3.9}$$

where, $\Delta\, h_1$, $\Delta\, h_2$, $\Delta\, h_3$ and $\Delta\, h_4$ are the change in levels of the tanks T_1, T_2, T_3 and T_4 respectively.

The change in tank levels are due to continuous load disturbance $d(t)$.

3.3.2 Proposed Optimisation Problem

The closed loop representation of QTP with continuous load disturbance controlled by the proposed FOLQI controller is shown in Fig. 3.3. The FOLQI controller has the advantage of using fractionality in the integral part of the conventional LQI controller shown in (3.9). The FOLQI controller parameters are obtained by formulating the optimisation problem and as follows:

Cost function:

$$\underset{\text{(Controller Parameters},Q,R)}{\text{Minimise}} J = \int_0^T (\Delta u_1^2(t) + \Delta u_2^2(t))dt \tag{3.10}$$

subject to constraints:

$$\left.\begin{aligned} &\text{Maximum overshoot / undershoot } (M_p): \\ &|\frac{\Delta h_1}{h_{1o}}| * 100 < \%M_p; |\frac{\Delta h_2}{h_{2o}}| * 100 < \%M_p \\ &\text{Settling time } (t_s): \\ &|\frac{\Delta h_1}{h_{1o}}| * 100 < x\% \text{ of } h_{1o}; |\frac{\Delta h_2}{h_{2o}}| * 100 < x\% \text{ of } h_{2o} \\ &\text{Steady state error } (e_{ss}): \\ &|\frac{\Delta h_1}{h_{1o}}| * 100 < \%e_{ss}; |\frac{\Delta h_2}{h_{2o}}| * 100 < \%e_{ss} \end{aligned}\right\} \tag{3.11}$$

This design provides better controller performance in order to reject the continuous load disturbance $d(t)$ with the desired time domain specifications and minimal control effort at the given operating conditions.

3.4 Summary

This chapter describes the fundamental concepts associated with FC, FOC, LQR, LQI and FOLQI controllers. Additionally, it introduces a method for approximating continuous domain functions using Oustaloups approximation which is particularly beneficial for rationalising FO TF's. It explores the proposed constrained optimisation problem for obtaining the parameters of the proposed FOLQI controller under continuous load disturbance conditions. The feasible values of the constraints are selected by iterating the simulations for different optimisation methods. For deterministic approach, the constraints are limited to (i) maximum overshoot/undershoot (M_p) $= 15\%$ (ii) settling time (t_s) $= 70\ sec$ (iii) maximum steady state error (e_{ss}) $= 3\ \%$ and (iv) $\pm\ 5\%$ of parameter variations. For heuristic methods, the constraints are limited to (i) maximum overshoot/undershoot (M_p) $= 10\%$ (ii) settling time (t_s) $= 70\ sec$ (iii) maximum steady state error (e_{ss}) $= 1\ \%$ and $\pm\ 30\%$ of parameter variations.

Chapter 4

Tuning of FOLQI Controller using Deterministic Approach

4.1 Introduction

Tuning FOC using deterministic approach requires a significant understanding of system dynamics and FC principles. This method typically integrates theoretical analysis, mathematical modelling, optimisation and practical experimentation to attain optimal control performance. Deterministic optimisation stands as a mathematical strategy for identifying the best solution to a given problem within specific constraints, excluding consideration of random variations or uncertainty. Unlike stochastic optimisation methods which accommodate randomness in system dynamics or parameters, deterministic optimisation centres on discovering the most suitable solution grounded on known and constant data [106]. Deterministic optimisation defines the optimisation problem and identify the objective function for maximisation or minimisation along with any required equality/inequality constraints.

The objective function signifies the parameters to optimise such as minimising costs, maximising profits and reducing time for allocating resources. The search space encompasses all feasible solutions to the optimisation problem within the defined constraints. It is used to systematically explore this space to ascertain the solution that optimises the objective function. Applying diverse deterministic optimisation algorithms attempts to navigate the solution space effectively and identify the optimal solution. These algorithms fall into distinct categories based on their search methodologies including gradient based methods, direct search methods, dynamic programming, linear programming, nonlinear programming, integer programming and mixed integer programming [107]. In general, set of constraints introduced in the optimisation problem is complex to solve. In specific, deterministic optimisation techniques are devised to navigate the solution space efficiently while

reducing computational effort which include gradient descent, Newton's method, simplex method, branch and bound, interior point methods etc. Convergence denotes a solution that satisfies predefined termination criteria such as reaching a specified tolerance threshold or maximum iteration count. The solution quality introduced by deterministic optimisation hinges on factors such as selected algorithm, problem formulation, initial conditions and convergence criteria [108] and [109].

4.2 Sequential Quadratic Programming

SQP methods are generally efficient for solving medium to large scale optimisation problems with nonlinear objective functions along with constraints. This method can handle problems with a moderate number of variables and constraints effectively. This algorithm typically converge to a solution relatively faster in specific, for problems with smooth and well behaved objective functions with constraints. With proper initialisation and convergence criteria, SQP methods can often find a solution within a reasonable number of iterations and can handle a wide range of optimisation problems including problems with equality/inequality constraints. They can also accommodate nonlinear and nonconvex objective functions. By approximating the objective function and constraints with quadratic models at each iteration provide a good balance between accuracy and computational efficiency [108].

The SQP method may not guarantee global optimality since it often converge to a local minimum or maximum depending on the problem's nature. With appropriate initialisation and problem setup, SQP algorithms can effectively find high quality solutions and have been successfully applied to a wide range of real world optimisation problems in engineering, economics, finance and other fields. Its ability to handle complex, nonlinear optimisation problems makes it valuable tool for practical decision making and problem solving [110]. The fmincon function in MATLAB is a powerful optimisation tool specifically designed for solving constrained nonlinear optimisation problems. It employs various algorithms to efficiently find the optimal solution including SQP, Interior Point, and Trust Region Reflective algorithms.

In this research work, the simulation uses fmincon function available in the MATLAB tool with SQP algorithm for solving the proposed constrained optimisation problem to obtain the controller parameters of FOLQI. Fig. 4.1 represents the flowchart indicating the sequence of operations performed behind fmincon function for solving the proposed problem.

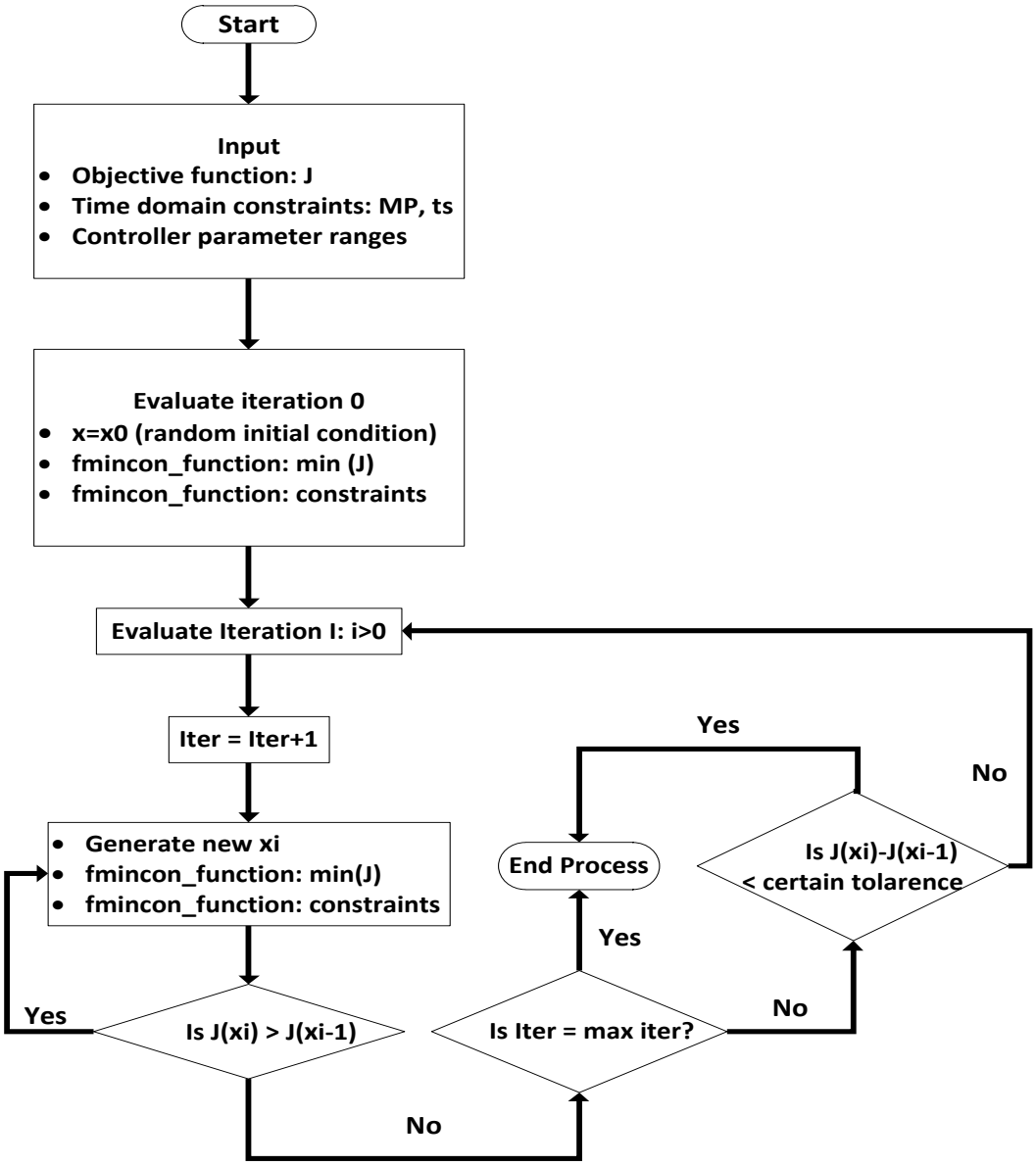

Figure 4.1: Flow chart representing sequence of steps for fmincon function

4.3 Optimisation Specifications

In this section, the controller parameters of the proposed FOLQI controller of QTP are tuned using deterministic method. Subsequently, the controller parameters for IOLQI and LADR controllers are tuned using the same optimisation method with suitable ranges for the controller parameters. The performance of the proposed FOLQI controller is compared with the existing IOLQI and LADR controllers. The details of LADR controller is provided in the Appendix A.

Table 4.1 illustrates the parameters of QTP and its equilibrium points for both minimum and non-minimum phase operating conditions.

Table 4.1: QTP parameters and its equilibrium points

Parameters	Minimum phase	Non-minimum phase
$A_i(cm^2)$, $i = 1$ to 4	176.71	176.71
$a_i(cm^2)$, $i = 1, 2$	2.54	2.54
$a_i(cm^2)$, $i = 3, 4$	1.43	1.43
$h_ieq(cm)$, $i = 1$ to 4	16.47, 16.71, 8.69, 8.09	20.20, 13.33, 22.94, 15.29
k_i, $i = 1, 2$	180.29	186.86
γ_i, $i = 1, 2$	0.60, 0.60	0.45, 0.35
$g(cm/sec^2)$	981	981

The parameters of the FOLQI controller shown in Fig. 3.3 are tuned by solving the proposed optimisation problem using SQP algorithm available in MATLAB [111]. The simulation considers design specifications (i) overshoot M_p constrained to be less than 15% (ii) settling time (t_s) is limited to 70 sec (iii) settling time band of 5% tolerance and (iv) Steady state error constraint which is less than 3%. The bounds used for the controller parameters during optimisation are as follows: Q_{ii} ($i = 1$ to 4) $\in [0.01, 2.5]$, R_{ii} ($i = 1$ and 2) $\in [0.1, 5]$, $K_{i1} \in [0.1, 10]$, $K_{i2} \in [0.1, 10]$, $\alpha_1 \in [0.1, 2]$ and $\alpha_2 \in [0.1, 2]$.

The objective of the proposed FOLQI controller is to ensure the effective rejection of continuous load disturbances while meeting the desired time domain specifications with minimal control effort. To accomplish this optimisation, (i) an Oustaloup approximation [99] is utilised to realise the fractional component of the LQI controller with an approximation order set to 5 and validity across the frequency range $[0.001, 1000] rad/sec$ and (ii) simulation is conducted for 350 sec with a continuous load disturbance of magnitude 1 cm introduced at the 50^{th} sec.

The selected fmincon optimisation algorithm operates according to the sequence pre-

sented in Fig. 4.1. This algorithm runs for 1000 randomly generated initial guesses with the maximum of 100 iterations. A convergence tolerance of 10^{-6} is defined for the cost function resulting in numerous converged controller parameters that meet the desired specifications.

Tables 4.2 and 4.3 display the chosen initial guesses and converged values of the FOLQI controller for minimum phase of QTP. Similarly, Tables 4.4 and 4.5 present the selected initial guesses and converged values of FOLQI controller for the non-minimum phase of QTP. Among the converged parameter sets, FOLQI controller with minimal control effort is selected for the closed loop simulation and is highlighted in Tables 4.3 and 4.5.

To illustrate the superiority of the proposed FOLQI controller, the performances are compared with the conventional IOLQI and LADR controllers. The parameters of the IOLQI and LADR controllers for both minimum and non-minimum phase conditions of QTP are obtained by solving the proposed optimisation problem using the SQP algorithm. For IOLQI controller, the optimisation bounds are chosen as follows: Q_{ii} ($i = 1$ to 4) $\in [0.01, 2.5]$, R_{ii} ($i = 1$ and 2) $\in [0.1, 5]$, $K_{i1} \in [0.1, 10]$, and $K_{i2} \in [0.1, 10]$. For LADR controller, the controller parameters (β_{11} to β_{41}, β_{12} to β_{42}, β_{13} to β_{43}, b_1 to b_4 and r_1 to r_4) presented in [72] are selected and the optimisation bounds for the controller parameters are chosen as follows: β_{ij} ($i = 1$ to 4; $j = 1$ to 3) $\in [0, 150]$, b_i ($i = 1$ to 4) $\in [0, 10]$ and r_i ($i = 1$ to 4) $\in [0, 10]$. From the resulting set of converged solutions, IOLQI and LADR controllers provide the minimum control effort and are given in Tables 4.6 and 4.7 respectively.

Table 4.2: Random initial guesses of FOLQI controller parameters for minimum phase system

S.no	Q_{11}	Q_{22}	Q_{33}	Q_{44}	R_{11}	R_{22}	K_{i1}	K_{i2}	α_1	α_2
1	0.9197	1.8302	0.4455	0.6012	0.8131	0.7667	8.7060	5.8391	0.9100	0.8290
2	1.6378	1.2567	1.0118	0.6100	1.3647	2.4569	2.3507	0.5812	0.8338	0.8517
3	0.2441	0.2025	1.1085	1.5804	4.6767	0.7365	5.7314	4.7470	0.8024	0.8674
4	0.9197	1.8302	0.4455	0.6012	0.8131	0.7667	8.7060	5.8391	0.9100	0.8290
5	0.6973	1.7025	1.6412	0.4149	0.6831	2.5420	9.6015	3.4698	0.9171	0.8448

Table 4.3: Converged values of FOLQI controller parameters for minimum phase system

$S.no$	Q_{11}	Q_{22}	Q_{33}	Q_{44}	R_{11}	R_{22}	K_{i1}	K_{i2}	α_1	α_2	$(J * 10^3)$
1	0.9285	1.8205	0.4402	0.6060	0.7819	0.8117	8.7059	5.8392	0.9074	0.8348	4.0119
2	1.6121	1.7976	1.3507	0.6392	1.9367	1.6321	2.0377	0.2372	0.8338	0.8517	3.3025
3	0.2370	0.1688	1.0956	1.5823	4.6756	0.7695	5.7316	4.7467	0.8220	0.8644	3.9008
4	0.9266	1.8225	0.4413	0.6049	0.7886	0.8020	8.7060	5.8391	0.9144	0.8354	4.0051
5	0.1042	1.7308	1.7500	0.2024	1.6658	2.2580	9.6084	3.4441	0.8938	0.8009	4.0125

Table 4.4: Random initial guesses of FOLQI controller parameters for non-minimum phase system

$S.no$	Q_{11}	Q_{22}	Q_{33}	Q_{44}	R_{11}	R_{22}	K_{i1}	K_{i2}	α_1	α_2
1	1.7639	1.3069	0.2848	1.8260	0.2716	0.2948	9.8868	6.8932	0.8753	0.9009
2	1.9963	1.9985	0.5263	1.9891	0.1261	0.1000	0.5141	0.1376	0.8393	0.8243
3	0.9084	0.8682	0.8606	0.3127	2.1791	3.1064	9.8818	2.2770	0.8708	0.8532
4	1.1079	0.2408	0.6925	1.8008	4.1904	0.1115	6.4381	8.0515	0.8490	0.8128
5	0.6911	1.8544	0.9174	0.4512	4.5339	4.9008	4.4448	1.2001	0.8516	0.8817

Table 4.5: Converged values of FOLQI controller parameters for non-minimum phase system

$S.no$	Q_{11}	Q_{22}	Q_{33}	Q_{44}	R_{11}	R_{22}	K_{i1}	K_{i2}	α_1	α_2	$(J * 10^3)$
1	0.8931	0.7372	1.9876	1.9980	0.2275	0.4175	5.6151	0.5002	0.8753	0.9009	4.2109
2	1.9737	1.9897	0.4951	1.9812	0.4053	0.3233	0.7192	0.1004	0.9768	0.9968	4.1012
3	1.9537	1.4782	1.9105	1.7601	1.3936	2.7536	7.9721	3.1429	0.8708	0.8532	4.5988
4	1.3497	0.1935	1.9878	1.9850	0.1532	0.2685	2.8742	3.0758	0.8490	0.8128	4.1867
5	0.7869	1.8420	0.2456	0.7864	4.4042	4.9829	4.4422	1.1555	0.9146	0.8956	3.9321

Table 4.6: IOLQI controller parameters from the set of converged values resulting minimal controller effort

Operating condition	Q_{11}	Q_{22}	Q_{33}	Q_{44}	R_{11}	R_{22}	K_{i1}	K_{i2}	$(J * 10^3)$
Minimum phase	1.6734	1.0641	0.7957	0.5306	2.7207	1.5185	0.7769	0.9412	3.795
Non-minimum phase	1.6688	1.7685	1.5879	1.7679	0.9602	1.5284	0.8265	0.1952	4.461

Table 4.7: LADR controller parameters from the set of converged values resulting minimal controller effort

Operating condition	Controller parameters
Minimum phase	$\beta_{11} = 27.6941$, $\beta_{21} = 67.8033$, $\beta_{31} = 52.1144$, $\beta_{41} = 38.7474$, $\beta_{12} = 91.4081$, $\beta_{22} = 64.4205$, $\beta_{32} = 60.5146$, $\beta_{42} = 100.8996$, $\beta_{13} = 31.5137$, $\beta_{23} = 83.3163$, $\beta_{33} = 82.9348$, $\beta_{43} = 41.9110$, $b_1 = 0.8493$, $b_2 = 1.8323$, $b_3 = 1.5865$, $b_4 = 1.9194$, $r_1 = 0.6592$, $r_2 = 0.0454$, $r_3 = 0.8506$, $r_4 = 0.9347$
Non-minimum phase	$\beta_{11} = 91.7276$, $\beta_{21} = 28.6553$, $\beta_{31} = 75.7443$, $\beta_{41} = 75.3975$, $\beta_{12} = 38.1065$, $\beta_{22} = 56.8254$, $\beta_{32} = 7.6778$, $\beta_{42} = 5.4896$, $\beta_{13} = 53.1267$, $\beta_{23} = 77.9388$, $\beta_{33} = 93.4077$, $\beta_{43} = 13.0776$, $b_1 = 1.7648$, $b_2 = 4.1558$, $b_3 = 2.9305$, $b_4 = 2.7531$, $r_1 = 9.1728$, $r_2 = 2.8655$, $r_3 = 7.5744$, $r_4 = 7.5398$

4.4 Results and Discussions

4.4.1 Performance under Disturbance Condition

The closed loop simulation for both minimum and non-minimum phase operating conditions of QTP are performed with the converged controller parameters of FOLQI controller under continuous load disturbance $d(t)$. A constant disturbance level of $1\ cm$ (step disturbance) is introduced in $h_1(t)$ and $h_2(t)$ as a continuous load disturbance at $50^{th} sec$ which is shown in Fig. 4.2. To show the superiority of FOLQI controller, the simulation is carried out for QTP with the converged controller parameters of existing IOLQI and LADR controllers. The obtained output responses ($h_1(t)$ and $h_2(t)$) and controller responses ($u_1(t)$ and $u_2(t)$) with FOLQI along with IOLQI and LADR controllers are shown in Figs. 4.3 and 4.4.

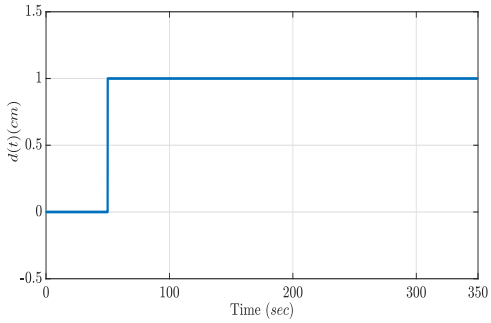

Figure 4.2: Load disturbance signal

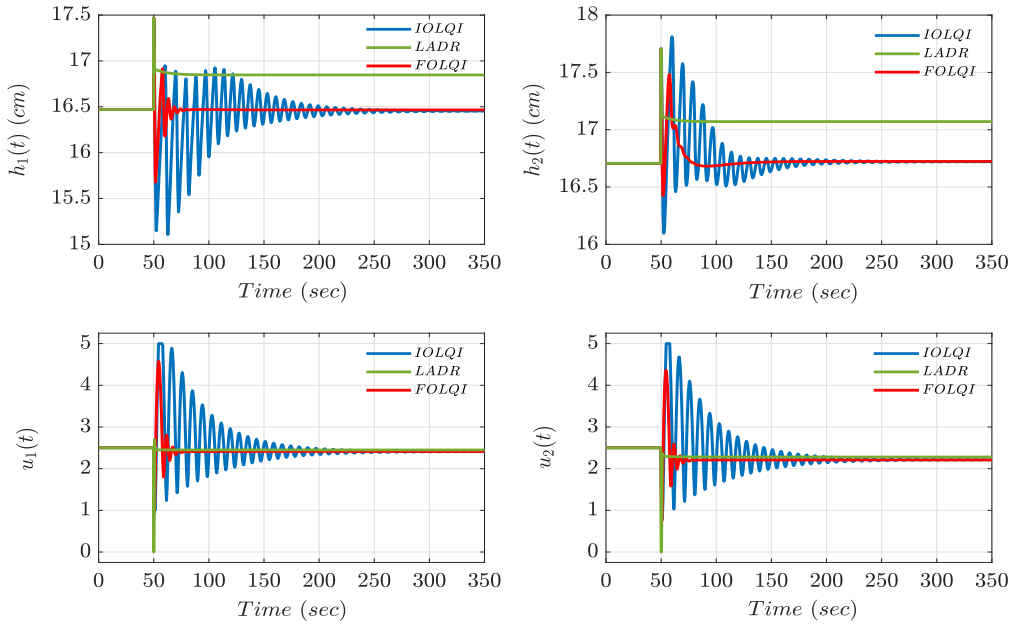

Figure 4.3: Output and controller responses for minimum phase condition under $d(t)$

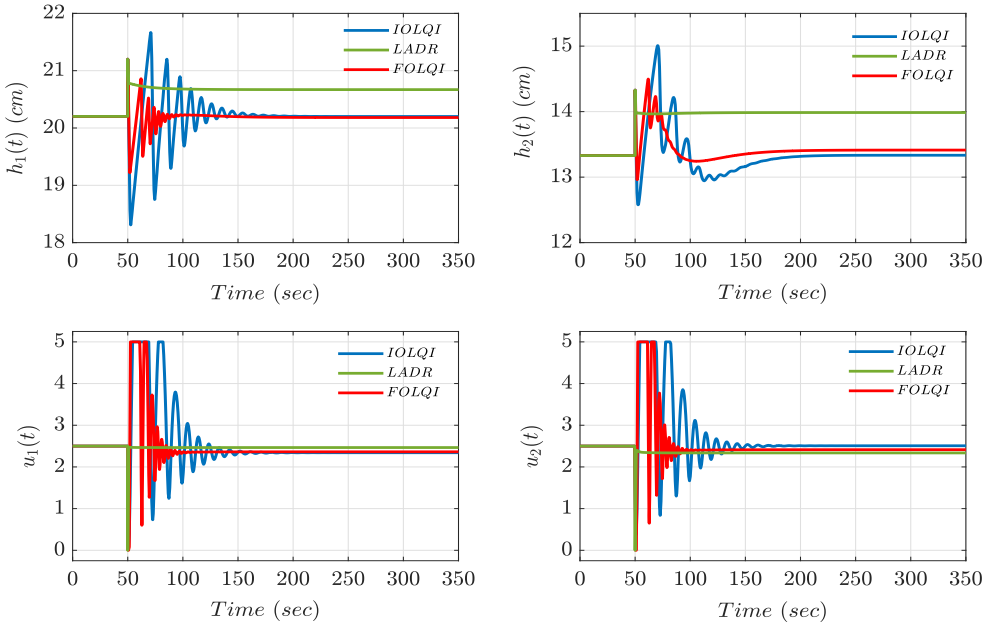

Figure 4.4: Output and controller responses for non-minimum phase condition under $d(t)$

Table 4.8: Time domain performance metrices under $d(t)$ condition for minimum and non-minimum phase systems

Operating condition	Controller	Level of the tank	Overshoot $(\%)$	Settling time (sec)	Steady state error (ess) $(\%)$	Controller effort $(*10^3)$	Effective controller effort $(J * 10^3)$
Minimum phase	IOLQI	h_1 h_2	8.2777 6.6129	32.5670 20.1600	0.1066 0.0775	2.040 1.755	3.795
	LADR	h_1 h_2	6.0725 5.9856	0.1180 0.1060	2.2960 2.1806	2.109 1.871	3.980
	FOLQI	h_1 h_2	6.0720 5.9856	0.2050 0.2780	0.0180 0.0993	1.794 1.509	3.302
Non-minimum Phase	IOLQI	h_1 h_2	9.3713 12.5970	26.3810 36.8130	0.0056 0.0358	2.128 2.333	4.461
	LADR	h_1 h_2	4.9500 7.5023	0 0.4090	2.3150 4.9263	2.133 1.948	4.082
	FOLQI	h_1 h_2	4.9500 8.7694	0 19.7290	0.0963 0.6284	1.932 2.001	3.932

From Figs. 4.3 and 4.4, the time domain performance indices such as maximum overshoot M_p (%), settling time t_s (sec), steady state error e_{ss} (%) and controller effort (J) are measured and listed in Table 4.8. Following are the observations from the obtained performance indices: (i) FOLQI controller requires less controller effort compared to both IOLQI and LADR controllers (ii) FOLQI and IOLQI controllers provide better steady state error compared to LADR controller and (iii) FOLQI and LADR controllers provide better overshoot and settling time compared to IOLQI controller. From the above findings, it is concluded that FOLQI controller provides better performance characteristics than IOLQI and LADR controllers.

4.4.2 Performance under Disturbance and Parameter Uncertainty

The performance of the proposed FOLQI controller is further analysed by introducing $\pm$ 5% uncertainty in the system parameters (A_i and a_i; where $i = 1$ to 4) along with $d(t)$ at 50^{th} sec. The performance of the FOLQI controller is compared with the existing IOLQI and LADR controllers. The output responses ($h_1(t)$ and $h_2(t)$) are shown in Fig. 4.5 for minimum and Fig. 4.6 for non-minimum phase operating mode of QTP. The corresponding controller responses are shown in Figs. 4.7 and 4.8 for minimum and non-minimum phase operating mode respectively. From these figures, the time domain performance indices such as maximum overshoot (%), settling time (sec), steady state error (%) and controller effort (J) are obtained and listed in Tables 4.9 and 4.10 respectively.

Following are the inferences from the obtained performance indices: (i) IOLQI and LADR controllers require more controller effort in comparison to FOLQI controller (ii) LADR controller provides larger steady state error compared to FOLQI and IOLQI controllers and (iii) IOLQI controller underperforms in terms of overshoot and settling time compared to FOLQI and LADR controllers. From the above insights, it is found that FOLQI controller outperforms IOLQI and LADR controllers in the presence of parameter uncertainty and disturbance conditions.

Remarks [1]: It is noted that the introduction of parameter variations beyond $\pm 5\%$, LADR controller fails to meet the required specifications and hence simulation is limited to $\pm 5\%$.

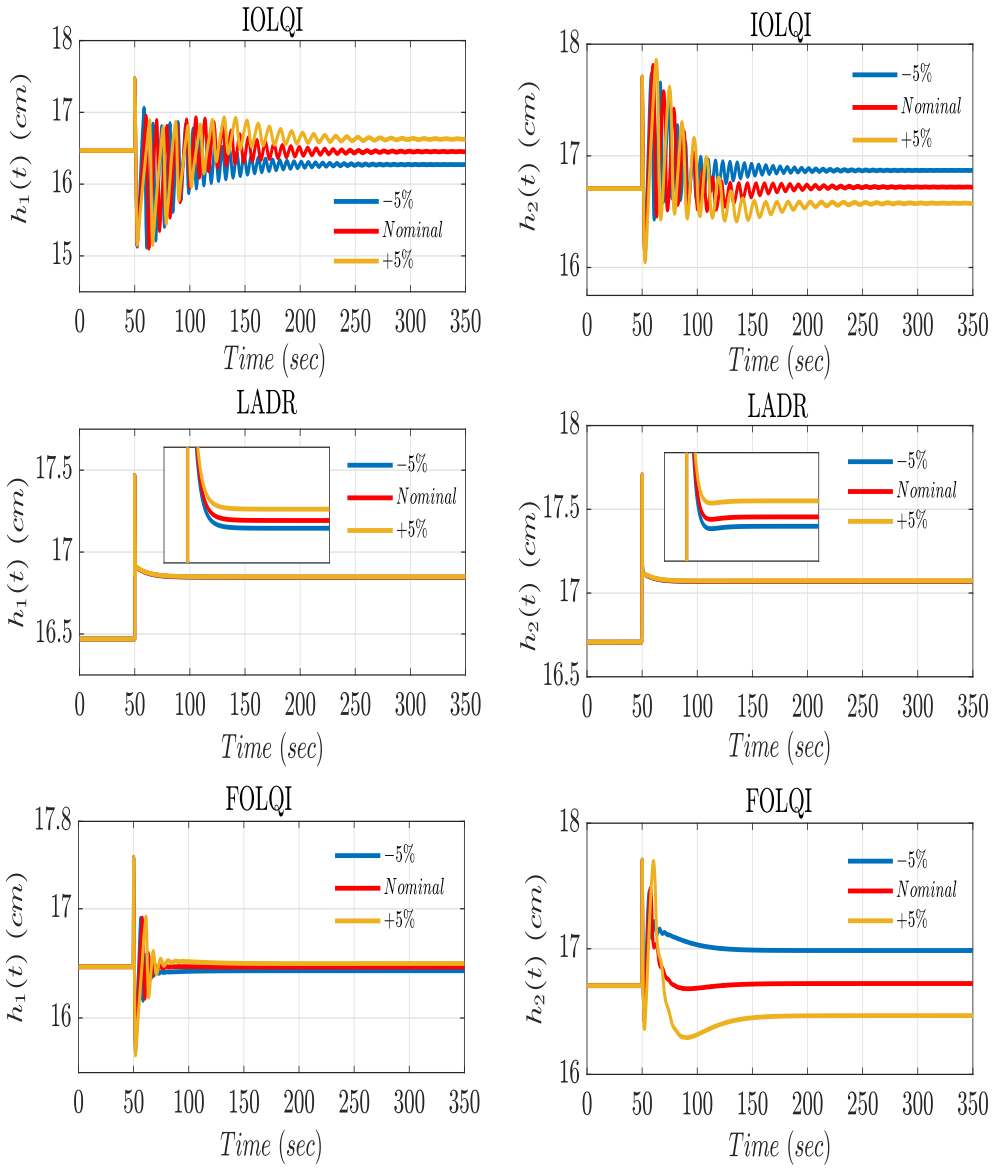

Figure 4.5: Output responses under $d(t)$ and parameter variations for minimum phase condition

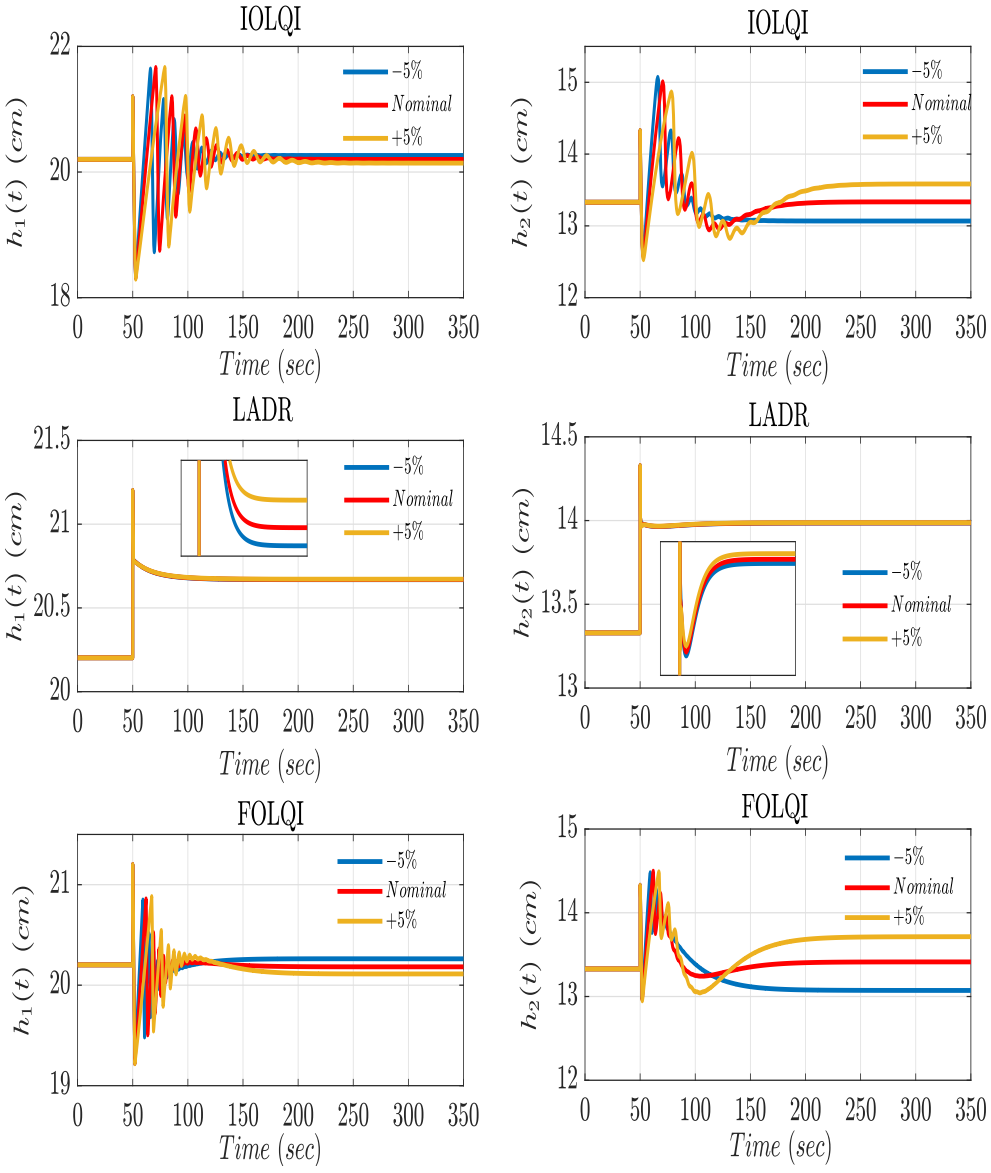

Figure 4.6: Output responses under $d(t)$ and parameter variations for non-minimum phase condition

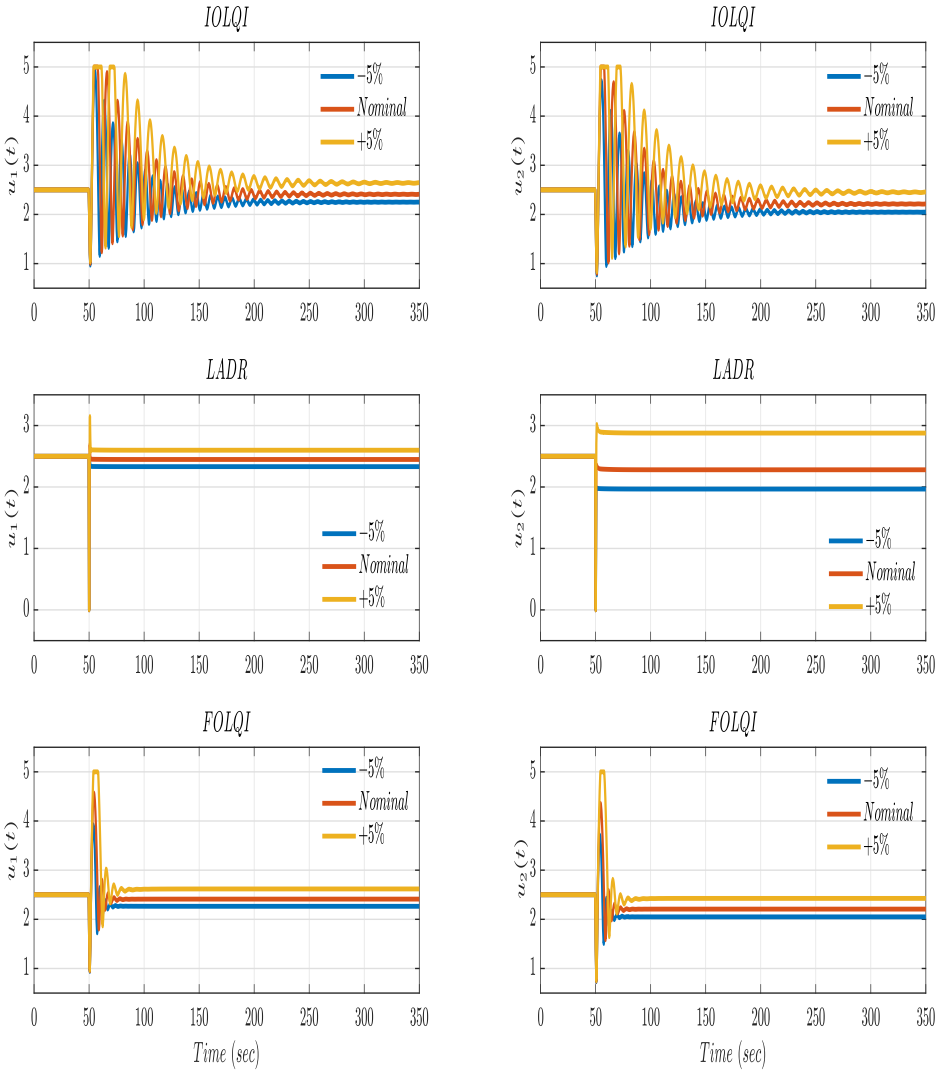

Figure 4.7: Controller responses under $d(t)$ and parameter variations for minimum phase condition

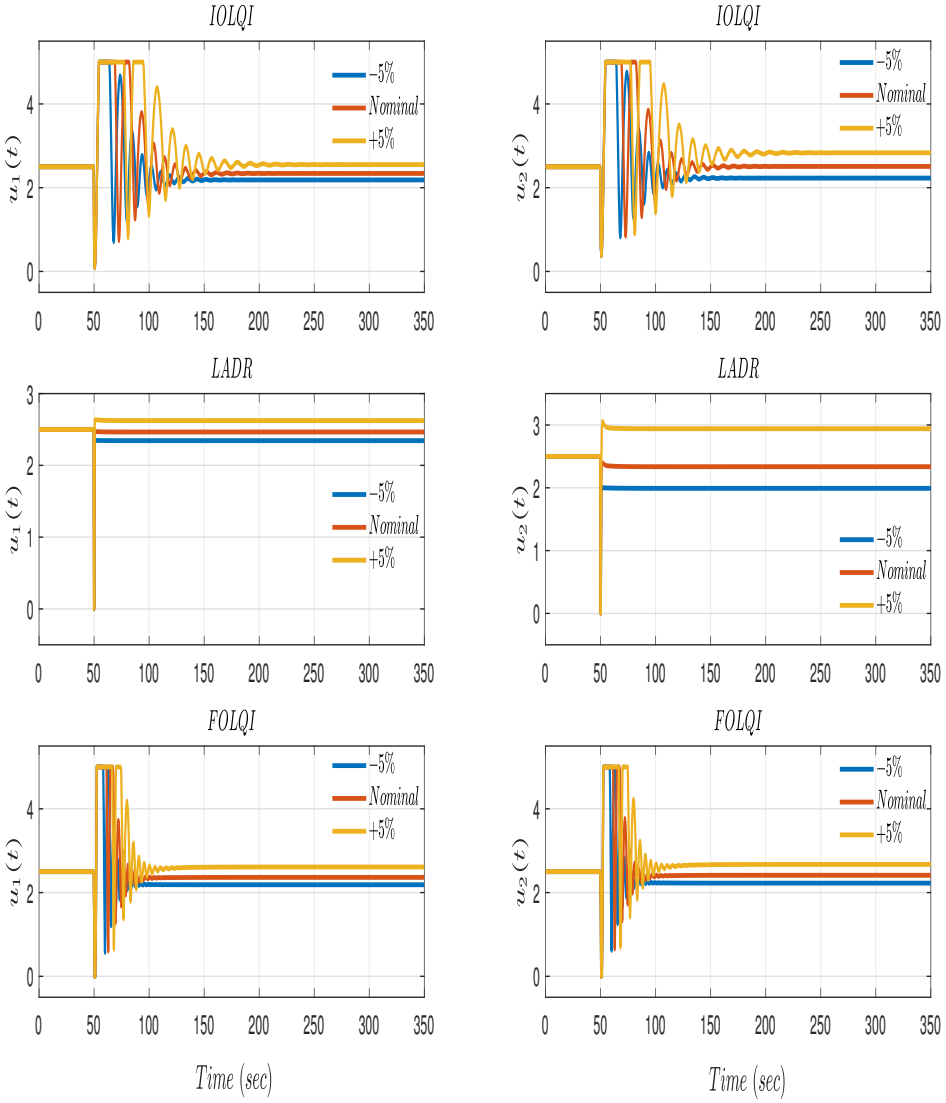

Figure 4.8: Controller responses under $d(t)$ and parameter variations for non-minimum phase condition

Table 4.9: Time domain performance metrices under $d(t)$ and parameter uncertainty for minimum phase condition

Controllers	Parameter variation	Level of the tank	Overshoot $(\%)$	Settling time (sec)	Steady state error (ess) $(\%)$	Controller effort $(*10^3)$	Effective controller effort $(J * 10^3)$
IOLQI	-5%	h_1	8.1929	34.8860	1.1906	1.703	3.132
		h_2	6.1403	17.1890	0.9752	1.429	
	Nominal	h_1	8.2777	32.5670	0.1066	2.040	3.795
		h_2	6.6129	20.1600	0.0775	1.753	
	$+5\%$	h_1	7.9717	29.7610	0.9649	2.560	4.824
		h_2	6.8839	25.8410	0.7878	2.263	
LADR	-5%	h_1	6.0729	0.1180	2.2879	1.941	3.413
		h_2	5.9856	0.1060	2.1729	1.472	
	Nominal	h_1	6.0725	0.1180	2.2960	2.109	3.980
		h_2	5.9856	0.1060	2.1806	1.871	
	$+5\%$	h_1	6.0721	0.1180	2.3079	2.338	5.132
		h_2	5.9856	0.1060	2.1939	2.795	
FOLQI	-5%	h_1	6.0720	0.2100	0.2231	1.566	2.852
		h_2	5.9856	0.2920	1.6713	1.286	
	Nominal	h_1	6.0720	0.2050	0.0180	1.794	3.302
		h_2	5.9856	0.2780	0.0993	1.509	
	$+5\%$	h_1	6.0720	0.2000	0.1807	2.167	4.043
		h_2	5.9856	11.7360	1.4299	1.876	

Table 4.10: Time domain performance metrices under $d(t)$ and parameter uncertainty for non-minimum phase condition

Controllers	Parameter variation	Level of the tank	Overshoot $(\%)$	Settling time (sec)	Steady state error (ess) $(\%)$	Controller effort $(*10^3)$	Effective controller effort $(J * 10^3)$
IOLQI	-5%	h_1	9.2972	21.1750	0.3061	1.752	3.572
		h_2	13.0600	29.7010	1.9642	1.819	
	Nominal	h_1	9.3713	26.3810	0.0056	2.128	4.461
		h_2	12.5970	36.8130	0.0358	2.333	
	$+5\%$	h_1	9.4515	34.8930	0.2974	2.681	5.704
		h_2	11.5327	47.6580	1.9086	3.024	
LADR	-5%	h_1	4.9500	0	2.3094	1.960	3.461
		h_2	7.5023	0.4190	4.9193	1.501	
	Nominal	h_1	4.9500	0	2.3150	2.133	4.082
		h_2	7.5023	0.4090	4.9263	1.948	
	$+5\%$	h_1	4.9500	0	2.3235	3.376	5.280
		h_2	7.5023	0.4020	4.9358	2.904	
FOLQI	-5%	h_1	4.9500	0	0.2981	1.621	3.293
		h_2	8.6241	19.6690	1.9282	1.672	
	Nominal	h_1	4.9500	0	0.0963	1.932	3.932
		h_2	8.7694	19.7290	0.6284	2.001	
	$+5\%$	h_1	4.9500	0	0.4456	2.409	4.906
		h_2	8.7110	26.4800	2.8879	2.497	

4.4.3 Stability Analysis

In this section, the stability analysis of QTP with the proposed FOLQI controller is studied using frequency response. Figs. 4.9 and 4.10 show the open loop frequency responses of various control loops of QTP. From these figures (i) phase crossover frequencies and gain margins are found to be ∞ for all control loops and (ii) obtained phase margins and gain crossover frequencies for all control loops are measured and given in Table 4.11. The results indicates that all four control loops are stable with enough stability margins. Similarly, Table 4.12 show the open loop frequency responses of all the control loops of QTP tuned using IOLQI and LADR controllers respectively and it shows that FOLQI controller outperforms IOLQI and LADR controllers in terms of phase margin measures for stability conditions.

Remarks [2]: From Section 4.4.2 it is noted that FOLQI controller provided better time response characteristics with minimum control effort compared with IOLQI and LADR controllers for both minimal and non-minimal phase conditions. Hence, Bode response of open loop TF with FOLQI controller is only plotted under minimum and non-minimum phase conditions. However, the stability details of IOLQI and LADR controllers are shown in Table 4.12 for the reference.

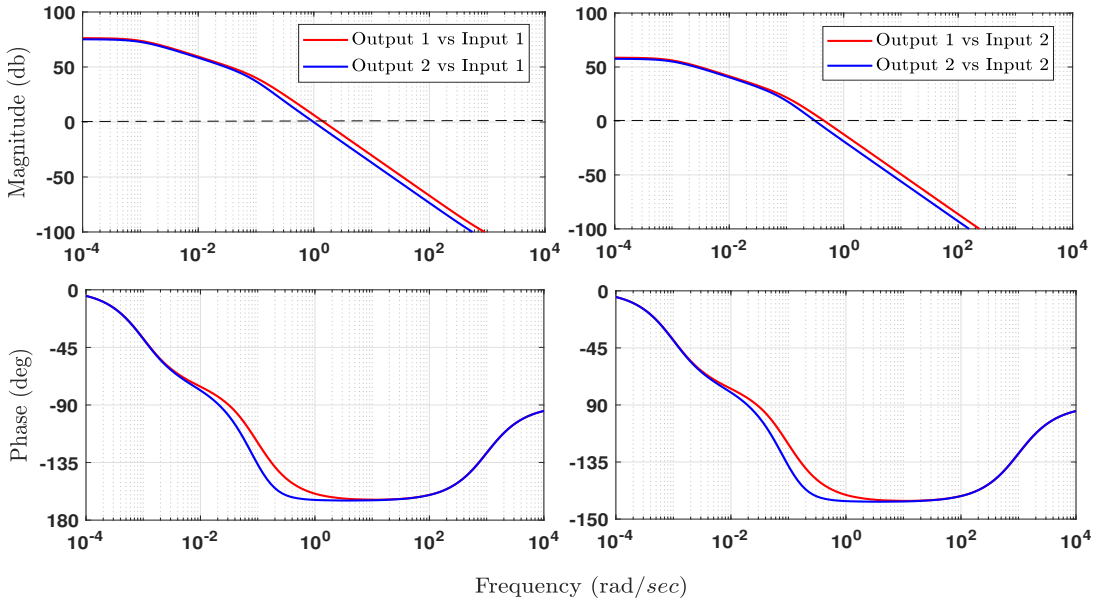

Figure 4.9: Bode response of FOLQI controller for minimum phase condition

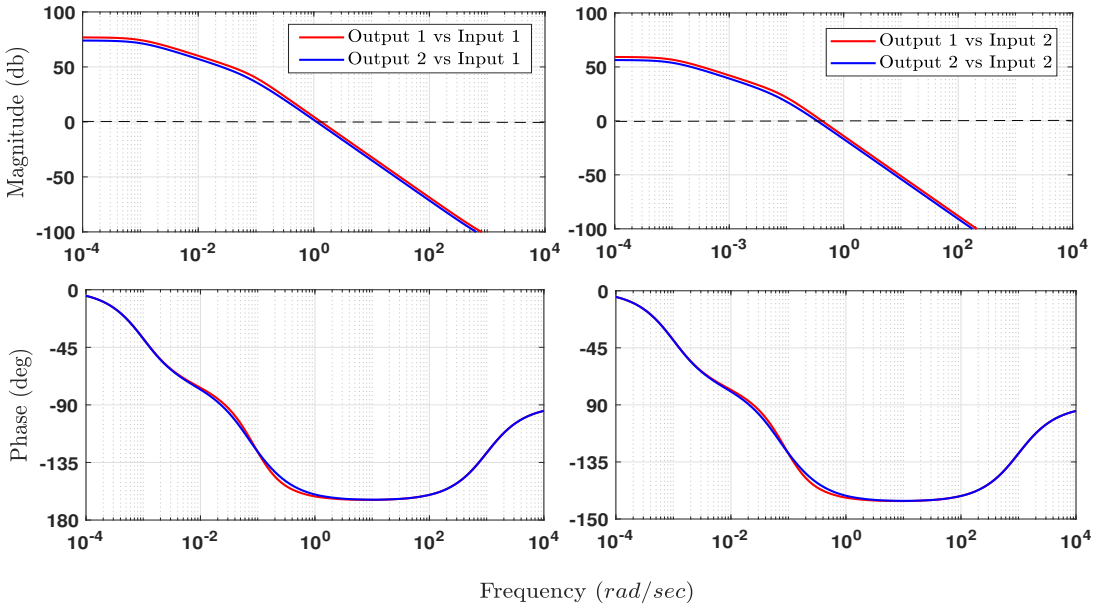

Figure 4.10: Bode response of FOLQI controller for non-minimum phase condition

Table 4.11: Stability analysis of FOLQI controller for minimum and non-minimum phase condition

Controller / Operating condition	Loop interaction		Gain crossover frequency (rad/sec)	Phase margin (deg)
	Input	Output		
FOLQI / Minimum	1	1	1.490	18.9
	1	2	0.989	15.8
	2	1	0.459	25.6
	2	2	0.318	17.7
FOLQI / Non-minimum	1	1	1.340	17.6
	1	2	1.120	19.4
	2	1	0.418	21.9
	2	2	0.345	27.3

Table 4.12: Controller performance of IOLQI and FOLQI controller under $d(t)$ and parameter uncertainty conditions

Controller / Operating condition	Loop interaction		Gain crossover frequency (rad/sec)	Phase margin (deg)
	Input	Output		
IOLQI / Minimum	1	1	0.690	4.57
	1	2	0.701	5.66
	2	1	0.759	4.16
	2	2	0.772	5.15
IOLQI / Non-minimum	1	1	0.610	8.39
	1	2	0.554	8.45
	2	1	0.292	17.00
	2	2	0.268	18.90
LADR / Minimum	1	1	6.090	0.49
	1	2	6.200	0.69
	2	1	7.860	0.38
	2	2	8.000	0.54
LADR / Non-minimum	1	1	1.880	2.91
	1	2	1.690	3.14
	2	1	1.590	3.44
	2	1	1.430	3.71

4.5 Summary

This section introduces SQP algorithm for tuning FOLQI controller parameters to accommodate both minimum and non-minimum phase operating conditions of QTP. The FOLQI controller is tuned to reject continuous load disturbances effectively while adhering to desired time domain specifications with minimal control effort. Extensive simulation studies are conducted under disturbance, parameter uncertainty conditions and stability analysis to validate the performance of the proposed FOLQI controller with the results obtained from IOLQI and LADR controllers. Even though IOLQI and FOLQI controllers have better steady state error performance, there exists minor steady state error due to system nonlinearity and disturbances as referred in [112] and [113].

Chapter 5

Tuning of FOLQI Controller using Heuristic Approach

5.1 Introduction

Optimisation using heuristic algorithms involves applying problem solving approaches that rely on intuition, experience or thumb rule rather than systematic and deterministic methods. Unlike classical optimisation techniques that guarantee finding the optimal solution, heuristic algorithms provide efficient but not necessarily optimal solutions. Heuristic algorithms can efficiently find near optimal solutions, particularly for large scale and complex optimisation problems by exploring promising regions of the solution space and offer computational efficiency by avoiding extensive search techniques [114]. These algorithms are versatile and adaptable to different types of optimisation problems including those with nonlinear objectives, discrete decision variables and complex constraints.

Heuristic algorithms exhibit robustness to uncertainties, noise and changes in problem parameters. They can handle real world optimisation problems where exact information may not be available or incomplete [115]. Many heuristic algorithms perform global search efficiently by exploring diverse regions of the solution space. While they may not guarantee to find the global optimum, they often converge to satisfactory solutions that are close to the global optimum [116].

These algorithms find applications across various fields including engineering, finance, logistics and healthcare. They provide versatile tools for solving optimisation problems in diverse domains [117]. There is a wide variety of heuristic algorithms, each suited to different types of optimisation problems. Common heuristic algorithms include genetic algorithms, simulated annealing, PSO, Ant Colony Optimisation (ACO), tabu search, CS, APSO, FF and various evolutionary strategies.

5.2 Heuristic Algorithms

In this section, nature inspired meta heuristic based algorithms - CS, APSO and FF are used to solve the proposed constraint optimisation problem given in Section 3.3.2.

5.2.1 CS Algorithm

CS algorithm effectively explore the solution space due to its combination of random walk and Levy flights which allow rapid convergence to promising regions. It demonstrates strong global optimisation capabilities often finding near optimal solutions for various optimisation problems. It is easy to implement and adapt different problem domains making it suitable for various control applications and show robustness to noise and uncertainties in optimisation problems which enable reliable performance in the real world scenarios [118].

The CS algorithm [119] introduced by Xin-She Yang in 2009, is inspired by the obligate brood parasitic behaviour of cuckoo birds and the levy flight behaviour observed in some birds and fruit flies. In this algorithm, the process of egg laying by cuckoo birds in the nests of other host birds is considered. The eggs that successfully hatch are selected as the best and are passed on to the next generation. This behaviour is mathematically represented using the levy flight mechanism which describes the stochastic movement pattern of foraging animals. When a host bird discovers a foreign egg in its nest, it either ejects the egg or abandons the nest leaving the foreign egg behind which typically fails to hatch. Based on this process, the operation of CS algorithm is sequenced in three stages. The detailed sequence of the process is shown in Fig. 5.1 and the procedure as follows:

1. A cuckoo lays an egg in one randomly selected nest at a time.
2. The nest with the highest quality egg is deemed successful and is carried forward to the next generation. The best egg or solution from the current generation is replaced by the best egg or solution from the next generation.
3. The number of host nests (n) is predetermined and the probability of a host bird encountering a foreign egg (p_a) is typically assumed to be 0.25.

The solution generated by the levy flight formulation is expressed as:

$$x_i(t+1) = x_i(t) + \mu \oplus + Levy(\lambda) \tag{5.1}$$

where, (μ, $\oplus$ and λ) represents step size, entry wise multiplication and Levy distribution parameter respectively.

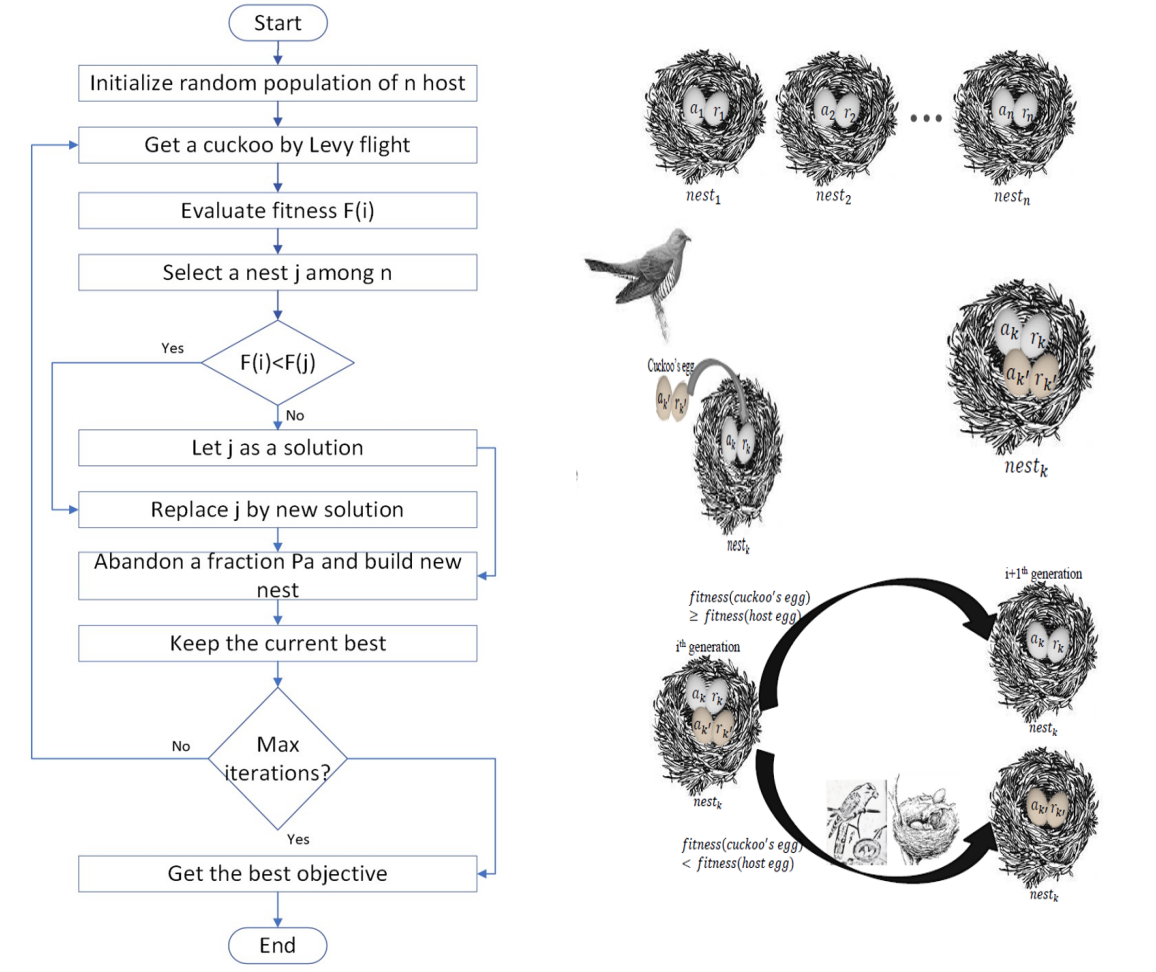

Figure 5.1: Flowchart and process sequence of CS algorithm

The pseudocode of CS algorithm is given as follows:

Algorithm 5.1: CS algorithm

Require: (i) Objective function: J (ii) Inequality constraints: $\%M_p$, t_s and e_{ss}, (iii) Maximum number of iterations: T, and (iv) Probability of encountering a new solution: p_a

1: Generate an initial population of n host nests x_i, where $i = 1, 2, ..., n$
2: While $t \leq T$ do
3: Randomly select a cuckoo using Levy flights
4: Evaluate its objective function $f(x_i(t))$ along with the inequality constraints
5: Randomly choose one nest among the n nests (denoted as j)
6: If $F_i > F_j$ then
7: Replace the nest j with the new solution
8: End if loop
9: Abandon a fraction (p_a) of worse nests and build new ones
10: Retain the best solutions
11: Rank the solutions and determine the current best
12: Increment t by 1
13: End while loop
14: Post-process results using the best solution

5.2.2 APSO Algorithm

APSO algorithm dynamically adjusts its parameters during optimisation by improving convergence speed and solution quality. It balances acceleration and ranges effectively allowing for thorough solution space exploration while exploiting promising regions. APSO's adaptability makes it well suited for optimisation problems in dynamic or uncertain environments, where traditional optimisation methods may struggle [120].

The PSO algorithm introduced by Kennedy and Eberhart in 1995 [121], draw inspiration from the collective behaviour observed in fish and bird swarms during foraging. In this algorithm, each individual bird referred as a particle navigates through the search space adjusting its flight characteristics based on the proximity of other particles to potential prey.

APSO is an updated version of PSO distinguished by deviating from the conventional approach of computing individual bests and this introduces randomness into the initial guesses leading to enhanced accuracy and faster convergence [122]. The detailed sequence of the process and its procedure is shown in Fig. 5.2 and as follows:

During each iteration of the algorithm, velocity vectors are computed and corresponding positions are updated. The updated velocity and position vectors are denoted as $v_i(t+1)$

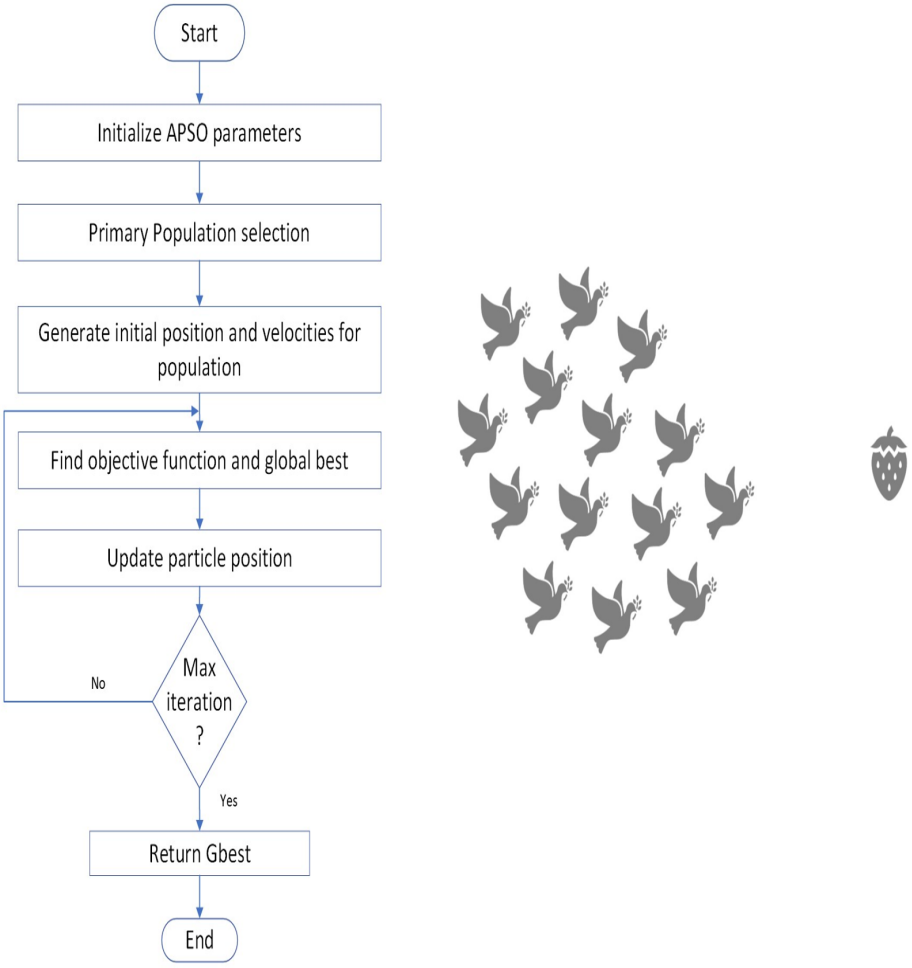

Figure 5.2: Flowchart and process sequence of APSO algorithm

and $x_i(t+1)$ and expressed as follows:

$$v_{i(t+1)} = v_{i(t)} + \lambda(g^* - x_i(t)) + \mu \in_t \tag{5.2}$$

$$x_{i(t+1)} = x_{i(t)} + v_{i(t+1)} \tag{5.3}$$

where, λ and μ are the acceleration constants, g^* is the global best value, x_i represents position of i^{th} particle at time 't' and $\in_t$ is drawn from N [0,1].

The pseudocode of APSO algorithm is given as follows:

Algorithm 5.2: APSO algorithm

Require: (i) Objective function: J (ii) Inequality constraints: $\%M_p$, t_s, and e_{ss}, and (iii) Maximum number of iterations: T

1: Generate an initial population of N particles x_i, where $i = 1, 2, ..., N$
2: While $t \leq T$ do
3: For $i = 1$ to N do
4: Update the velocity vector
5: Update the position vector
6: Evaluate objective functions at the new locations x_i^{t+1} along with constraints
7: Determine the current best
8: End for loop
9: Find the global best
10: Increment t by 1
11: End while loop
12: Post-process results using the best solution

5.2.3 FF Algorithm

The FF algorithm demonstrates strong global search capabilities, efficiently exploring the solution space and converging towards the global optimum. Its easiness of understanding and implementation makes it accessible to practitioners and researchers across various disciplines. FF algorithm shows the robust performance across different optimisation problems which includes continuous, discrete and dynamic optimisation scenarios [123].

The FF algorithm proposed by Xin-She Yang in 2008 [124], draw attention and inspired from the flashing behaviour exhibited by fireflies of a particular species. The behavioural characteristics of fireflies is studied and the process sequence is presented in algorithm form. It is as follows:

1. Fireflies are genderless and are drawn to one another based on the brightness of their emitted light.

2. Fireflies with lower light intensity are attracted to those emitting higher light intensity.

3. The brightness of light increases as fireflies approach each other.

If two fireflies emit the same level of brightness, they move randomly without mutual attraction. The relative motion between a less bright firefly and brighter one is described as

follows:

$$x_{i(t+1)} = x_{i(t)} + \beta_0 e^{-\gamma r_{ij}^2}(x_j(t) - x_i(t)) + \mu_t \in_i (t) \tag{5.4}$$

where, β_0 is the brightness of the firefly, γ indicates light absorption co-efficient, r represents euclidean distance between fireflies and it is given as: $r_{ij} = \sqrt{(x_i - x_j)^2}$, μ(t) is the random parameter and $\in_i$(t) is a vector of random numbers which belongs to Gaussian or random distribution at time t.

The detailed sequence of the process and its procedure is shown in Fig. 5.3. The corresponding pseudocode of FF algorithm is given as follows:

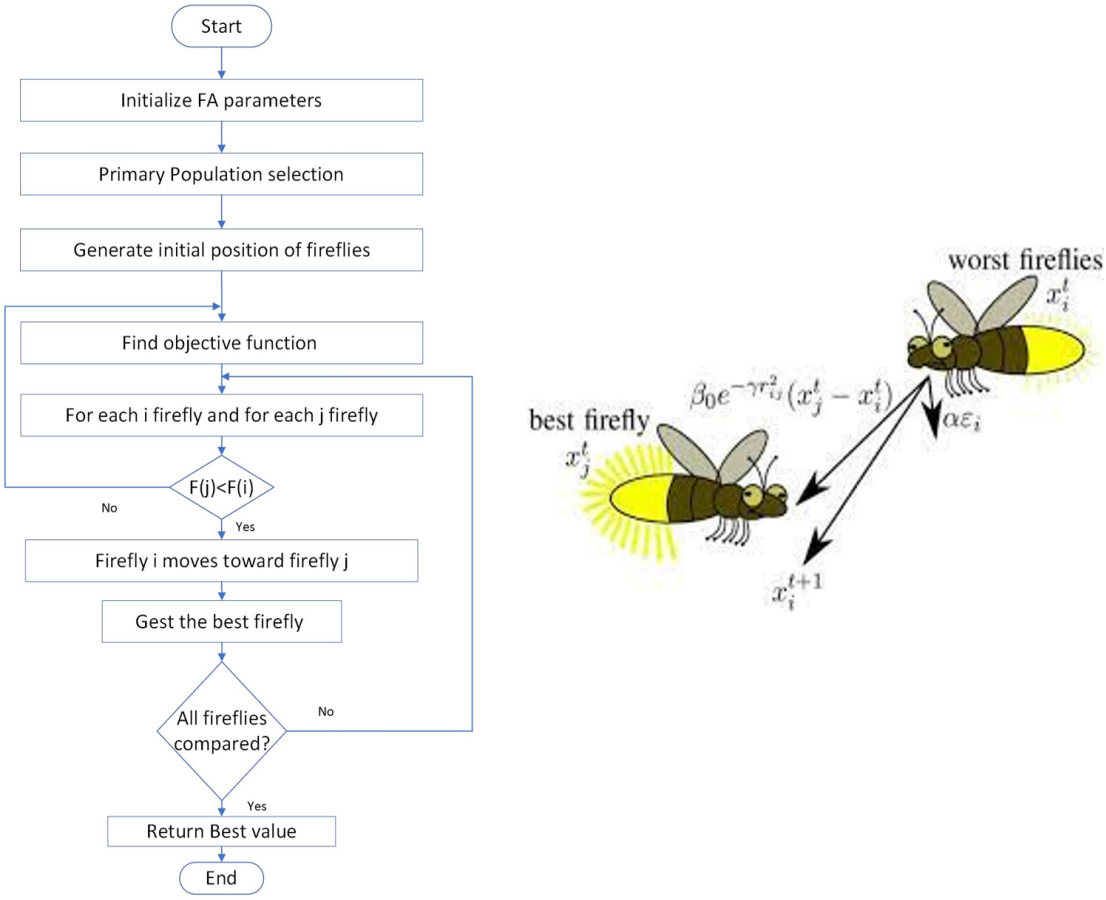

Figure 5.3: Flowchart and process sequence of FF algorithm

Algorithm 5.3: FF algorithm

Require: (i) Objective function: J, (ii) Inequality constraints: $\%M_p$, t_s, and e_{ss} and (iii) Maximum iterations: $Max_{iterations}$

1: Generate an initial population of fireflies X_i (where $i = 1, 2, ..., n$)
2: Determine the light intensity I_i at X_i using the objective function $f(X_i)$
3: While $t < Max_{iterations}$
4: For $i = 1$ to n, for all n fireflies
5: For $j = 1$ to n, for all n fireflies
6: If $I_j > I_i$, move firefly i towards firefly j in d-dimension
7: End if
8: Evaluate new solutions and update light intensity
9: End for loop for j
10: End for loop for i
11: Rank the fireflies and find the best
12: End while loop
13: Post-process results and visualization

5.3 Optimisation and its Specifications

In this section, heuristic algorithms CS, APSO and FF are used to tune the parameters of FOLQI controller and subsequently compare the results with IOLQI controller. To implement FOLQI controller, the fractional element in the integrator is approximated to an integer order using the Oustaloup approximation of order 5 over the frequency range [0.001, 1000] rad/sec [99]. The closed loop simulation is conducted in the presence of continuous load disturbance $d(t) = 1$ cm introduced at $t = 50^{th}$ sec. The parameters and equilibrium points of QTP for both minimum and non-minimum phase operating conditions are detailed in Table 4.1.

The parameters of the FOLQI controller are adjusted to eliminate continuous load disturbance while minimising controller effort and adhering to specified constraints: (i) less than 10% in $\%M_p$ (ii) less than 70 seconds in t_s (with a tolerance band of $\pm 3\%$) and (iii) less than 1% in e_{ss}. The bounds for the controller parameters are defined as follows: Q_{ii} ($i = 1$ to 4) within the range of $[0.01, 2.5]$, R_{ii} ($i = 1$ and 2) within $[0.1, 5]$, K_{i1} within $[0.1, 10]$, K_{i2} within $[0.1, 10]$, α_1 within $[0.1, 2]$ and α_2 within $[0.1, 2]$. For optimisation, the parameters of the CS, APSO and FF algorithms are presented in Table 5.1 are used with a convergence tolerance of 10^{-6}. Similarly, these algorithms are used to tune the parameters of the existing IOLQI controller. The converged values of both FOLQI and IOLQI controllers satisfying the specified time domain specifications with minimal control effort for

Table 5.1: Parameters of CS, APSO and FF algorithms

Heuristic algorithm	Parameters
CS	n=25 p_a=0.25 T=100
APSO	n=25 T=100
FF	n=100 T=100 $\mu = 0.3$ $\beta = 0.3$ $\gamma = 1$

both minimum and non-minimum phase operating conditions are presented in Table 5.2.

The convergence of the objective function J using the CS, APSO and FF algorithms for both IOLQI and FOLQI controllers under minimum and non-minimum phase operating conditions of QTP are shown in Figs. 5.4 and 5.5. Table 5.3 provide information on convergence epochs and statistical parameters (mean and standard deviation) for CS, APSO and FF algorithms of both IOLQI and FOLQI controllers. It is observed that FF algorithm exhibits (i) faster convergence epochs for FOLQI minimum, IOLQI minimum and non-minimum conditions compared to CS and APSO algorithms (ii) lower statistical parameter - Mean compared to CS and APSO algorithms and (iii) improved statistical parameter - Standard Deviation for minimum phase systems. Hence, it is inferred that FF algorithm outperforms the CS and APSO algorithms.

Table 5.2: Converged controller parameters of IOLQI and FOLQI controllers

Heuristic algorithm	Controller/ Operating condition	Q_{11}	Q_{22}	Q_{33}	Q_{44}	R_{11}	R_{22}	K_{i1}	K_{i2}	α_1	α_2
CS	IOLQI / Minimum	2.4409	0.9294	0.0743	1.5406	2.8543	1.6239	4.9467	0.5440	-	-
	IOLQI / Non-minimum	2.4266	1.1754	0.1141	2.3565	4.9639	3.8190	1.0003	1.0205	-	-
	FOLQI / Minimum	0.4431	0.3027	0.4434	1.5722	4.2253	2.5994	1.7411	7.1716	0.9814	0.8437
	FOLQI / Non-minimum	1.0788	1.0036	0.1676	1.7933	3.6276	3.7317	6.9248	2.6781	0.8020	0.8700
APSO	IOLQI/ Minimum	0.5514	0.9915	1.5566	1.0882	2.8910	4.2427	0.8557	4.8845	-	-
	IOLQI/ Non-minimum	1.9712	1.3166	1.6154	1.6593	2.4662	4.6690	5.5342	0.1686	-	-
	FOLQI/ Minimum	0.4670	0.5505	0.3838	1.0798	4.3735	4.0577	7.1449	1.7352	0.8212	0.9198
	FOLQI/ Non-minimum	2.1809	2.2659	0.7991	1.9047	3.2796	4.1326	8.5300	2.8451	0.8229	0.9219
FF	IOLQI/ Minimum	1.2571	0.8219	1.8114	1.5922	3.0720	2.9747	2.0416	0.6452	-	-
	IOLQI/ Non-minimum	1.2201	0.6425	1.4486	1.8297	1.0615	1.7583	2.9393	5.3533	-	-
	FOLQI/ Minimum	0.8815	0.4995	0.6352	1.5440	2.4191	1.8231	8.3252	5.8941	0.9099	0.9834
	FOLQI/ Non-minimum	1.0342	0.8677	0.1859	0.6687	4.0277	4.7713	0.2204	1.2102	0.9994	0.8071

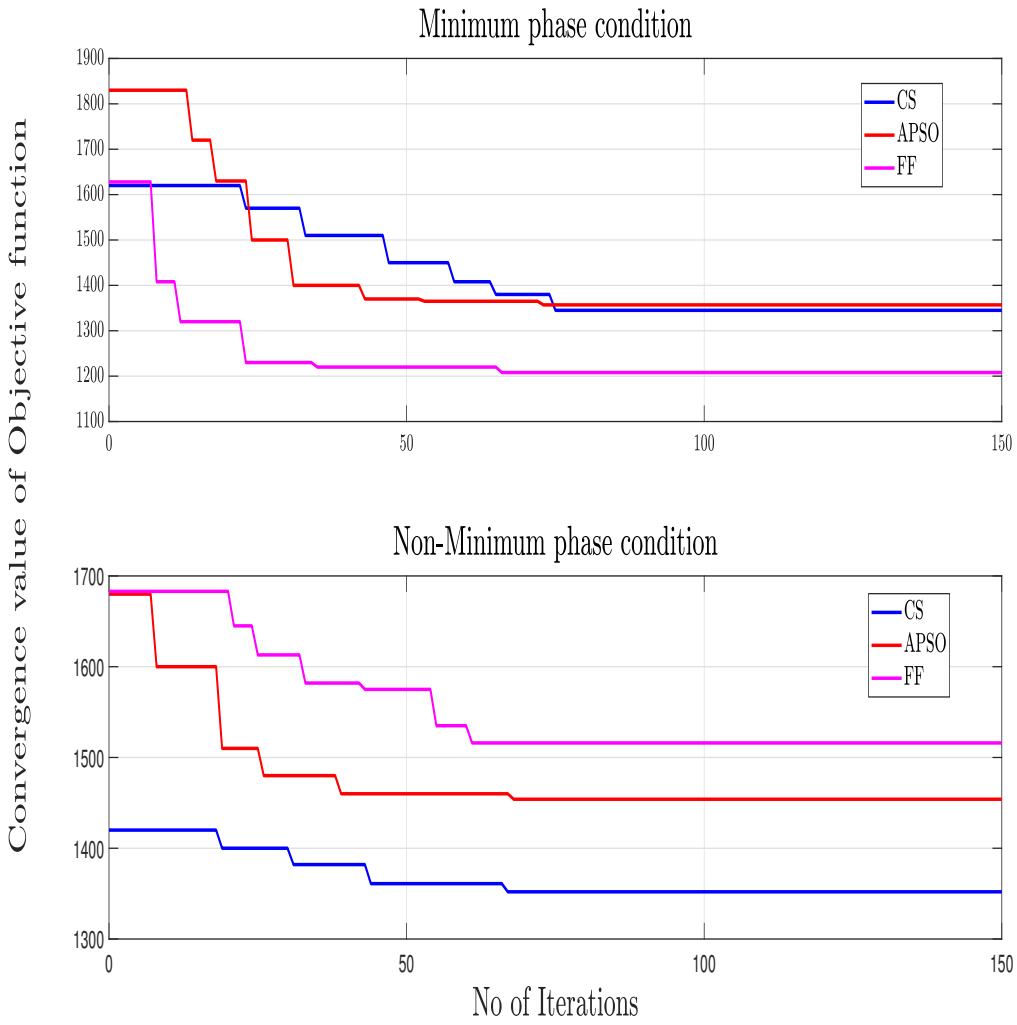

Figure 5.4: Convergence response of CS, APSO and FF algorithms for IOLQI Controller

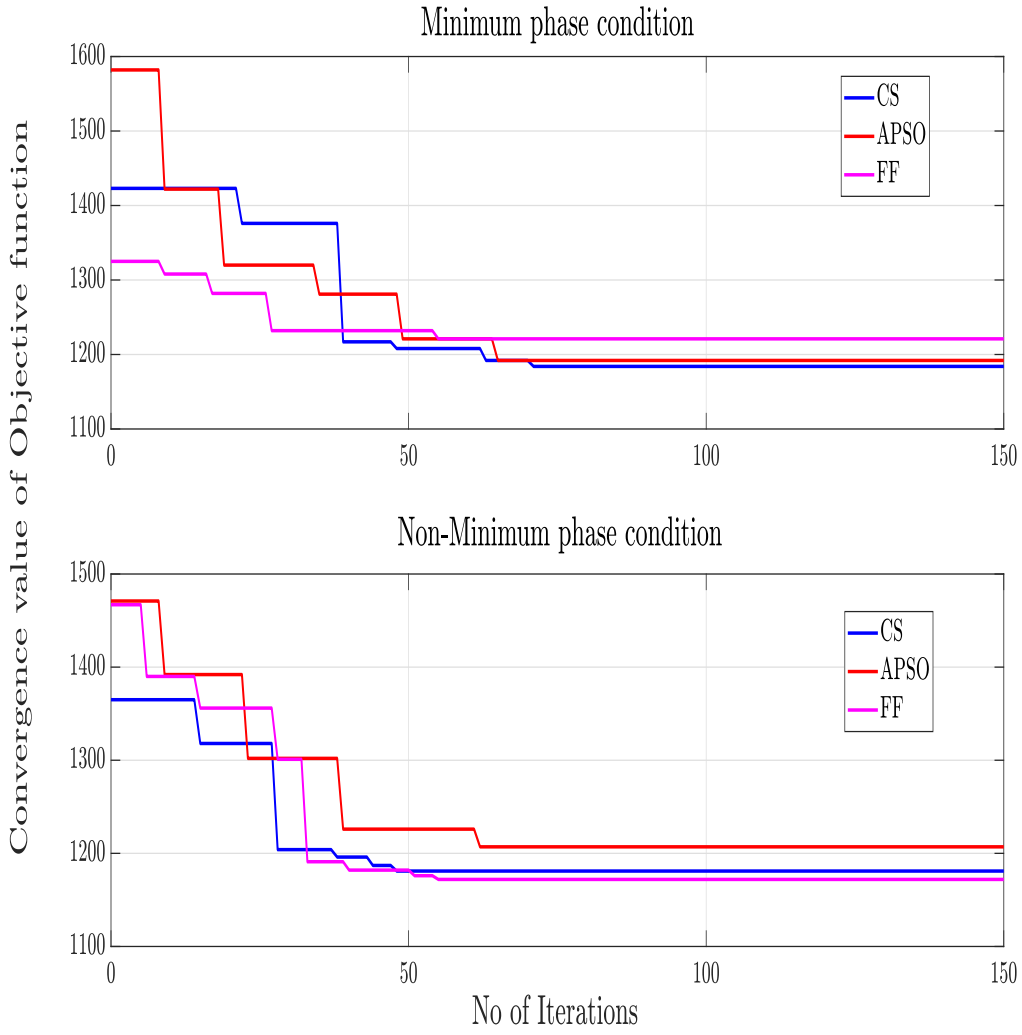

Figure 5.5: Convergence response of CS, APSO and FF algorithms for FOLQI Controller

Table 5.3: Convergence epochs and statistical indices of CS, APSO and FF algorithms

Methods	Controllers	Convergence epochs	Statistical indices	
			Mean	SD
CS	IOLQI: Minimum phase	74	1403.34	118.10
	IOLQI: Non-minimum phase	66	1334.19	40.07
	FOLQI: Minimum phase	70	1241.73	91.88
	FOLQI: Non-minimum phase	47	1222.34	55.06
APSO	IOLQI: Minimum phase	72	1442.49	161.13
	IOLQI: Non-minimum phase	67	1490.91	61.44
	FOLQI: Minimum phase	64	1239.97	98.09
	FOLQI: Non-minimum phase	61	1250.20	78.12
FF	IOLQI: Minimum phase	65	1288.23	102.02
	IOLQI: Non-minimum phase	60	1541.80	62.71
	FOLQI: Minimum phase	54	1237.66	30.62
	FOLQI: Non-minimum phase	54	1213.70	88.50

5.4 Results and Discussion

5.4.1 Performance under Disturbance Condition

The simulation is performed using the proposed FOLQI and existing IOLQI controller parameters obtained using CS, APSO and FF algorithms for the duration of $350\ sec.$ At 50^{th} sec (as depicted in Fig. 4.2), a continuous load disturbance of $1\ cm$ magnitude is introduced to the outputs $h_1(t)$ and $h_2(t)$. The time domain performance metrics $\%M_p$, t_s, e_{ss} and J are evaluated for IOLQI and FOLQI controllers under minimum and non-minimum phase operating conditions. The results are summarised in Table 5.4. The output responses ($h_1(t)$ and $h_2(t)$) and controller responses ($u_1(t)$ and $u_2(t)$) for QTP with IOLQI and FOLQI controllers operating under minimum and non-minimum phase operating conditions are shown in Figs. 5.6 - 5.13. Observations from the Table 5.4, show that FOLQI controllers exhibit superior time related characteristics $\%M_p$, t_s and J compared to their IOLQI counterparts. However, it is noted that IOLQI controllers outperform FOLQI controllers in terms of e_{ss}.

Remarks 1: The data presented in Table 5.4 suggest that controllers optimised using CS, APSO and FF algorithms doesn't provide consistency in time characteristics under minimum and non-minimum phase conditions of IOLQI and FOLQI controllers. The simulation results demonstrate that in all cases, the control effort required to regulate h_2 is more compared to control effort necessary for regulating h_1.

Table 5.4: Performance characteristics for IOLQI and FOLQI controllers of QTP under $d(t)$ condition

Controller/ Operating condition	Heuristic algorithm	Output (cm)	Overshoot $(\%)$	Settling time (sec)	Steady state error (e_{ss})	Controller effort $(*10^3)$	Effective controller effort $(J*10^3)$
IOLQI / Minimum phase	CS	h_1	5.7977	24.1030	0.0014	1.827	3.6639
		h_2	6.1123	24.1750	0.0077	1.836	
	APSO	h_1	5.5180	28.3980	0.0425	1.845	3.7028
		h_2	5.8153	29.9640	0.0105	1.858	
	FF	h_1	5.6629	26.9330	0.0148	1.792	3.5972
		h_2	5.9180	29.2720	0.0334	1.805	
FOLQI / Minimum phase	CS	h_1	4.3728	2.7920	0.0069	1.765	3.5371
		h_2	4.6702	2.7200	0.0040	1.772	
	APSO	h_1	4.3744	1.7480	0.0141	1.761	3.5342
		h_2	4.6647	1.7800	0.0317	1.773	
	FF	h_1	5.2375	4.9460	0.1809	1.766	3.5719
		h_2	5.5283	4.9670	0.1615	1.806	
IOLQI / Non-minimum phase	CS	h_1	6.2989	51.5870	0.0322	1.720	3.6708
		h_2	8.1258	62.0230	0.0355	1.951	
	APSO	h_1	4.9419	26.5330	0.0035	1.784	3.8153
		h_2	8.3099	55.8790	0.1366	2.032	
	FF	h_1	6.5241	46.7880	0.0622	1.804	3.8519
		xh_2	7.5291	48.4790	0.0503	2.048	
FOLQI / Non-minimum phase	CS	h_1	4.2540	2.2600	0.1369	1.627	3.5416
		h_2	3.4549	23.2500	0.3901	1.914	
	APSO	h_1	4.4437	2.2310	0.0264	1.650	3.5494
		h_2	3.7544	21.5190	0.1069	1.900	
	FF	h_1	5.6173	13.8690	0.7047	1.700	3.5129
		h_2	4.6486	9.5570	0.6279	1.813	

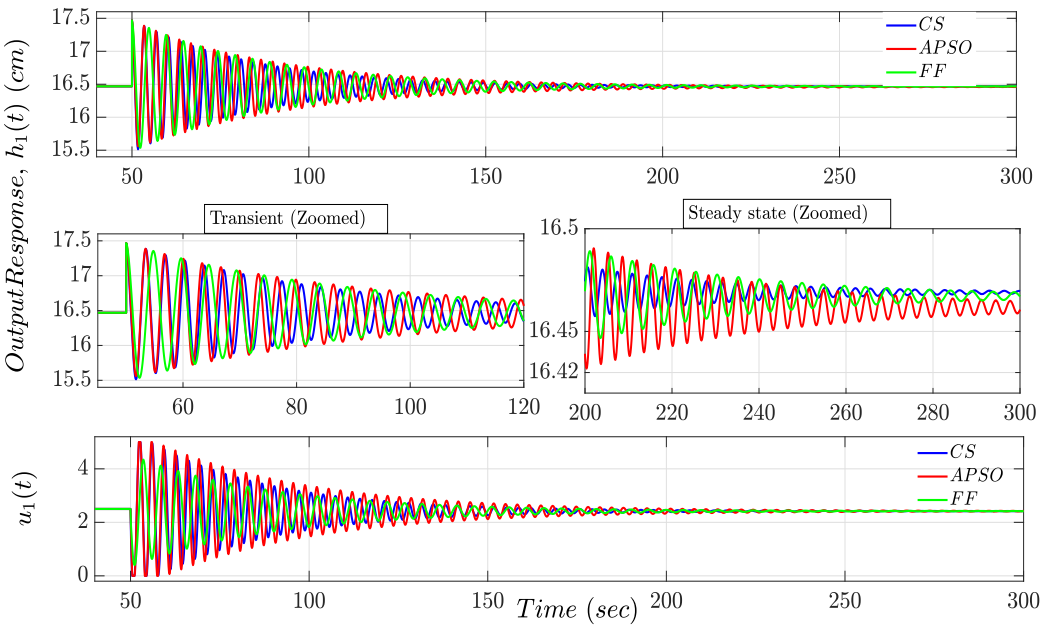

Figure 5.6: Output $h_1(t)$ and controller $u_1(t)$ responses for minimum phase condition of QTP with IOLQI controller

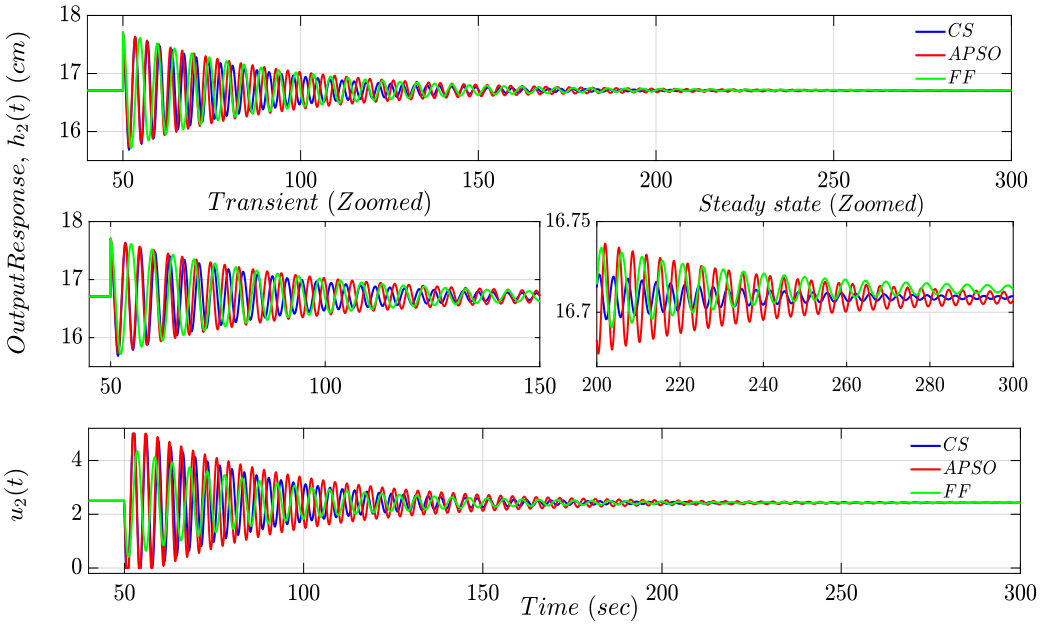

Figure 5.7: Output $h_2(t)$ and controller $u_2(t)$ responses for minimum phase condition of QTP with IOLQI controller

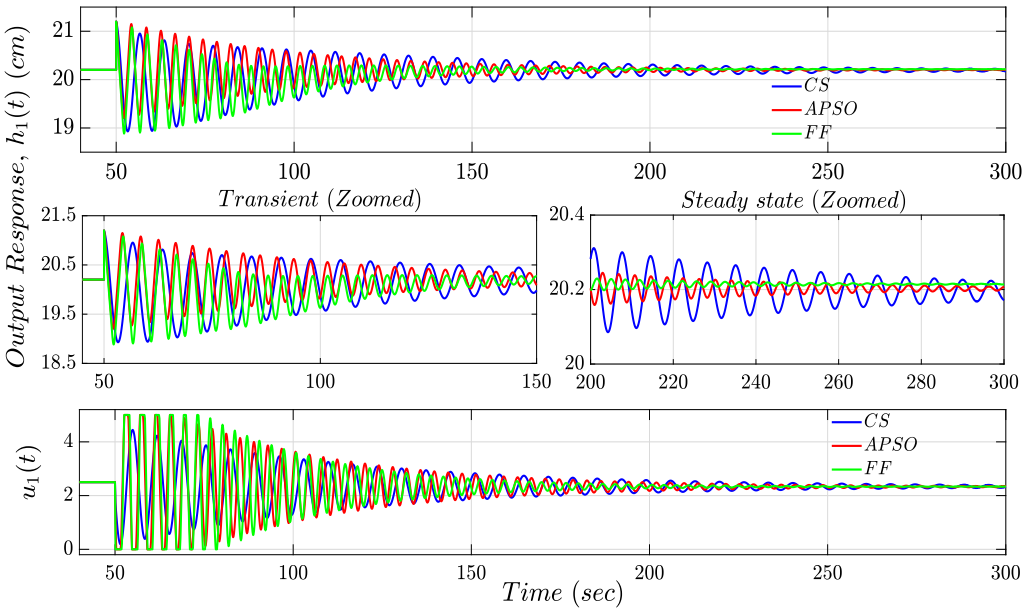

Figure 5.8: Output $h_1(t)$ and controller $u_1(t)$ responses for non-minimum phase condition of QTP with IOLQI controller

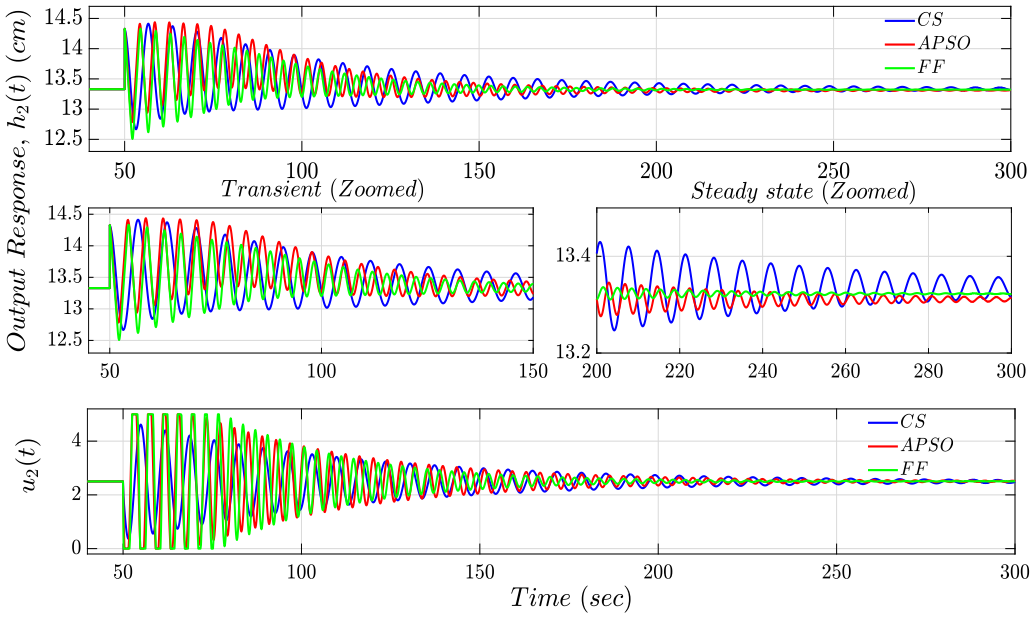

Figure 5.9: Output $h_2(t)$ and controller $u_2(t)$ responses for non-minimum phase condition of QTP with IOLQI controller

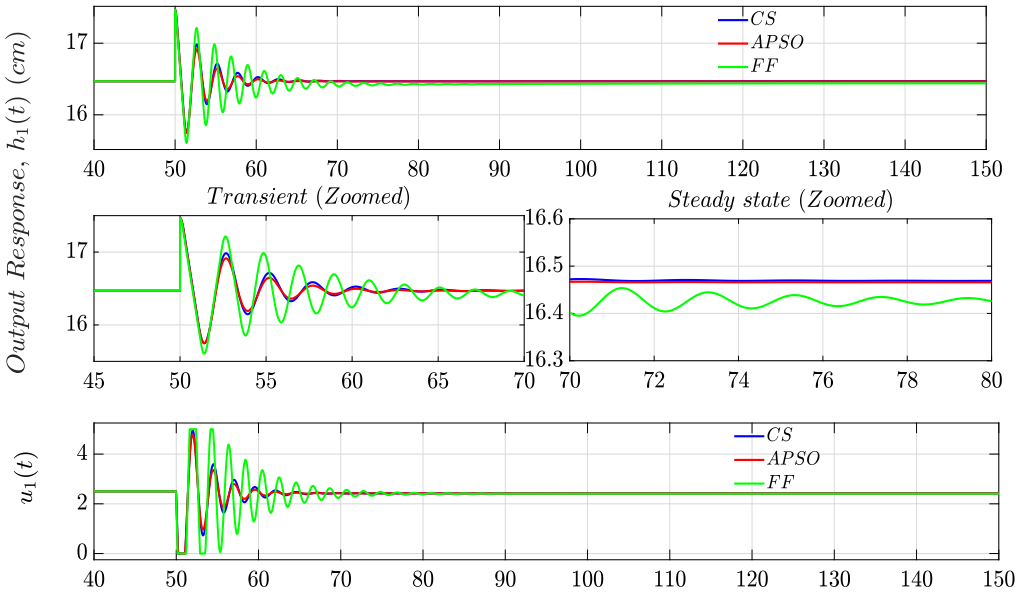

Figure 5.10: Output $h_1(t)$ and controller $u_1(t)$ responses for minimum phase condition of QTP with FOLQI controller

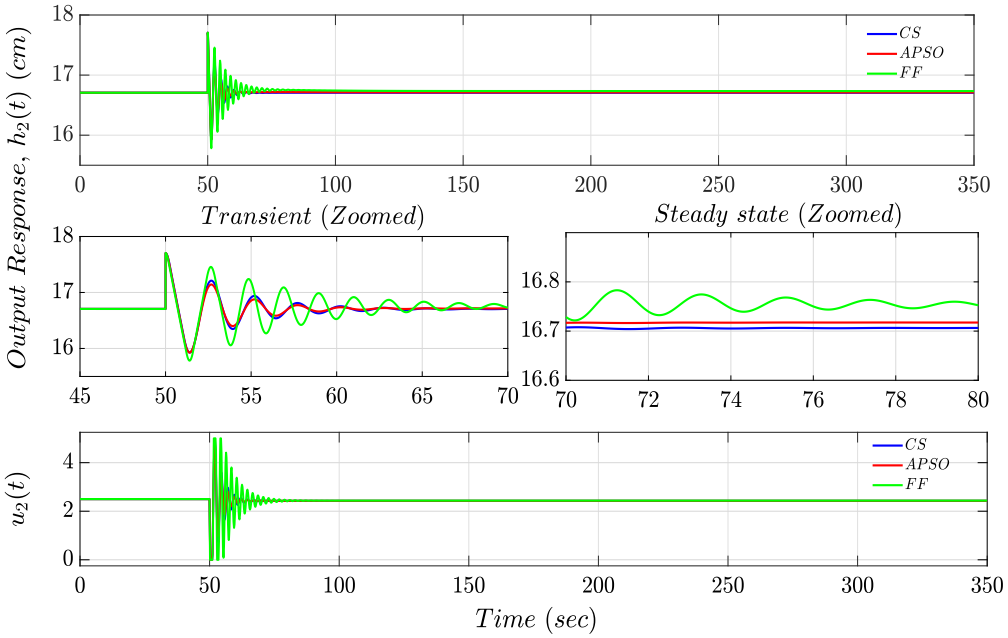

Figure 5.11: Output $h_2(t)$ and controller $u_2(t)$ responses for minimum phase condition of QTP with FOLQI controller

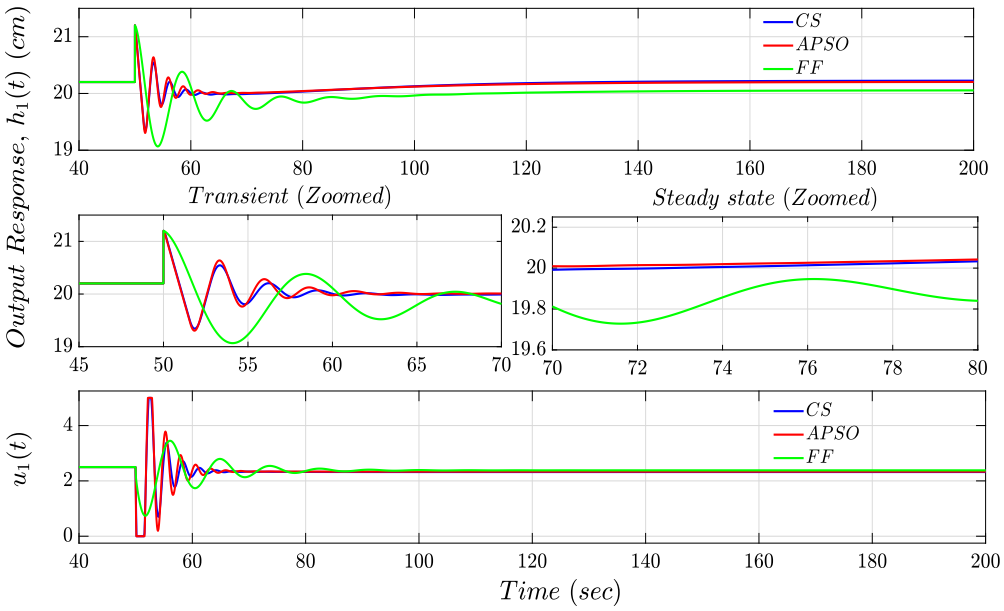

Figure 5.12: Output $h_1(t)$ and controller $u_1(t)$ responses for non-minimum phase condition of QTP with FOLQI controller

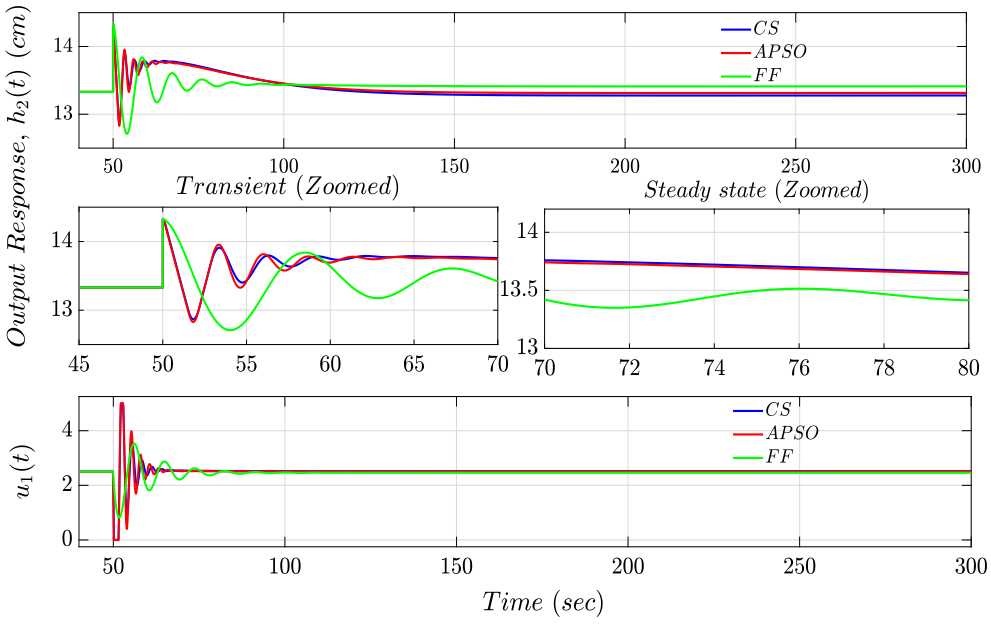

Figure 5.13: Output $h_2(t)$ and controller $u_2(t)$ responses for non-minimum phase condition of QTP with FOLQI controller

5.4.2 Performance under Disturbance and Parameter Uncertainty

The robustness of the FOLQI controller is assessed by introducing parameter uncertainty in A_i and a_i, varied by $\pm$ 30 $\%$ along with a continuous load disturbance $d(t)$ at 50^{th} sec. The performance of FOLQI controller is compared with their IO counterpart. Time domain characteristics including $\%M_p$, t_s, e_{ss} and J of both IOLQI and FOLQI controllers are computed for minimum and non-minimum phases of QTP and presented in Tables 5.5 - 5.7. The output responses $h_1(t)$ and $h_2(t)$ of QTP with IOLQI and FOLQI controllers obtained using (i) CS algorithm are shown in Figs. 5.14 - 5.17 (ii) APSO algorithm are shown in Figs. 5.18 - 5.21 and (iii) FF algorithm are shown in Figs. 5.22 - 5.25.

From Tables 5.5 - 5.7, the following results are inferred: (i) FOLQI controllers exhibit superior time characteristics ($\%M_p$, t_s and J) compared to IOLQI controllers (ii) IOLQI controllers demonstrate better performance in terms of e_{ss} compared to FOLQI controllers (iii) CS algorithm tuned IOLQI and FOLQI controllers fail to meet the required t_s and e_{ss} for non-minimum phase respectively (iv) APSO tuned IOLQI controller fails to achieve the required t_s for non-minimum phase mode (v) FF tuned IOLQI and FOLQI controllers successfully meet all the required specifications for minimum and non-minimum phases of QTP. Based on the above observations, it is concluded that FF tuned FOLQI controller exhibits superior time response characteristics ($\%M_p$, t_s, e_{ss} and J) compared to APSO and CS tuned FOLQI controllers.

Table 5.5: Performance characteristics for IOLQI and FOLQI controllers of QTP under $d(t)$ and parameter uncertainty conditions using CS algorithm

Controller / Operating condition	Parameter uncertainty $(\%)$	Output (cm)	Overshoot $(\%)$	Settling time (sec)	Steady state error (e_{ss})	Controller effort $(*10^3)$	Effective controller effort $(J * 10^3)$
IOLQI / Minimum phase	-30 %	h_1	5.8089	20.6680	0.0049	0.903	1.8122
		h_2	6.1224	20.7270	0.0425	909.2	
	Nominal	h_1	5.7977	24.1030	0.0014	1.827	3.6639
		h_2	6.1123	24.1750	0.0077	1.836	
	+30 %	h_1	6.0560	29.0490	0.0008	3.072	6.1559
		h_2	6.3768	30.8900	0.0132	3.084	
FOLQI / Minimum phase	-30 %	h_1	4.3322	2.5380	0.0119	0.865	1.735
		h_2	4.6280	2.4840	0.0083	0.870	
	Nominal	h_1	4.3728	2.7920	0.0069	1.765	3.5371
		h_2	4.6702	2.7200	0.0040	1.772	
	+30 %	h_1	4.5716	3.5200	0.0168	2.982	5.9742
		h_2	4.8736	3.4840	0.0113	2.992	
IOLQI / Non-minimum phase	-30 %	h_1	6.4819	43.6580	0.3433	0.8305	1.8160
		h_2	8.3504	52.2830	0.4847	0.9855	
	Nominal	h_1	6.2989	51.5870	0.0322	1.720	3.6708
		h_2	8.1258	62.0230	0.0355	1.951	
	+30 %	h_1	6.6453	67.0240	0.2686	2.949	6.1970
		h_2	8.1421	79.1180	0.3158	3.248	
FOLQI / Non-minimum phase	-30 %	h_1	4.1406	2.1340	0.4431	0.7718	1.7361
		h_2	3.2853	27.1110	1.1946	0.9643	
	Nominal	h_1	4.2540	2.2600	0.1369	1.627	3.5416
		h_2	3.4549	23.2500	0.3901	1.914	
	+30 %	h_1	4.9472	2.4790	0.0416	2.802	5.9831
		h_2	7.4975	17.7240	0.0761	3.182	

Table 5.6: Performance characteristics for IOLQI and FOLQI controllers of QTP under $d(t)$ and parameter uncertainty conditions using APSO algorithm

Controller / Operating condition	Parameter uncertainty $(\%)$	Output (cm)	Overshoot $(\%)$	Settling time (sec)	Steady state error (e_{ss})	Controller effort $(*10^3)$	Effective controller effort $(J*10^3)$
IOLQI / Minimum phase	-30 %	h_1	5.7473	29.9520	0.0944	0.9212	1.8513
		h_2	6.0479	29.8620	0.0145	0.9302	
	Nominal	h_1	5.5180	28.3980	0.0425	1.845	3.7028
		h_2	5.8153	29.9640	0.0105	1.858	
	+30 %	h_1	5.6510	32.0650	0.0170	3.087	6.1898
		h_2	5.9519	33.9000	0.0048	3.103	
FOLQI / Minimum phase	-30 %	h_1	4.2845	1.6550	0.0295	0.8623	1.7333
		h_2	4.5714	1.6820	0.0715	0.8709	
	Nominal	h_1	4.3744	1.7480	0.0141	1.761	3.5342
		h_2	4.6647	1.7800	0.0317	1.773	
	+30 %	h_1	4.6015	1.8930	0.0065	2.977	5.9695
		h_2	4.8976	1.9390	0.0091	2.993	
IOLQI / Non-minimum phase	-30 %	h_1	4.8412	22.8300	0.0173	0.8599	1.8835
		h_2	9.2901	47.4860	0.9350	1.024	
	Nominal	h_1	4.9419	26.5330	0.0035	1.784	3.8153
		h_2	8.3099	55.8790	0.1366	2.032	
	+30 %	h_1	5.1532	38.5570	0.0232	3.040	6.3955
		h_2	8.0681	76.7930	0.3393	3.355	
FOLQI / Non-minimum phase	-30 %	h_1	4.3313	2.1080	0.2745	0.7881	1.7407
		h_2	3.5948	25.2610	0.7400	0.9526	
	Nominal	h_1	4.4437	2.2310	0.0264	1.650	3.5497
		h_2	3.7544	21.5190	0.1069	1.900	
	+30 %	h_1	4.5975	2.4820	0.1237	2.829	5.9944
		h_2	3.9476	13.9610	0.2747	3.165	

Table 5.7: Performance characteristics for IOLQI and FOLQI controllers of QTP under $d(t)$ and parameter uncertainty conditions using FF algorithm

Controller / Operating condition	Parameter uncertainty (%)	Output (cm)	Overshoot (%)	Settling time (sec)	Steady state error (e_{ss})	Controller effort ($*10^3$)	Effective controller effort ($J * 10^3$)
IOLQI / Minimum phase	-30 %	h_1	5.8759	26.7950	0.0258	0.8852	1.7790
		h_2	6.1253	28.7900	0.0749	0.8938	
	Nominal	h_1	5.6629	26.9330	0.0148	1.792	3.5972
		h_2	5.9180	29.2720	0.0334	1.805	
	+30 %	h_1	6.0770	30.7940	0.0003	3.026	6.0686
		h_2	6.3546	33.4520	0.0192	3.043	
FOLQI / Minimum phase	-30 %	h_1	5.2602	4.2330	0.2694	0.8644	1.7563
		h_2	5.5461	4.2860	0.2415	0.8919	
	Nominal	h_1	5.2375	4.9460	0.1809	1.766	3.5719
		h_2	5.5283	4.9670	0.1615	1.806	
	+30 %	h_1	5.3317	6.4830	0.1315	2.984	6.0210
		h_2	5.6275	6.4840	0.1165	3.037	
IOLQI / Non-minimum phase	-30 %	h_1	6.4270	36.0870	0.3769	0.8716	1.8973
		h_2	7.5023	37.4690	0.3136	1.026	
	Nominal	h_1	6.5241	46.7880	0.0622	1.804	3.8519
		h_2	7.5291	48.4790	0.0503	2.048	
	+30 %	h_1	6.7010	67.7480	0.1609	3.068	6.4556
		h_2	7.6919	69.7580	0.1291	3.388	
FOLQI / Non-minimum phase	-30 %	h_1	5.3932	12.0800	0.4283	0.8233	1.7244
		h_2	4.1344	8.4150	0.4153	0.901	
	Nominal	h_1	5.6173	13.8690	0.7047	1.700	3.5129
		h_2	4.6486	9.5570	0.6279	1.813	
	+30 %	h_1	6.3565	15.6810	0.8626	2.894	5.9369
		h_2	5.6796	10.7130	0.7417	3.043	

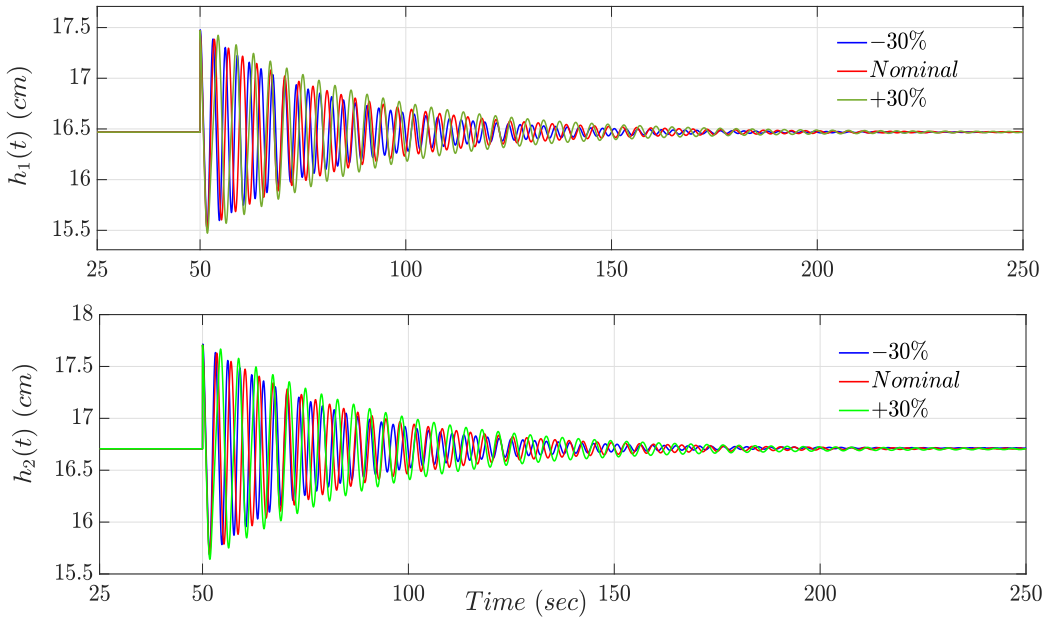

Figure 5.14: Output responses ($h_1(t)$ and $h_2(t)$) for minimum phase operating condition of QTP with IOLQI controller using CS algorithm

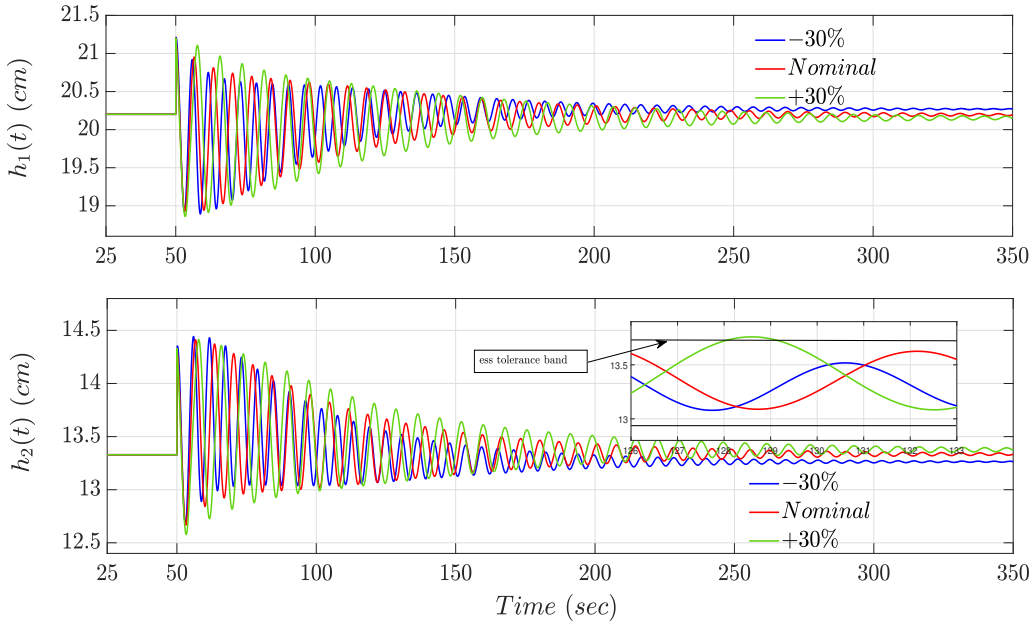

Figure 5.15: Output responses ($h_1(t)$ and $h_2(t)$) for non-minimum phase operating condition of QTP with IOLQI controller using CS algorithm

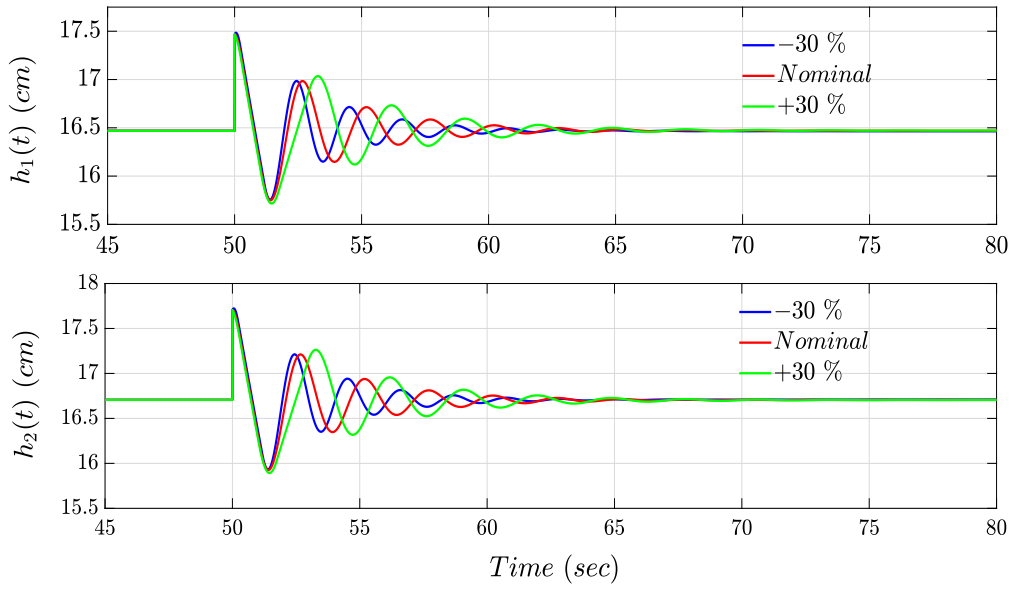

Figure 5.16: Output responses ($h_1(t)$ and $h_2(t)$) for minimum phase operating condition of QTP with FOLQI controller using CS algorithm

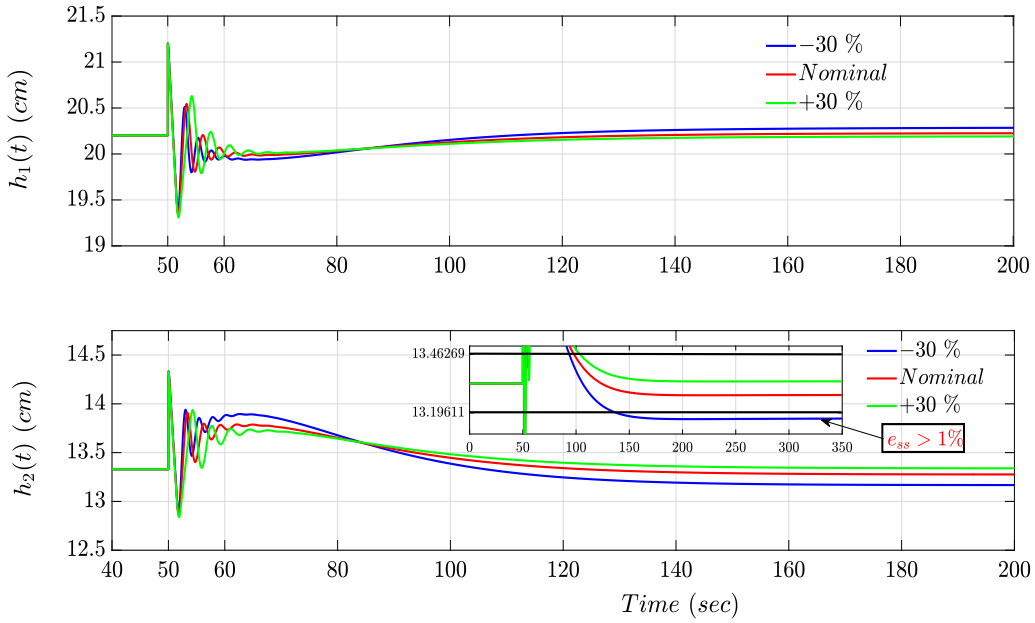

Figure 5.17: Output responses ($h_1(t)$ and $h_2(t)$) for non-minimum phase operating condition of QTP with FOLQI controller using CS algorithm

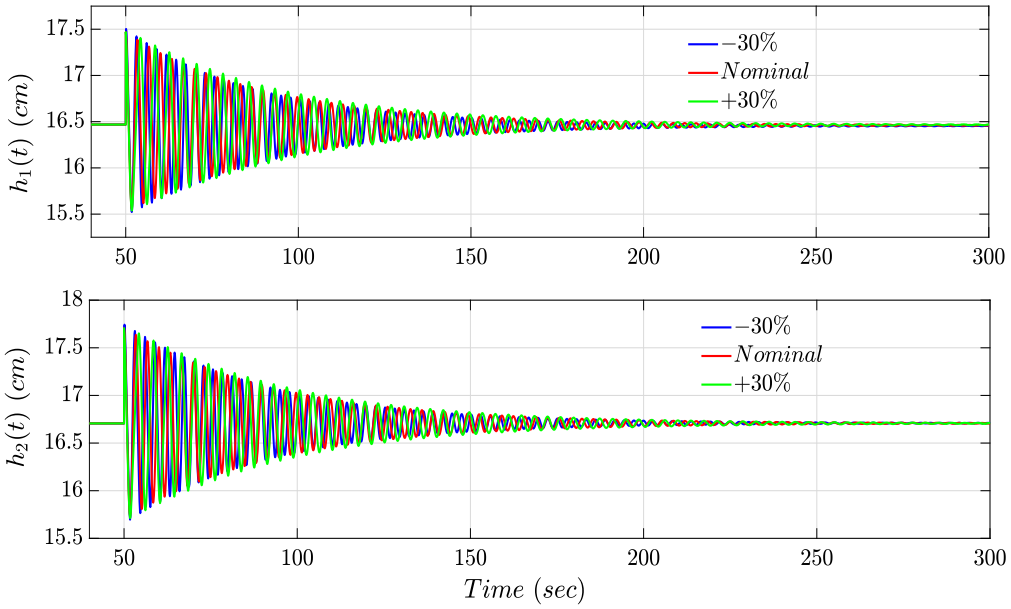

Figure 5.18: Output responses ($h_1(t)$ and $h_2(t)$) for minimum phase operating condition of QTP with IOLQI controller using APSO algorithm

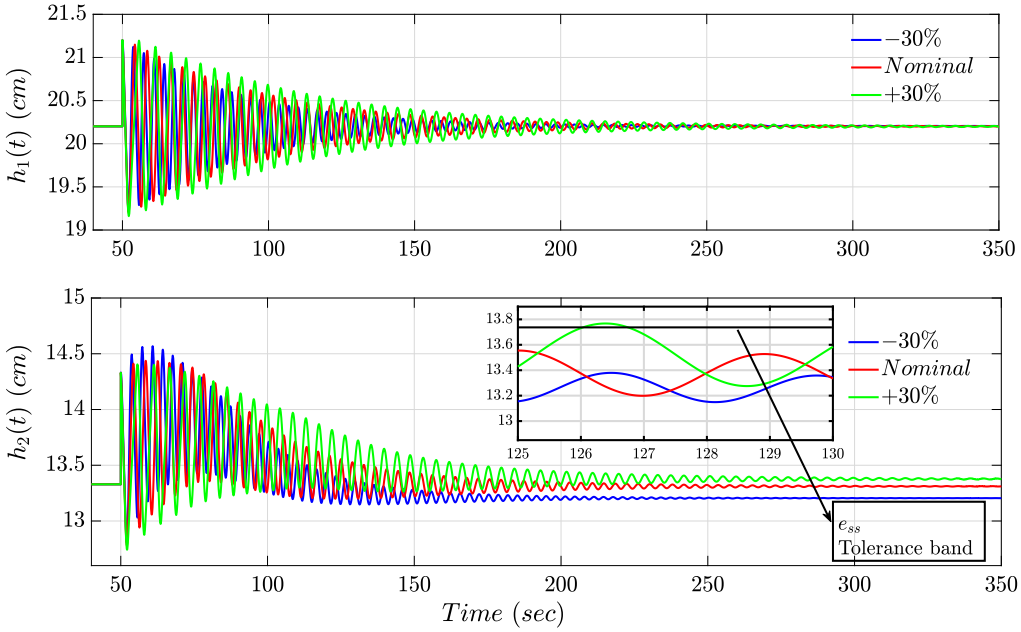

Figure 5.19: Output responses ($h_1(t)$ and $h_2(t)$) for non-minimum phase operating condition of QTP with IOLQI controller using APSO algorithm

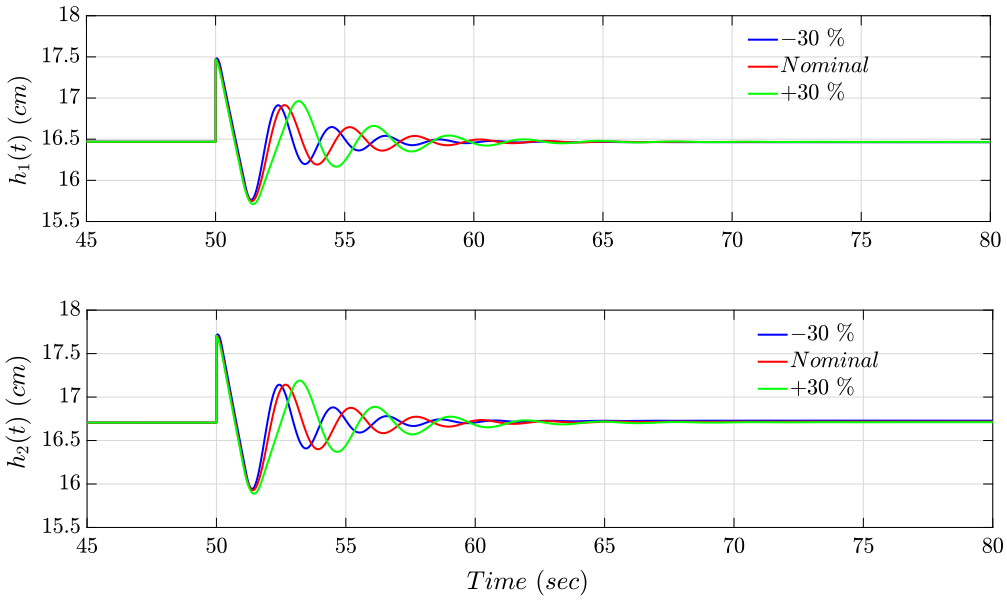

Figure 5.20: Output responses ($h_1(t)$ and $h_2(t)$) for minimum phase operating condition of QTP with FOLQI controller using APSO algorithm

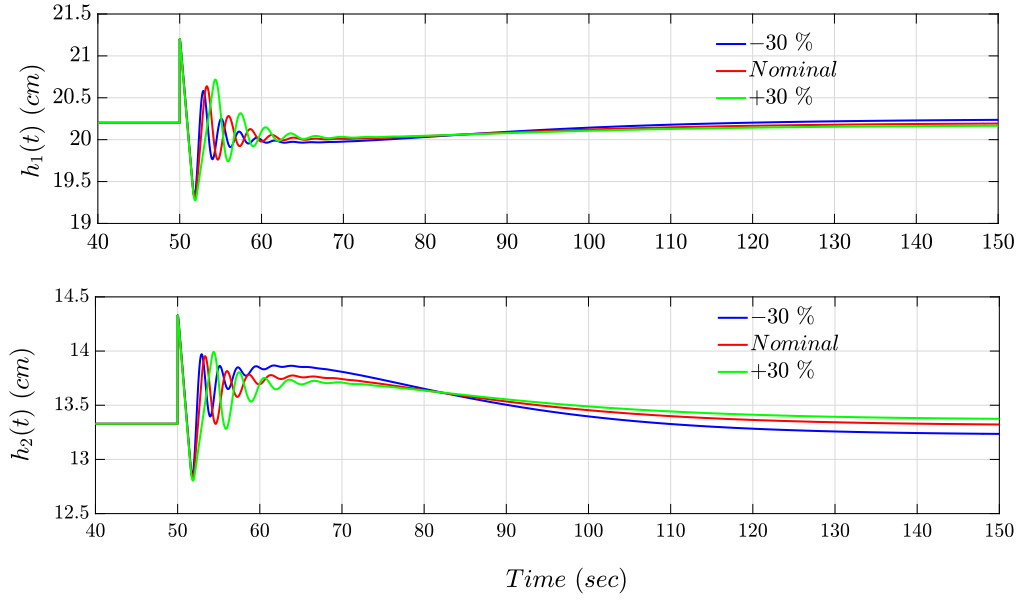

Figure 5.21: Output responses ($h_1(t)$ and $h_2(t)$) for non-minimum phase operating condition of QTP with FOLQI controller using APSO algorithm

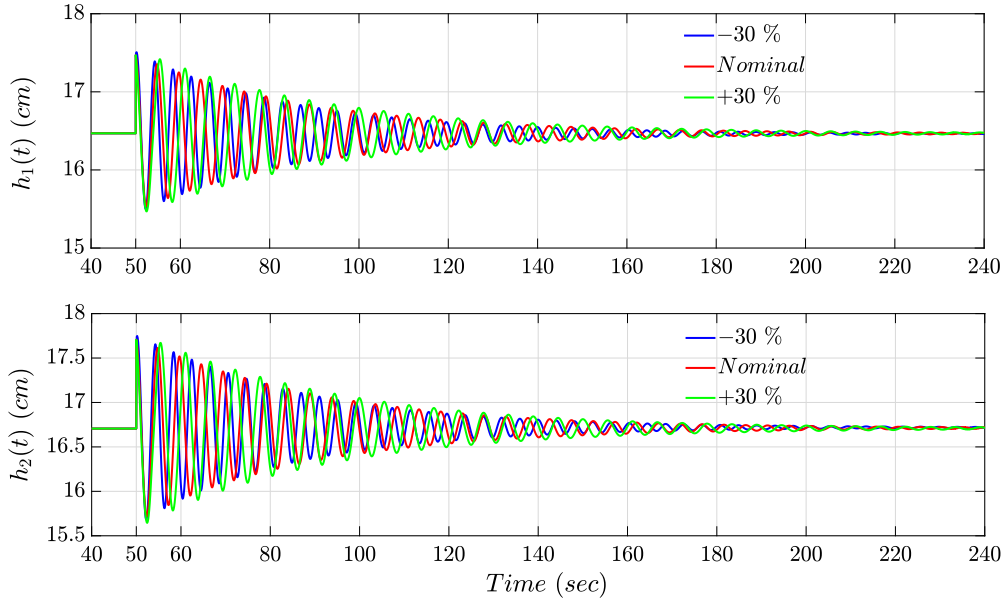

Figure 5.22: Output responses ($h_1(t)$ and $h_2(t)$) for minimum phase operating condition of QTP with IOLQI controller using FF algorithm

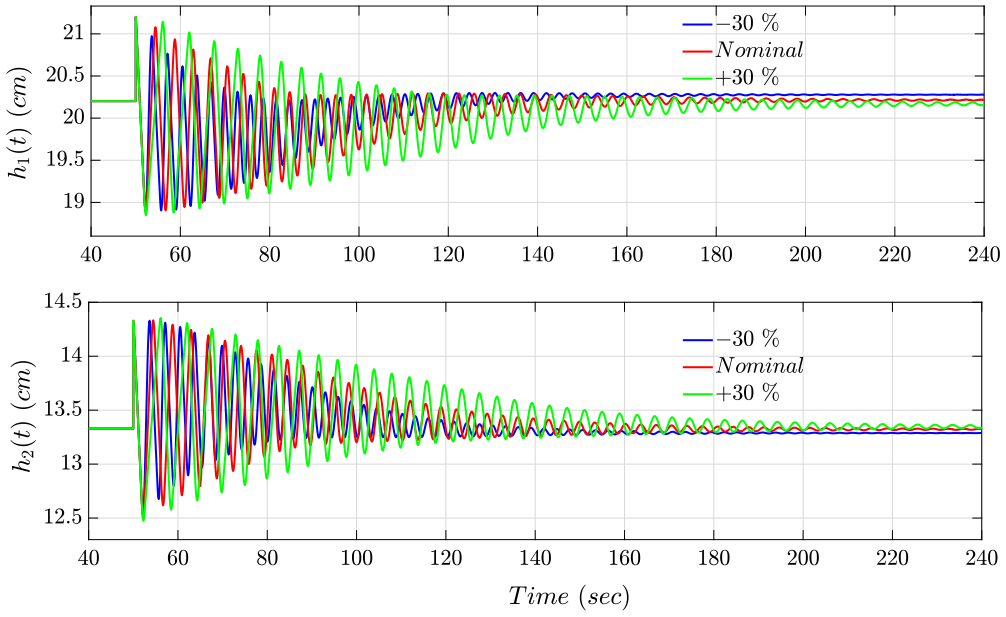

Figure 5.23: Output responses ($h_1(t)$ and $h_2(t)$) for non-minimum phase operating condition of QTP with IOLQI controller using FF algorithm

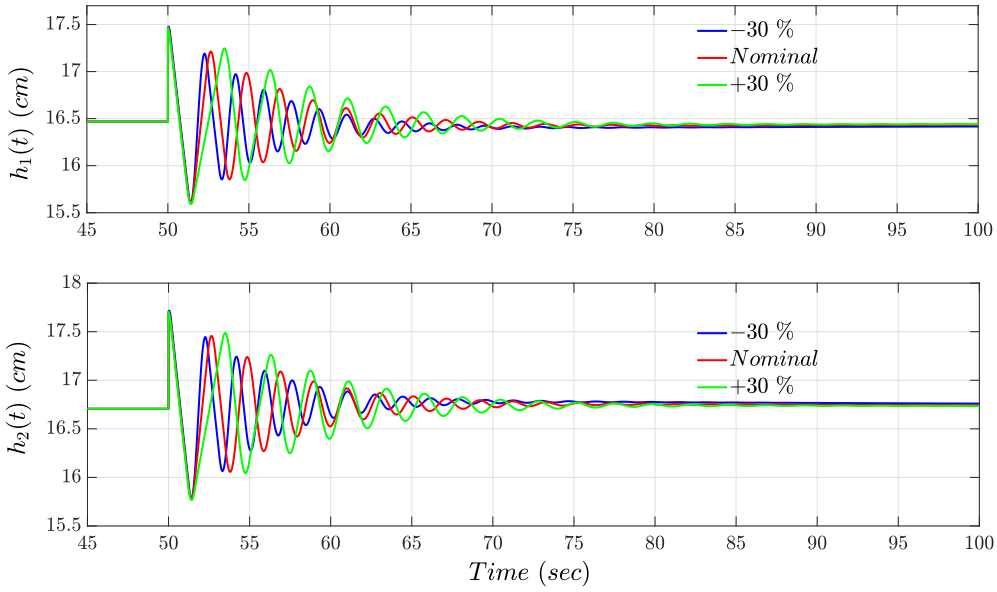

Figure 5.24: Output responses ($h_1(t)$ and $h_2(t)$) for minimum phase operating condition of QTP with FOLQI controller using FF algorithm

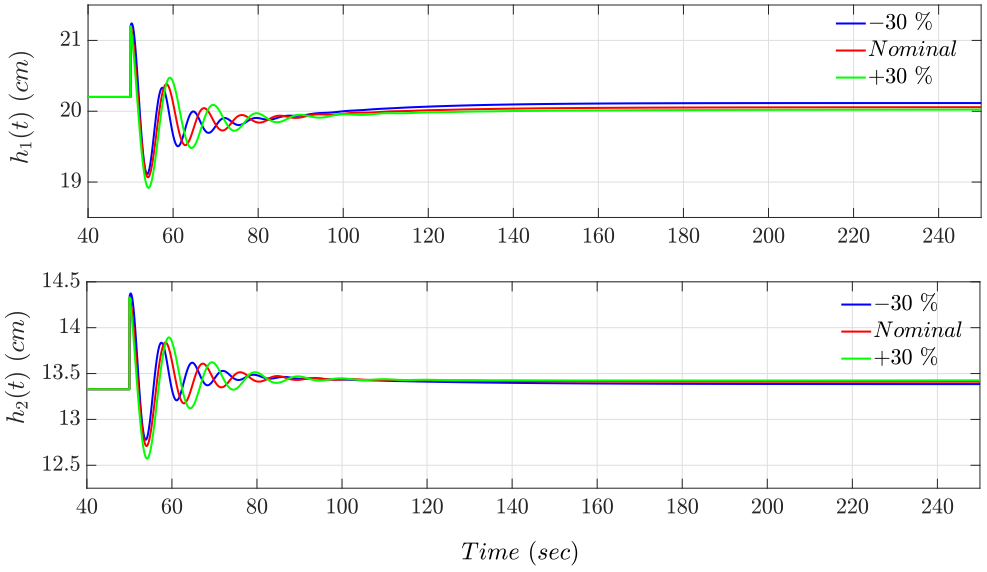

Figure 5.25: Output responses ($h_1(t)$ and $h_2(t)$) for non-minimum phase operating condition of QTP with FOLQI controller using FF algorithm

5.4.3 Stability Analysis

The stability of QTP with IOLQI and FOLQI controllers tuned using CS, APSO and FF algorithms are ensured using frequency response. The phase margin and its corresponding gain crossover frequencies of all the loops under minimum and non-minimum phase conditions of IOLQI and FOLQI controllers tuned using CS, APSO and FF algorithms are computed and shown in Tables 5.8 - 5.10.

Table 5.8: Stability analysis of controllers tuned using CS algorithm

Controller	Operating mode	Loop interaction		Gain crossover frequency (rad/sec)	Phase margin (deg)
		Input	Output		
IOLQI	Minimum	1	1	1.740	2.09
		1	2	1.770	2.07
		2	1	0.576	6.34
		2	2	0.587	6.28
	Non - minimum	1	1	0.617	2.71
		1	2	0.611	2.74
		2	1	0.685	2.91
		2	2	0.617	2.71
FOLQI	Minimum	1	1	1.030	4.17
		1	2	1.050	4.15
		2	1	2.230	15.3
		2	2	2.270	15.3
	Non - minimum	1	1	1.900	18.9
		1	2	1.690	18.7
		2	1	1.120	13.5
		2	2	0.997	13.2

It is noted that (i) phase margin for all control loops are finite in order to satisfy the required time response specifications and (ii) gain margin is infinite which is due to the absence of phase crossover frequency (not listed in tables). This leads to ensure adequate stability margin for both IOLQI and FOLQI controllers.

Remarks 2: Since LADR controller fails to provide the performance when it exceeds the uncertainty level of $\pm 5\%$, the comparison with IOLQI and FOLQI controllers for the uncertainty ($\pm 30\%$) are not attempted and hence the characteristics of LADR controller is excluded in this chapter.

Table 5.9: Stability analysis of controllers tuned using APSO algorithm

Controller	Operating mode	Loop interaction		Gain crossover frequency (rad/sec)	Phase margin (deg)
		Input	Output		
IOLQI	Minimum	1	1	0.724	3.77
		1	2	0.737	3.73
		2	1	1.730	1.57
		2	2	1.760	1.55
	Non - minimum	1	1	1.590	1.63
		1	2	1.430	1.51
		2	1	0.277	9.44
		2	2	0.253	10.30
FOLQI	Minimum	1	1	2.250	17.30
		1	2	2.290	17.30
		2	1	0.164	9.67
		2	2	0.160	9.64
	Non - minimum	1	1	2.110	17.20
		1	2	1.880	17.10
		2	1	1.150	9.24
		2	2	1.030	9.09

Table 5.10: Stability analysis of controllers tuned using FF algorithm

Controller	Operating mode	Loop interaction		Gain crossover frequency (rad/sec)	Phase margin (deg)
		Input	Output		
IOLQI	Minimum	1	1	1.120	2.72
		1	2	1.140	2.70
		2	1	0.628	4.85
		2	2	0.640	4.82
	Non - minimum	1	1	1.160	3.56
		1	2	1.040	3.35
		2	1	1.570	2.64
		2	2	1.410	2.46
FOLQI	Minimum	1	1	2.350	9.54
		1	2	2.390	9.48
		2	1	1.910	3.21
		2	2	1.940	3.14
	Non - minimum	1	1	0.319	4.77
		1	2	0.289	5.55
		2	1	0.723	19.40
		2	2	0.643	19.60

5.5 Summary

This section uses heuristic algorithms - CS, APSO and FF to tune FOLQI controller parameters for the proposed constrained optimisation problem under continuous load disturbance. Simulations were conducted for minimum and non-minimum phase operating modes of QTP under conditions of (i) disturbance and (ii) disturbance along with parameter uncertainty. The time response characteristics along with stability of FOLQI controller are compared with optimally tuned IOLQI controller with the given uncertainty limit along with disturbance condition.

Chapter 6

Tuning of FOLQI Controller using BG Approach

6.1 Introduction to BG

A BG method is a powerful tool for modelling and analysing dynamical systems across various engineering domains and it provides a unified framework for representing complex physical system using graphical structure applied in both continuous and discrete domain. Henry M. Paynter introduced BG during 1960s and since become widely adopted due to their ability to capture the multidomain nature of engineering systems and improve the system level understanding / analysis [125].

BG provide a unified framework for modelling complex inter disciplinary systems allowing engineers to represent and analyse interactions between electrical, mechanical, hydraulic and thermal components within a single model [126]. It is based on the concept of energy flow allowing for energy based analysis of system behaviour. This enables engineers to analyse energy storage, transfer and dissipation within the system which lead to better insights into system performance and efficiency [125]. It offers a clear and intuitive representation of the causal relationships between system components making it to understand the dynamics of the system. The causal nature of BG provides better understanding of the cause and effect relationships between different components of the system aiding the design of effective control strategies [127].

BG enable a dynamic analysis of systems under various operating conditions to assess the performance of control strategies and detect faults in real time. It also serves as the foundation for model based control approaches where controllers are designed based on system's dynamical behaviour represented in BG [128]. Due to multidisciplinary nature of BG, it makes them suitable for a wide range of applications including mechanical, electri-

cal, aerospace, automotive, biomedical and robotics engineering [129].

6.2 BG Elements

BG elements are fundamental components used in modelling, facilitating the representation and analysis of dynamic systems across multiple domains. The key idea behind BG is to represent the flow and storage of energy within a system using graphical elements called bonds and junctions. Bonds represent the flow of energy, while junctions represent the storage or interaction of energy. By combining bonds and junctions, complex systems can be represented and analysed in a systematic manner. These elements provide a standard way to represent the dynamics of the physical system. The half arrow is used to connect one BG element/junction with other and it represent a straight line with a half arrowhead at one end which is shown in Fig. 6.1. Here, line represents the bond and the direction of arrowhead indicates the direction of energy flow which points from source of effort or flow to the destination.

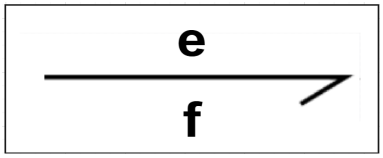

Figure 6.1: Representation of bond in BG

The common elements used in BG for representing the physical system is as follows:

- R Element (Resistor): The R element represents energy dissipation or resistance within the system. It is analogous to resistors in electrical circuit which models the dissipative process such as friction or damping.
- C Element (Capacitor): The C element represents energy storage or capacitance within the system. It is analogous to electrical capacitors and used to model the energy storage in the forms of compliance.
- I Element (Inductor): The I element represents energy storage due to magnetic effects. It is analogous to electrical inductors and used to model systems using magnetic energy storage such as inductors or flywheels.
- TF Element (Transformer): A transformer in BG represents the energy conversion between same engineering domain. It is analogous to a mechanical gearbox or electrical transformer where output is changing with respect to the input.

- GY Element (Gyrator): A gyrator element represents the element transferring energy between components of two different domains. It is analogous to energy exchange between an electric motor and mechanical shaft and vice versa.
- Effort source: An effort source is an element that represents a source of effort/force within a dynamic system. It typically represents a voltage source in electrical systems or a force or torque source in mechanical systems.
- Flow source: A flow source is an element that represents a source of flow within a dynamic system. It typically represents a current source in electrical systems or a flow rate in fluid or thermal systems.
- 0 Junction (Zero Junction): The 0 junction represents a point where variables are conserved. It is used to connect BG elements and ensures the conservation of energy and effort within the system.
- 1 Junction (One Junction): The 1 junction represents a point where effort is divided among multiple paths, but energy is conserved. It is used to model branching or distribution of energy or effort within the system.

In BG modelling, ports are pivotal junctions that facilitate the exchange of energy between different components within a system. These ports serve as connection points where energy flows into or out of a component allow to transfer power and signals. Each port is characterised by (i) power variables and (ii) directionality. Power variables such as effort and flow, represent the type of effort and flow being exchanged through the port which may vary depending on the system's physical domain.

Effort represents the driving force or input and flow signifies the resultant output. Directionality defines the nature of energy exchange with ports in either bidirectional or unidirectional. In BG, ports are typically depicted as small circles or squares and arrows denoting the direction of energy flow. By interconnecting ports of different elements, engineers can model the dynamic flow of energy through complex systems which enables comprehensive analysis and understanding of system behaviour across diverse domains. Each port of these elements is associated with power variables (effort and flow) and the directionality of energy flow is indicated by arrows on the ports.

One Port Elements:

- One port elements have a single port through which energy flows into or out of the component.

- Examples of one port elements include resistors, capacitors, inductors, mechanical springs, dampers and electrical sources such as batteries or voltage sources.
- One port elements are fundamental building blocks in BG modelling and are used to represent basic components and interactions within a system.

Two Ports Elements:

- Two port elements have two ports which allows energy exchange between two distinct parts of the system.
- Examples of two port elements include transformers, gyrators, mechanical transmissions, electrical transmission lines and hydraulic pipes.
- Two port elements are crucial for modelling interactions between different subsystems or components within a larger system. It enable the representation of energy transfer and conversion between multiple domains (e.g., electrical to mechanical, mechanical to hydraulic).

MultiPort Elements:

- Multiport elements have more than two ports which allow complex interactions and energy exchanges between multiple components.
- Examples of multiport elements include junctions, transformers with multiple windings, multimass mechanical systems and complex electrical networks.
- Multiport elements are used in BG models to represent interconnected subsystems, distributed parameter systems and networks with multiple pathways for energy flow.

6.2.1 Element Description

BG elements represent physical components relating their interaction within the system and are described as follows:

C type elements:

In a C type element, the BG representation and its constitutive relation is given as follows:

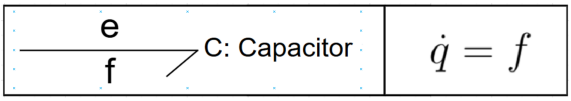

The following examples are used to present the constitutive relation:

(i) The deformation (x) and effort (e) of spring element is given by,

$$x = \int_{-\infty}^{t} v dt \qquad and \qquad e = Kx$$

(ii) The charge (q) and effort (e) of capacitor element is given by,

$$q = \int_{-\infty}^{t} i dt \qquad and \qquad e = \frac{1}{C} q$$

I type elements

I type element, BG representation and its constitutive relation is given as follows:

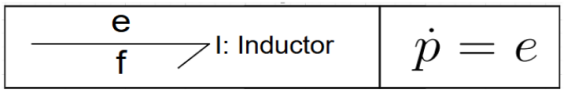

$$\dot{p} = e$$

The following examples are used to present the constitutive relation:

(i) The momentum (p) and velocity (v) of mass element is given by,

$$p = \int_{-\infty}^{t} F dt \qquad and \qquad v = \frac{1}{M} p$$

(ii) The flux linkage (ϕ) and current (i) in the inductor element is given by,

$$\phi = \int_{-\infty}^{t} V dt \qquad and \qquad i = \frac{1}{L} \phi$$

R type elements

In a R type element, the BG representation and its constitutive relation is given as follows:

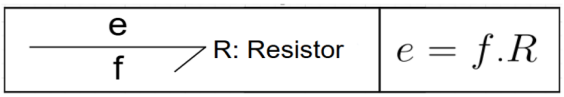

$$e = f.R$$

The following examples are used to present the constitutive relation:

(i) The effort (voltage V) and flow (current i) of resistor element is given by,

$$e = R * f \qquad and \qquad V = R * i$$

(ii) The effort (force) and flow (velocity) of damper element is given by,

$$f = \frac{1}{R}e \qquad and \qquad v = \frac{1}{B}F$$

Effort Sources

The effort e is represented as $e = E(t)$ and BG representation is shown as follows:

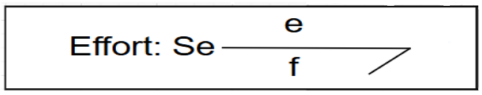

It is defined that the flow f is independent of effort e and is provided by the system to which the source is connected.

Flow Sources

The flow f is represented as $f = F(t)$ and the BG representation is shown as follows:

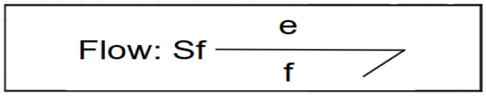

It is defined that the effort e is independent of flow f and is provided by the system to which the source is connected.

Transformer

The BG representation of transformer is shown as follows:

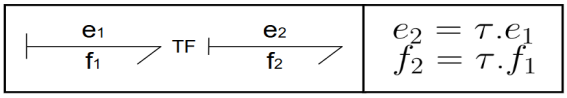

where, τ represents the transformer turns ratio.

Gyrator

The BG representation of gyrator is shown as follows:

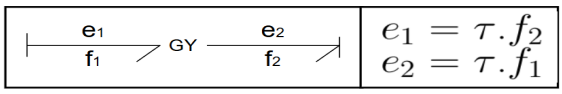

where, τ represents gyrator ratio.

0 junctions

The BG representation and its constitutive relations of 0 junction are shown as follows:

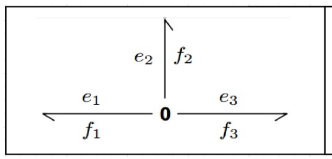

$$e_1 = e_2 = e_3$$
$$f_1 + f_2 + f_3 = 0$$

1 junctions

The BG representation and its constitutive relations of 1 junction are shown as follows:

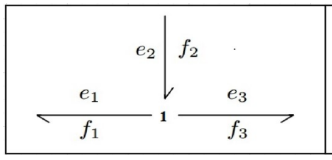

$$f_1 = f_2 = f_3$$
$$e_1 + e_2 + e_3 = 0$$

6.2.2 Representation of BG Variables and its Causal Relations

The effort and flow variables of different engineering domain are given in Table 6.1 and the casual relations of each elements are presented in Table 6.2.

Table 6.1: Effort and Flow representation in various domain

Element type	Element name	Symbol	Causal Relation (Preferred causality)
Source	Effort source	Se	-
	Flow source	Sf	-
Storage element	Capacitance	C	$e = \phi_c^- 1 \int f dt$
	Inertance	I	$f = \phi_L^- 1 \int e dt$
Resistance	Resistance	R	$e = \phi_R(f), f = \phi_R^- 1(e)$
Transductor	Transformer	TF	$f_2 = n * f_1$ $e_1 = n * e_2$
	Gyrator	GY	$e_2 = r * f_1$ $e_1 = r * f_2$
Junction	0 Junction	0	$e_1 = e_1 = ... = e_n$ $f_1 + f_2 + ... + f_n = 0$
	1 Junction	1	$f_1 = f_2 = ... = f_n$ $e_1 + e_2 + ... + e_n = 0$

Table 6.2: Casual relationship of BG elements

Domain	Effort (e)	Flow (f)
Electrical	Voltage (V)	Current (i)
Mechanical	Force (F)	Velocity (v)
	Torque (τ)	Angular Velocity (ω)
Hydraulic	Pressure (P)	Volume Flow Rate (dQ/dt)
Thermal	Temperature (T)	Entropy Change Rate (dS/dt)
Chemical	Chemical Potential (μ)	Mass Flow Rate (dN/dt)
Magnetic	Magneto motive Force (e_m)	Magnetic Flux Rate ($d\phi/dt$)

6.3 BG Model

6.3.1 BG Model of QTP

The BG representation of QTP is shown in Fig. 6.2.

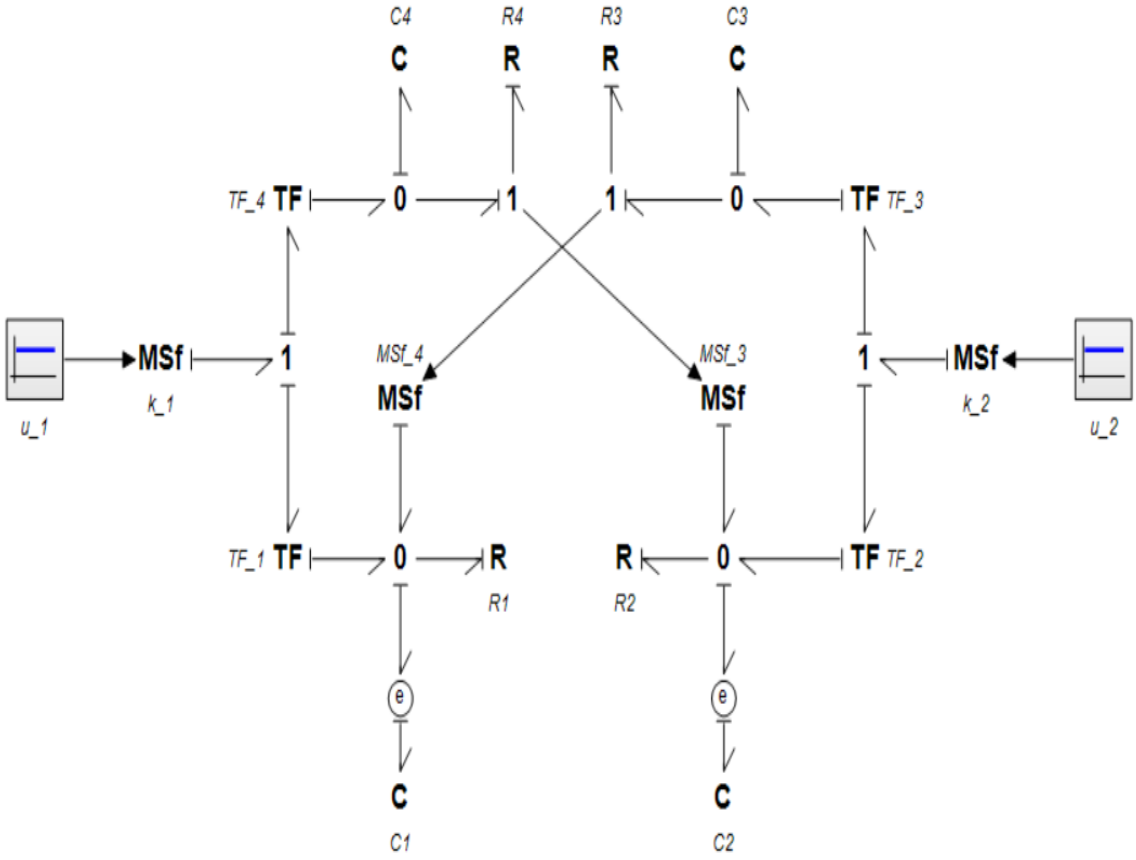

Figure 6.2: BG model of QTP

The description of various elements presented in Fig. 6.2 is as follows: (i) R_i represents resistor element which equals $a_i\sqrt{P_i}$ ($i \in$ Tank $1-4$) (ii) C_i ($i \in$ Tank $1-4$) represents capacitor element and (iii) TF_i ($i \in$ Tank $1-4$) represents transformer element, where TF_1 represents γ_1, TF_2 represents γ_2, TF_3 represents $(1-\gamma_2)$ and TF_4 represents $(1-\gamma_1)$. The parameters and their equilibrium points for minimum and non-minimum phase operating mode of QTP are given in Table 4.1. The nonlinear mathematical model with pressure term (P - effort variable) are considered as state variables and as follows [81]:

$$\dot{P}_1 = -\frac{a_1\sqrt{P_1}}{C_1} + \frac{a_3\sqrt{P_3}}{C_1} + \frac{\gamma_1}{C1}u_1 \tag{6.1}$$

$$\dot{P}_2 = -\frac{a_2\sqrt{P_2}}{C_1} + \frac{a_4\sqrt{P_4}}{C_2} + \frac{\gamma_1 2}{C1}u_2 \tag{6.2}$$

$$\dot{P}_3 = \frac{a_3\sqrt{P_3}}{C_3} + \frac{1-\gamma_2}{C3}u_2 \tag{6.3}$$

$$\dot{P}_4 = \frac{a_4\sqrt{P_4}}{C_4} + \frac{1-\gamma_1}{C4}u_1 \tag{6.4}$$

These equations are similar to state space representation of QTP shown in Section 2.3.

6.3.2 BG Model of FOLQI Controller

The FOLQI controller in BG representation is shown in Fig. 6.3.

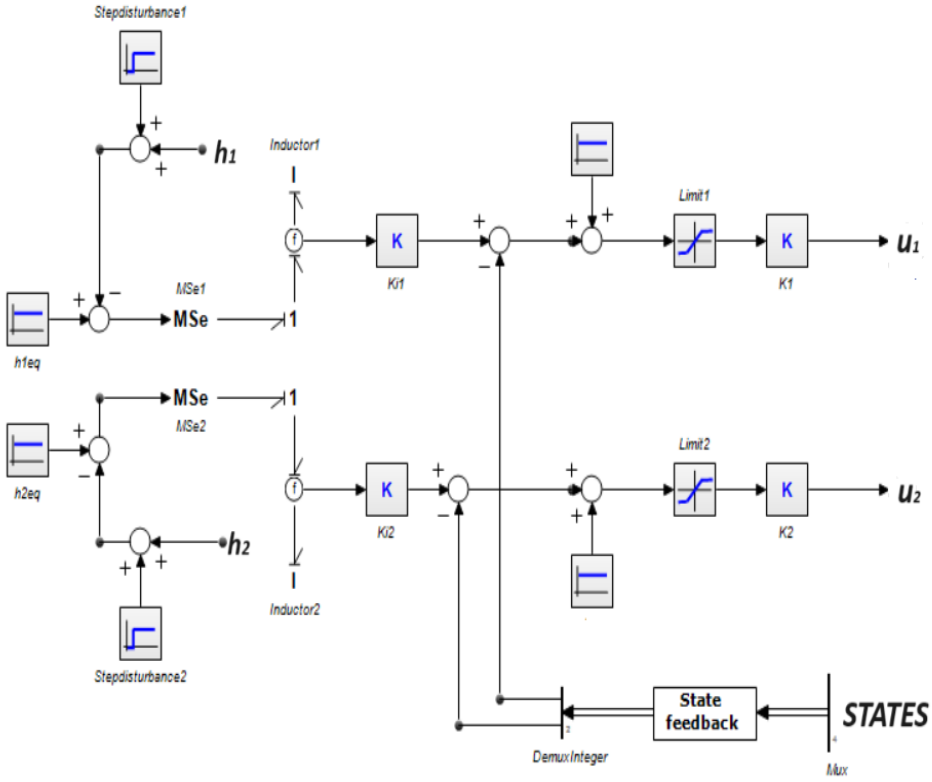

Figure 6.3: BG model of FOLQI controller

In BG domain, the dynamic behaviour of the controller is captured by the power flow through bonds, junctions and ports. The error values e_1 and e_2 i.e. ($h_i - h_{ieq}$, $i \in 1$ and 2) are assigned as effort values by using modulated effort source component MSe. The

effort value is given to inductor element (I) and in consequence, it provides the integration value of errors as per the dynamics of junction 1 presented in Section 6.2.1. The states of QTP are given to state feedback block presented in Fig. 6.3 where, the values of states are communicated to MATLAB by using "$doMatlab$" function available in 20-sim. Further, LQI function is performed to execute the IOLQI and FOLQI optimisation for calculating the required control actions. The integral values of error and state feedback outputs are combined and given to pump constants k_1 and k_2 to generate u_1 and u_2.

6.3.3 BG Model of QTP and FOLQI Controller in Closed Loop

The QTP along with FOLQI controller represented in BG is shown in Fig. 6.4. This is similar to the closed loop representation of plant with controller in feedback. The 20-sim software is used for implementing and simulating the closed loop representation of BG model.

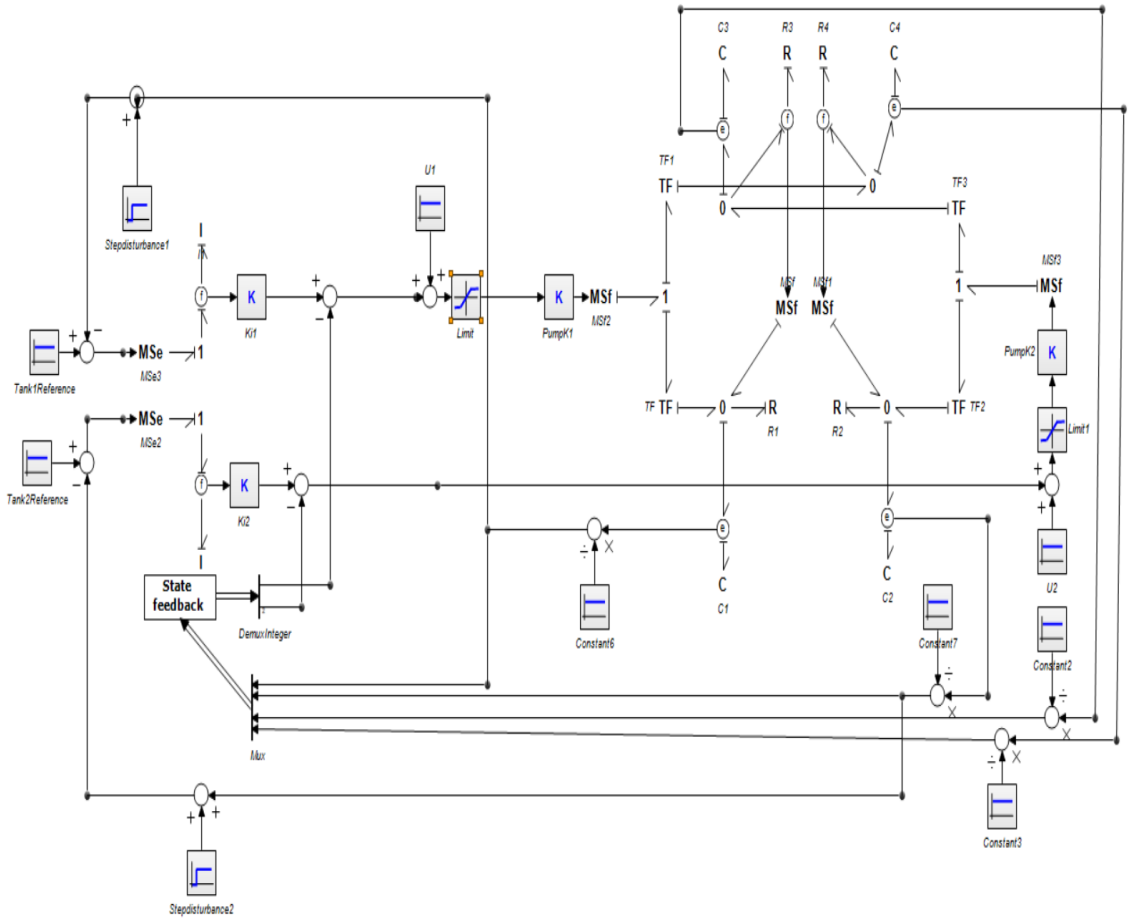

Figure 6.4: Closed loop BG representation of QTP with FOLQI controller

6.4 Optimisation and its Specifications

The FOLQI controller parameters are obtained by solving the unconstrained optimisation problem using 20-sim software. The following algorithms are used for optimising the controller parameters: (i) Newton-Raphson (NR) [130] (ii) Davidon-Fletcher-Powell (DFP) [131–133] (iii) Steepest Descent (SD) [108] and (iv) Broydon-Fletcher-Goldfarb-Shanno (BFGS) [132, 134–136]. The cost function used for solving the unconstrained optimisation problem is as follows:

$$\underset{\text{(Controller Parameters},Q,R)}{\text{Minimise}} J = \int_0^T (\Delta u_1^2(t) + \Delta u_2^2(t))dt \tag{6.5}$$

For FOLQI controller, the fractional term in the integrator is approximated to an integer order using the Oustaloup approximation of degree 5 with the frequency range of 0.001 to 1000 rad/sec [99]. A closed loop simulation is performed with the given optimisation problem by introducing the continuous load disturbance $d(t) = 1$ cm at $t = 50\ sec$ to obtain the parameters of IOLQI and FOLQI controllers. The bounds for the IOLQI and FOLQI controllers are tabulated in Chapter. 4.

6.4.1 Optimisation Algorithms

6.4.1.1 Newton Raphson method:

NR method is an iterative numerical method which is used for finding successively better approximations to the roots (or zeros) of a real valued function. It is particularly useful for solving complex nonlinear equations. The method involves using the first and second derivatives of the function to refine the solution until convergence is achieved iteratively. The pseudo code of the algorithm is given as:

NR algorithm
1. Define initial guess X_0, and set k=0
2. Obtain descent direction d_k = $\{H\}\ x_k^{-1}\ \nabla\ f(x_k)$
3. Set α_k = 1
4. Calculate the step S_k = $\alpha_k\ d_k$
5. Update the design x_{k+1}=x_k+s_k
6. If $\mid x_{k+1}$ - $x_k \mid <$ tot or $\nabla \mid f(x_{k+1}) \mid <$ tot, then stop
7. Increase the iterator k=k+1 and goto 2

6.4.1.2 Davidon–Fletcher–Powell method:

The DFP algorithm is a quasi-Newton optimisation algorithm used for unconstrained non-linear optimisation. It belongs to the class of quasi-Newton methods which seek to approximate the inverse Hessian matrix of the objective function using successive updates. The algorithm is known for its efficiency and robustness in many optimisation problems. The pseudo code of the algorithm is given as:

DFP algorithm
1. Define initial guesses X_0, and A_0, and set k=0
2. Obtain descent direction d_k = $\{-A_k\}\ x_k^{-1}\ \nabla\ f(x_k)$
3. Set α_k = 1
4. Calculate the step S_k = $\alpha_k\ d_k$
5. Update the design $x_k + 1$=x_k+s_k
6. If $\mid x_k + 1$ - $x_k \mid <$ tot or $\nabla \mid f(x_k + 1) \mid <$ tot, then stop
7. Obtain the variation in the gradient y_k = $\nabla\ f(x\_\{k + 1\})$ - $f(x\_k)$
8. Update the inverse Hessian approximation A_{k+1} = A_k+ $\frac{s_k S_k^T}{s_k^T y_k} - \frac{A_k y_k y_k^T A_k}{y_k^T A_k y_k}$
9. Increase the iterator k=k+1 and goto 2

6.4.1.3 Steepest Descent Method:

SD method is also known as gradient descent method. This method uses first order optimisation algorithm for finding the minimum of a function and works by iteratively moving in the direction towards the negative gradient of the function at each point. This algorithm is simple to implement and converge slowly especially in highly non convex functions or ill conditioned problems. The pseudo code of the algorithm is given as:

SD Method algorithm

1. Given an initial x_0, $d_0 = -g_0$ and a convergence tolerance tol
2. for $k = 0$ to max iter do
3. set α k = argmin($\phi\ \alpha$) = f(k)- $\alpha\ g_k$
4. x_{k+1}=x_k- $\alpha_k\ g_k$
5. Compute $g_{k+1} = \nabla \mid f(x_k + 1)$
6. if $\parallel g_{k+1} \parallel 2 \leq$ tol then
7. converged
8. end if
9. end for

6.4.1.4 Broyden–Fletcher–Goldfarb–Shanno algorithm:

Like DFP, BFGS is also a quasi-Newton method used to solve the unconstrained optimisation problems. It iteratively updates an approximation of the Hessian matrix using rank one updates which aim to converge optimal point. This algorithm offers faster convergence compared to DFP and is widely used in practice for its efficiency and reliability. The pseudo code of the algorithm is given as:

BFGS algorithm

1. Define initial guesses X_0, and B_0, and set k=0
2. Obtain descent direction $d_k = \{-B_k\}^{-1}\ x_k^{-1}\ \nabla\ f(x_k)$
3. Set α_k = 1
4. Calculate the step $S_k = \alpha_k\ d_k$
5. Update the design $x_k + 1$=x_k+s_k
6. If $\mid x_k + 1$ - $x_k \mid <$ tot or $\nabla \mid f(x_k + 1) \mid <$ tot, then stop
7. Obtain the variation in the gradient $y_k = \nabla\ f(x\_\{k + 1\})$ - $f(x\_k)$
8. Update the inverse Hessian approximation $B_{k+1} = B_k + \frac{y_k y_k^T}{y_k^T s_k} - \frac{B_k s_k s_k^T B_k}{s_k^T B_k s_k}$
9. Increase the iterator k=k+1 and goto 2

6.5 Results and Discussions

The simulation of QTP along with IOLQI and FOLQI controller parameters obtained using optimisation algorithms are performed under (i) disturbance and (ii) parameter uncertainty conditions. The converged values of IOLQI and FOLQI controller parameters for both minimum and non-minimum phase operating conditions are shown in Tables 6.3 and 6.4. Table 6.5 show the control effort utilised by the IOLQI and FOLQI controllers during the simulation and it is observed that (i) FOLQI controller tuned using all four optimisation

algorithms provide better controller effort for minimum and non-minimum phase operating modes of QTP (ii) controller tuned using BFGS algorithm provides least control effort to IOLQI controller under minimum phase operating mode (iii) controller tuned using SD algorithm provides least control effort to IOLQI controller under non-minimum phase operating mode (iv) controller tuned using NR algorithm provides least control effort to FOLQI controller under minimum phase operating mode and (v) controller tuned using SD algorithm provides least control effort to FOLQI controller under non-minimum phase operating mode. Based on the above observation, FOLQI controller provides minimum control effort than IOLQI controller.

Table 6.3: Converged parameters of IOLQI and FOLQI controllers obtained using NR and DFP methods

Algorithm	Controller/ Operating condition	Q_{11}	Q_{22}	Q_{33}	Q_{44}	R_{11}	R_{22}	K_{i1}	K_{i2}	α_1	α_2
NR	IOLQI / Minimum	0.3955	0.3683	1.5188	0.6436	1.6883	2.0687	4.1230	3.9232	-	-
	IOLQI / Non-minimum	1.3468	1.2102	0.6004	1.4849	1.9026	2.8487	4.7341	7.0607	-	-
	FOLQI / Minimum	0.0185	0.0021	0.0081	0.0118	0.0094	0.0124	0.0103	0.0056	0.4946	0.5439
	FOLQI / Non-minimum	0.0227	0.0035	0.0078	0.0372	0.0110	0.0064	0.0358	0.0022	0.5611	0.9465
DFP	IOLQI / Minimum	0.0417	0.7193	1.4108	1.6005	2.4317	3.8760	5.5505	6.1091	-	-
	IOLQI / Non-minimum	1.4006	1.7237	1.7326	1.4310	1.9111	4.2653	7.7950	1.2247	-	-
	FOLQI / Minimum	0.0074	0.0019	0.0012	0.0137	0.0095	0.0040	0.0068	0.0018	0.3240	0.5472
	FOLQI / Non-minimum	0.0131	0.0055	0.0045	0.0309	0.0029	0.0046	0.0229	0.0016	0.2475	0.4681

Table 6.4: Converged parameters of IOLQI and FOLQI controllers obtained using SD and BFGS methods

Algorithm	Controller/ Operating condition	Q_{11}	Q_{22}	Q_{33}	Q_{44}	R_{11}	R_{22}	K_{i1}	K_{i2}	α_1	α_2
SD	IOLQI / Minimum	2.3941	2.4125	0.4024	2.4267	4.7901	2.4783	0.8022	0.1504	-	-
	IOLQ / Non-minimum	1.3880	2.1256	1.7581	1.6629	2.1939	4.6155	8.0465	1.0545	-	-
	FOLQI / Minimum	0.0108	0.0033	0.0047	0.0123	0.0061	0.0212	0.0091	0.0095	0.8022	0.1504
	FOLQI / Non-minimum	0.0206	0.0037	0.0071	0.0620	0.0062	0.0041	0.0465	0.0014	0.2939	0.5353
BFGS	IOLQI / Minimum	0.1635	1.1498	0.9796	1.6108	3.1832	4.6364	0.8188	0.5863	-	-
	IOLQI / Non-minimum	2.0574	0.8043	1.6460	1.2684	0.8714	1.5948	0.1140	0.8719	-	-
	FOLQI / Minimum	0.0011	0.0023	0.0005	0.0114	0.0027	0.0052	0.0047	0.0025	0.8188	0.5863
	FOLQI / Non-minimum	0.0423	0.0057	0.0145	0.0549	0.0115	0.0057	0.0620	0.0019	0.1140	0.8719

Table 6.5: Controller effort of IOLQI and FOLQI controller under d(t) and parameter uncertainty conditions

Algorithm	Controller/ Operating mode	Control effort		
		-30%	Nominal	+30%
NR	IOLQI / Minimum	1.8120	3.6630	6.1550
	IOLQI / Non-minimum	2.0599	4.1129	6.7726
	FOLQI / Minimum	1.7162	3.5075	5.9324
	FOLQI / Non-minimum	1.7577	3.5693	6.0096
DFP	IOLQI / Minimum	1.8210	3.6551	6.1355
	IOLQI / Non-minimum	1.9665	3.9518	6.5691
	FOLQI / Minimum	1.7479	3.5530	5.9921
	FOLQI / Non-minimum	1.7620	3.7072	6.0557
SD	IOLQI / Minimum	1.7880	3.6108	6.0860
	IOLQI / Non-minimum	1.7910	3.6680	6.2082
	FOLQI / Minimum	1.5984	3.5397	6.0135
	FOLQI / Non-minimum	1.7530	3.5635	6.0066
BFGS	IOLQI Minimum	1.7338	3.5194	5.9585
	IOLQI / Non-minimum	1.9073	3.8727	6.4864
	FOLQI / Minimum	1.6393	3.4439	5.8828
	FOLQI / Non-minimum	1.7541	3.5688	6.0170

6.6 Summary

This chapter presents a graphical approach for representing the system and controller using BG. An unconstrained optimisation problem is presented to tune the IOLQI and FOLQI controller parameters to obtain the minimum controller effort using the optimisation methods (i) NR (ii) DFP (iii) SD and (iv) BFGS under minimum and non-minimum operating modes in the presence of disturbance condition. The performance of these controllers are evaluated under disturbance along with parameter uncertainty condition.

Chapter 7

Conclusions and Future Scope

This research work focused on solving constrained optimisation problem for obtaining FOLQI controller parameters of QTP using (i) deterministic and (ii) heuristic algorithms under disturbance conditions. The performance of FOLQI controller was compared with optimally tuned IOLQI and LADR controllers under disturbance and parameter uncertainty conditions. The research also extended to explore the possibility of representing QTP along with IOLQI and FOLQI controllers tuned using BG approach.

The summary of this research work is as follows:

(i) The constrained optimisation problem was proposed for tuning FOLQI controller under disturbance conditions. Time domain constraints such as $\%M_p$, t_s and e_{ss} with control effort as an objective function were used for tuning the controller parameters. The performance of the FOLQI controller was compared with optimally tuned IOLQI and LADR controllers and stability margins were computed and analysed. Frm the simulation study, it is evident that FOLQI controller performed better than existing IOLQI and LADR controllers.

(ii) The Heuristic based optimisation algorithms (i) CS (ii) APSO and (iii) FF were used to solve the proposed constrained optimisation problem for obtaining the controller parameters of FOLQI controller under disturbance conditions. The performance of (i) FOLQI controller was compared with an optimally tuned IOLQI controller and (ii) heuristic algorithms were compared among themselves. To show the stability of the closed loop system, the stability margins of FOLQI controller was presented and analysed. The result concluded that FF tuned FOLQI controller performs better than other controllers.

(iii) The QTP along with (i) FOLQI and (ii) IOLQI controllers were represented using the BG approach using 20-sim. An unconstrained optimisation problem was proposed

for minimising the control effort under disturbance conditions. The proposed optimisation problem was solved using optimisation algorithms like (i) NR (ii) DFP (iii) SD and (iv) BFGS for minimum and non-minimum operating modes of QTP. The result indicated that FOLQI controller provided better controller responses than the IOLQI controller.

The research work in this thesis points towards the following future directions:

- Various other optimisation algorithms in both (i) deterministic and (ii) heuristic approaches can be used to solve the optimisation problems with additional constraints and extended parameter variations.
- The proposed problem in this thesis can utilise the frequency domain constraints such as gain margin, phase margin, bandwidth etc., in order to get better visibility during external noise and disturbance conditions.
- Fractional order approximation method like Trigeassou et al. for the approximation of fractional integrator by keeping a low frequency integer effect.
- Controller parameter optimisation which ensure non zero steady state error in the presence of nonlinearities and parameter uncertainties.
- The optimisation problem can be incorporated with various other features like parameter estimation along with the guaranteed stability conditions.
- Introduction of constrained optimisation problem using BG approach for tuning FOLQI and IOLQI controllers.
- Using BG approach, synthesise of control law which helps to detect various faults occurring in QTP and developing strategies for fault isolation conditions.

Bibliography

[1] K. H. Johansson, "The quadruple-tank process: A multivariable laboratory process with an adjustable zero," *IEEE Transactions on control systems technology*, vol. 8, no. 3, pp. 456–465, 2000.

[2] M. Vidyasagar, *Control Systems Synthesis: A Factorization Approach, Part II*. Springer Nature, 2022.

[3] S. Tofighi and F. Merrikh-Bayat, "A benchmark system to investigate the non-minimum phase behaviour of multi-input multi-output systems," *Journal of Control and Decision*, vol. 5, no. 3, pp. 300–317, 2018.

[4] J.-G. Juang, W.-K. Liu, and R.-W. Lin, "A hybrid intelligent controller for a twin rotor mimo system and its hardware implementation," *ISA transactions*, vol. 50, no. 4, pp. 609–619, 2011.

[5] E. Rakhshani, I. M. H. Naveh, H. Mehrjerdi, and K. Pan, "An optimized lqg servo controller design using lqi tracker for vsp-based ac/dc interconnected systems," *International Journal of Electrical Power & Energy Systems*, vol. 129, p. 106752, 2021.

[6] K. J. Astrom, K. H. Johansson, and Q.-G. Wang, "Design of decoupled pid controllers for mimo systems," in *Proceedings of the 2001 American Control Conference.(Cat. No. 01CH37148)*, vol. 3. IEEE, 2001, pp. 2015–2020.

[7] M. Peres, C. Kallmeyer, M. Witter, R. Carneiro, F. D. Marques, and L. de Oliveira, "Advantages of multiple-input multiple-output testing," *Sound and Vibration*, vol. 49, no. 8, pp. 8–12, 2015.

[8] L. Liu, S. Tian, D. Xue, T. Zhang, Y. Chen, and S. Zhang, "A review of industrial mimo decoupling control," *International Journal of Control, Automation and Systems*, vol. 17, no. 5, pp. 1246–1254, 2019.

[9] K. H. Johansson and J. L. R. Nunes, "A multivariable laboratory process with an adjustable zero," in *Proceedings of the 1998 American Control Conference. ACC (IEEE Cat. No. 98CH36207)*, vol. 4. IEEE, 1998, pp. 2045–2049.

[10] K. H. Johansson, A. Horch, O. Wijk, and A. Hansson, "Teaching multivariable control using the quadruple-tank process," in *Proceedings of the 38th IEEE Conference on Decision and Control (Cat. No. 99CH36304)*, vol. 1. IEEE, 1999, pp. 807–812.

[11] M. Grebeck, "A comparison of controllers for the quadruple tank system," 1998.

[12] K. Astrom and A.-B. Ostberg, "A teaching laboratory for process control," *IEEE Control Systems Magazine*, vol. 6, no. 5, pp. 37–42, 1986.

[13] K. J. Astrom and M. Lundh, "Lund control program combines theory with hands-on experience," *IEEE Control Systems Magazine*, vol. 12, no. 3, pp. 22–30, 1992.

[14] P. Hušek, "Decentralized pi controller design based on phase margin specifications," *IEEE Transactions on Control Systems Technology*, vol. 22, no. 1, pp. 346–351, 2013.

[15] D. Rosinova and A. Kozakova, "Decentralized robust control of mimo systems: Quadruple tank case study," *IFAC Proceedings Volumes*, vol. 45, no. 11, pp. 72–77, 2012.

[16] D. Rosinová and M. Markech, "Robust control of quadruple tank process," *ICIC Express Letters*, vol. 2, no. 3, pp. 231–238, 2008.

[17] R. Vadigepalli, E. P. Gatzke, and F. J. Doyle, "Robust control of a multivariable experimental four-tank system," *Industrial & engineering chemistry research*, vol. 40, no. 8, pp. 1916–1927, 2001.

[18] D. Maghade and B. Patre, "Decentralized pi/pid controllers based on gain and phase margin specifications for tito processes," *ISA transactions*, vol. 51, no. 4, pp. 550–558, 2012.

[19] G. Park, C. Lee, and H. Shim, "On stealthiness of zero-dynamics attacks against uncertain nonlinear systems: A case study with quadruple-tank process," in *International symposium on mathematical theory of networks and systems (ISMTNS)*, 2018, pp. 10–17.

[20] G. Naami, M. Ouahi, A. Rabhi, F. Tadeo, and V. L. B. Tuan, "Design of robust control for uncertain fuzzy quadruple-tank systems with time-varying delays," *Granular Computing*, vol. 7, no. 4, pp. 951–964, 2022.

[21] X. Meng, H. Yu, H. Wu, and T. Xu, "Disturbance observer-based integral backstepping control for a two-tank liquid level system subject to external disturbances," *Mathematical Problems in Engineering*, vol. 2020, pp. 1–22, 2020.

[22] C. Huang, E. Canuto, and C. Novara, "The four-tank control problem: Comparison of two disturbance rejection control solutions," *ISA transactions*, vol. 71, pp. 252–271, 2017.

[23] N. N. Son, "Level control of quadruple tank system based on adaptive inverse evolutionary neural controller," *International Journal of Control, Automation and Systems*, vol. 18, no. 9, pp. 2386–2397, 2020.

[24] A. Osman, T. Kara, and M. Arıcı, "Robust adaptive control of a quadruple tank process with sliding mode and pole placement control strategies," *IETE Journal of Research*, vol. 69, no. 5, pp. 2412–2425, 2023.

[25] P. Navrátil, L. Pekař, and R. Matušů, "Control of a multivariable system using optimal control pairs: A quadruple-tank process," *IEEE Access*, vol. 8, pp. 2537–2563, 2019.

[26] M. Eltantawie, "Decentralized neuro-fuzzy controllers of nonlinear quadruple tank system," *SN Applied Sciences*, vol. 1, no. 1, p. 39, 2019.

[27] M. Herrera, O. Gonzales, P. Leica, and O. Camacho, "Robust controller based on an optimal-integral surface for quadruple-tank process," in *2018 IEEE Third Ecuador Technical Chapters Meeting (ETCM)*. IEEE, 2018, pp. 1–6.

[28] S. R. Mahapatro, B. Subudhi, and S. Ghosh, "Design of a robust optimal decentralized pi controller based on nonlinear constraint optimization for level regulation: An experimental study," *IEEE/CAA Journal of Automatica Sinica*, vol. 7, no. 1, pp. 187–199, 2019.

[29] S. Sondhi and Y. V. Hote, "Fractional order controller and its applications: A review," *Proc. of AsiaMIC*, 2012.

[30] J. Juchem, C. Muresan, R. De Keyser, and C.-M. Ionescu, "Robust fractional-order auto-tuning for highly-coupled mimo systems," *Heliyon*, vol. 5, no. 7, 2019.

[31] A. A. Kesarkar and N. Selvaganesan, "Superiority of fractional order controllers in limit cycle suppression," *International Journal of Automation and Control*, vol. 7, no. 3, pp. 166–182, 2013.

[32] A. A. Kesarkar, N. Selvaganesan, and H. Priyadarshan, "Novel controller design for plants with relay nonlinearity to reduce amplitude of sustained oscillations: Illustration with a fractional controller," *ISA transactions*, vol. 57, pp. 295–300, 2015.

[33] H. Gole, P. Barve, A. A. Kesarkar, and N. Selvaganesan, "Investigation of fractional control performance for magnetic levitation experimental set-up," in *2012 International conference on emerging trends in science, engineering and technology (INCOSET)*. IEEE, 2012, pp. 500–504.

[34] V. Mehra, S. Srivastava, and P. Varshney, "Fractional-order pid controller design for speed control of dc motor," in *2010 3rd international conference on emerging trends in engineering and technology*. IEEE, 2010, pp. 422–425.

[35] S. Perumal and N. Selvaganesan, "Input dependent nyquist plot for limit cycle prediction and its suppression using fractional order controllers," *Transactions of the Institute of Measurement and Control*, vol. 41, no. 13, pp. 3847–3860, 2019.

[36] P. Sathishkumar and N. Selvaganesan, "Fractional controller tuning expressions for a universal plant structure," *IEEE Control Systems Letters*, vol. 2, no. 3, pp. 345–350, 2018.

[37] D. Copot, M. Ghita, and C. M. Ionescu, "Simple alternatives to pid-type control for processes with variable time-delay," *Processes*, vol. 7, no. 3, p. 146, 2019.

[38] S. J. Wright, "Numerical optimization," 2006.

[39] D. Xue, Y. Chen, and D. P. Atherton, *Linear feedback control: analysis and design with MATLAB*. SIAM, 2007.

[40] P. Roy and B. K. Roy, "Dual mode adaptive fractional order pi controller with feedforward controller based on variable parameter model for quadruple tank process," *ISA transactions*, vol. 63, pp. 365–376, 2016.

[41] P. Roy and B. K. Roy, "Fractional order pi control applied to level control in coupled two tank mimo system with experimental validation," *Control Engineering Practice*, vol. 48, pp. 119–135, 2016.

[42] M. A. Nekoui, M. Pakzad, and S. Pakzad, "Optimal fractional order pid controllers design based on genetic algorithm for time delay systems," in *2017 international symposium on power electronics (Ee)*. IEEE, 2017, pp. 1–6.

[43] G. Prakash and V. Alamelumangai, "Design of predictive fractional order pi controller for the quadruple tank process," *wseas transactions on systems and control*, vol. 10, pp. 85–94, 2015.

[44] S. Sutha, P. Lakshmi, and S. Sankaranarayanan, "Fractional-order sliding mode controller design for a modified quadruple tank process via multi-level switching," *Computers & Electrical Engineering*, vol. 45, pp. 10–21, 2015.

[45] H. B. dos Santos, L. L. Carralero, F. A. d. C. Bahia, C. E. Nunes, and A. P. Tahim, "Lqi control applied to a dc-dc boost converter in a standalone pv system," in *2022 14th Seminar on Power Electronics and Control (SEPOC)*. IEEE, 2022, pp. 1–6.

[46] O. Saleem, J. Iqbal, and M. S. Afzal, "A robust variable-structure lqi controller for under-actuated systems via flexible online adaptation of performance-index weights," *Plos one*, vol. 18, no. 3, p. e0283079, 2023.

[47] A. Phillips and F. Sahin, "Optimal control of a twin rotor mimo system using lqr with integral action," in *2014 World Automation Congress (WAC)*. IEEE, 2014, pp. 114–119.

[48] J. C. Basilio, J. G. T. Ribeiro, A. Cunha Jr, and T. R. Oliveira, "An optimal fractional lqr-based control approach applied to a cart-pendulum system," in *Advances in Nonlinear Dynamics: Proceedings of the Second International Nonlinear Dynamics Conference (NODYCON 2021), Volume 2*. Springer, 2021, pp. 185–195.

[49] A. Ahmadi, B. Mohammadi-Ivatloo, A. Anvari-Moghaddam, and M. Marzband, "Optimal robust lqi controller design for z-source inverters," *Applied Sciences*, vol. 10, no. 20, p. 7260, 2020.

[50] A. F. Sagonda and K. A. Folly, "A comparative study between deterministic and two meta-heuristic algorithms for solar pv mppt control under partial shading conditions," *Systems and Soft Computing*, vol. 4, p. 200040, 2022.

[51] M. Nobre, I. Silva, and L. A. Guedes, "Routing and scheduling algorithms for wirelesshart networks: A survey," *Sensors*, vol. 15, no. 5, pp. 9703–9740, 2015.

[52] A. K. Sangaiah, A. A. R. Hosseinabadi, M. B. Shareh, S. Y. Bozorgi Rad, A. Zolfagharian, and N. Chilamkurti, "Iot resource allocation and optimization based on heuristic algorithm," *Sensors*, vol. 20, no. 2, p. 539, 2020.

[53] V. Sharma and A. K. Tripathi, "A systematic review of meta-heuristic algorithms in iot based application," *Array*, vol. 14, p. 100164, 2022.

[54] L. Abualigah, M. A. Elaziz, A. M. Khasawneh, M. Alshinwan, R. A. Ibrahim, M. A. Al-Qaness, S. Mirjalili, P. Sumari, and A. H. Gandomi, "Meta-heuristic optimization algorithms for solving real-world mechanical engineering design problems: a comprehensive survey, applications, comparative analysis, and results," *Neural Computing and Applications*, pp. 1–30, 2022.

[55] S. B. Joseph, E. G. Dada, A. Abidemi, D. O. Oyewola, and B. M. Khammas, "Meta-heuristic algorithms for pid controller parameters tuning: Review, approaches and open problems," *Heliyon*, vol. 8, no. 5, 2022.

[56] M. Ghalambaz, R. J. Yengejeh, and A. H. Davami, "Building energy optimization using grey wolf optimizer (gwo)," *Case Studies in Thermal Engineering*, vol. 27, p. 101250, 2021.

[57] S. Chaturvedi, N. Bhatt, R. Gujar, and D. Patel, "Application of pso and ga stochastic algorithms to select optimum building envelope and air conditioner size-a case of a residential building prototype," *Materials Today: Proceedings*, vol. 57, pp. 49–56, 2022.

[58] A. Altan, S. Karasu, and S. Bekiros, "Digital currency forecasting with chaotic meta-heuristic bio-inspired signal processing techniques," *Chaos, Solitons & Fractals*, vol. 126, pp. 325–336, 2019.

[59] A. Altan, S. Karasu, and E. Zio, "A new hybrid model for wind speed forecasting combining long short-term memory neural network, decomposition methods and grey wolf optimizer," *Applied Soft Computing*, vol. 100, p. 106996, 2021.

[60] A. Altan, "Performance of metaheuristic optimization algorithms based on swarm intelligence in attitude and altitude control of unmanned aerial vehicle for path fol-

lowing," in *2020 4th international symposium on multidisciplinary studies and innovative technologies (ISMSIT)*. IEEE, 2020, pp. 1–6.

[61] E. Belge, A. Altan, and R. Hacıoğlu, "Metaheuristic optimization-based path planning and tracking of quadcopter for payload hold-release mission," *Electronics*, vol. 11, no. 8, p. 1208, 2022.

[62] Q. Jin, L. Qi, B. Jiang, and Q. Wang, "Novel improved cuckoo search for pid controller design," *Transactions of the Institute of Measurement and Control*, vol. 37, no. 6, pp. 721–731, 2015.

[63] Z. Bingul and O. Karahan, "A novel performance criterion approach to optimum design of pid controller using cuckoo search algorithm for avr system," *Journal of the Franklin Institute*, vol. 355, no. 13, pp. 5534–5559, 2018.

[64] N. El Gmili, M. Mjahed, A. El Kari, and H. Ayad, "Particle swarm optimization and cuckoo search-based approaches for quadrotor control and trajectory tracking," *Applied Sciences*, vol. 9, no. 8, p. 1719, 2019.

[65] M. L. Lagunes, O. Castillo, and J. Soria, "Optimization of membership function parameters for fuzzy controllers of an autonomous mobile robot using the firefly algorithm," *Fuzzy logic augmentation of neural and optimization algorithms: theoretical aspects and real applications*, pp. 199–206, 2018.

[66] N. A. Al-Awad, "Optimal control of quadruple tank system using genetic algorithm," *International Journal of Computing and Digital Systems*, vol. 8, no. 01, pp. 51–59, 2019.

[67] D. A. Souza, V. A. de Mesquita, L. L. Reis, W. A. Silva, and J. G. Batista, "Optimal lqi and pid synthesis for speed control of switched reluctance motor using metaheuristic techniques," *International Journal of Control, Automation and Systems*, vol. 19, pp. 221–229, 2021.

[68] B. Zhang, W. Tan, and J. Li, "Tuning of linear active disturbance rejection controller with robustness specification," *ISA transactions*, vol. 85, pp. 237–246, 2019.

[69] H. Niu, Q. Gao, S. Tang, W. Guan *et al.*, "Linear active disturbance rejection control for lever-type electric erection system based on approximate model," *Journal of Control Science and Engineering*, vol. 2019, 2019.

[70] S. Shen and J. Xu, "Trajectory tracking active disturbance rejection control of the unmanned helicopter and its parameters tuning," *IEEE access*, vol. 9, pp. 56 773–56 785, 2021.

[71] C. Chen, H. Gao, L. Ding, W. Li, H. Yu, and Z. Deng, "Trajectory tracking control of wmrs with lateral and longitudinal slippage based on active disturbance rejection control," *Robotics and Autonomous Systems*, vol. 107, pp. 236–245, 2018.

[72] X. Meng, H. Yu, J. Zhang, T. Xu, and H. Wu, "Liquid level control of four-tank system based on active disturbance rejection technology," *Measurement*, vol. 175, p. 109146, 2021.

[73] Z. S. Hashim and I. K. Ibraheem, "A relative degree one modified active disturbance rejection control for four-tank level control system," *International Review of Applied Sciences and Engineering*, 2021.

[74] R. Mohankumar, N. Selvaganesan, M. Jayakumar, and P. Sathishkumar, "Centralised fractional order lqi controller design for quadruple tank process—an optimisation approach," *Results in Control and Optimization*, vol. 10, p. 100202, 2023.

[75] B. Nagalakshmia *et al.*, "Various domains of bond graph," *Turkish Journal of Computer and Mathematics Education (TURCOMAT)*, vol. 12, no. 2, pp. 772–779, 2021.

[76] P. J. Gawthrop and G. P. Bevan, "Bond-graph modeling," *IEEE Control Systems Magazine*, vol. 27, no. 2, pp. 24–45, 2007.

[77] S. Lichiardopol and C. Sueur, "Decoupling of linear time-varying systems with a bond graph approach," *ECMS 2006, Bonn, Germany*, 2006.

[78] A. Kumar, R. Singh, T. K. Bera, and A. Singla, "Heuristic controller design for inverted pendulum using bond graph approach," in *Recent Advances in Mechanical Engineering: Select Proceedings of CAMSE 2021*. Springer, 2022, pp. 547–557.

[79] E. Shojaei Barjuei, D. G. Caldwell, and J. Ortiz, "Bond graph modeling and kalman filter observer design for an industrial back-support exoskeleton," *Designs*, vol. 4, no. 4, p. 53, 2020.

[80] I. Dif, A. Kouzou, K. Benmahammed, and A. Hafaifa, "Trajectory tracking control design of a mass-damping-spring system with uncertainty using the bond graph approach," *Engineering, Technology & Applied Science Research*, vol. 10, no. 6, pp. 6427–6431, 2020.

[81] M. A. Nacusse and S. J. Junco, "Bond-graph-based controller design for the quadruple-tank process," *International Journal of Simulation and Process Modelling*, vol. 10, no. 2, pp. 179–191, 2015.

[82] B. Friedland, *Control system design: an introduction to state-space methods*. Courier Corporation, 2005.

[83] R. C. D. R. H. Bishop, *Modern control systems*, 2011.

[84] D. P. Atherton, "Nonlinear control engineering," *Van Nostrand Rheinhold*, 1975.

[85] K. Ogata, "Modern control engineering," 2020.

[86] K. B. Oldham and J. Spanier, "The fractional calculus, vol. 111 of mathematics in science and engineering," 1974.

[87] J. Sabatier, P. Lanusse, P. Melchior, and A. Oustaloup, "Fractional order differentiation and robust control design," *Intelligent systems, control and automation: science and engineering*, vol. 77, pp. 13–18, 2015.

[88] D. Xue and Y. Chen, "Fractional-order pid control: Theory, tuning, and application," *IEEE Transactions on Control Systems Technology*, vol. 21, no. 6, pp. 2391–2393, 2013.

[89] I. Podlubny, "Fractional-order systems and pi/sup/spl lambda," *D/sup/spl mu//-controllers. IEEE Trans. Autom. Control*, vol. 44, no. 1, pp. 208–214, 1999.

[90] Y. Luo, Y. Chen, I. Podlubny, and H. A. Barbosa, "Fractional-order control systems: Fundamentals and numerical implementations," *IET Control Theory & Applications*, vol. 5, no. 7, pp. 1033–1046, 2011.

[91] D. Valério and J. S. Da Costa, "Tuning of fractional pid controllers with ziegler–nichols-type rules," *Signal processing*, vol. 86, no. 10, pp. 2771–2784, 2006.

[92] C. A. Monje, B. M. Vinagre, V. Feliu, and Y. Chen, "Tuning and auto-tuning of fractional order controllers for industry applications," *Control engineering practice*, vol. 16, no. 7, pp. 798–812, 2008.

[93] S. Das, I. Pan, and S. Das, "Performance comparison of optimal tuning formulas for pid, piλdμ and pidd1 controllers in time delay systems," *ISA Transactions*, vol. 50, no. 3, pp. 376–388, 2011.

[94] Y. Chen and K. L. Moore, "Analytical stability bound for a class of delayed fractional-order dynamic systems," in *Proceedings of the 40th IEEE Conference on Decision and Control (Cat. No. 01CH37228)*, vol. 2. IEEE, 2001, pp. 1421–1426.

[95] C. Hwang, "Fractional-order pid controller design for time-delay systems," *Mechatronics*, vol. 13, no. 2, pp. 279–301, 2003.

[96] J. Jayaprakash and M. H. Kumar, "State variable analysis of four tank system," in *2014 International Conference on Green Computing Communication and Electrical Engineering (ICGCCEE)*. IEEE, 2014, pp. 1–8.

[97] S. N. M. Azam and J. B. Jørgensen, "Modeling and simulation of a modified quadruple tank system," in *2015 IEEE International Conference on Control System, Computing and Engineering (ICCSCE)*. IEEE, 2015, pp. 365–370.

[98] A. Loverro *et al.*, "Fractional calculus: history, definitions and applications for the engineer," *Rapport technique, Univeristy of Notre Dame: Department of Aerospace and Mechanical Engineering*, pp. 1–28, 2004.

[99] A. Oustaloup, F. Levron, B. Mathieu, and F. M. Nanot, "Frequency-band complex noninteger differentiator: characterization and synthesis," *IEEE Transactions on Circuits and Systems I: Fundamental Theory and Applications*, vol. 47, no. 1, pp. 25–39, 2000.

[100] I. Podlubny, *Fractional differential equations: an introduction to fractional derivatives, fractional differential equations, to methods of their solution and some of their applications*. elsevier, 1998.

[101] C. A. Monje, Y. Chen, B. M. Vinagre, D. Xue, and V. Feliu-Batlle, *Fractional-order systems and controls: fundamentals and applications*. Springer Science & Business Media, 2010.

[102] A. Oustaloup, B. Mathieu, and P. Lanusse, "The crone control of resonant plants: application to a flexible transmission," *European Journal of control*, vol. 1, no. 2, pp. 113–121, 1995.

[103] M. D. Ortigueira, *Fractional calculus for scientists and engineers*. Springer Science & Business Media, 2011, vol. 84.

[104] G. Feng, "A survey on analysis and design of model-based fuzzy control systems," *IEEE Transactions on Fuzzy systems*, vol. 14, no. 5, pp. 676–697, 2006.

[105] D. Baleanu, K. Diethelm, E. Scalas, and J. J. Trujillo, *Fractional calculus: models and numerical methods*. World Scientific, 2012, vol. 3.

[106] R. Fletcher and S. Leyffer, "Nonlinear programming without a penalty function," *Mathematical programming*, vol. 91, pp. 239–269, 2002.

[107] S. P. Boyd and L. Vandenberghe, *Convex optimization*. Cambridge university press, 2004.

[108] J. Nocedal and S. J. Wright, *Numerical optimization*. Springer, 1999.

[109] M. J. Osborne *et al.*, *An introduction to game theory*. Oxford university press New York, 2004, vol. 3, no. 3.

[110] D. Kraft, "A software package for sequential quadratic programming," *Forschungsbericht- Deutsche Forschungs- und Versuchsanstalt fur Luft- und Raumfahrt*, 1988.

[111] D. H. Tungadio, R. C. Bansal, and M. W. Siti, "Optimal control of active power of two micro-grids interconnected with two ac tie-lines," *Electric Power Components and Systems*, vol. 45, no. 19, pp. 2188–2199, 2017.

[112] H. Khalil, *Nonlinear Systems*, ser. Pearson Education. Prentice Hall, 2002. [Online]. Available: https://books.google.co.uk/books?id=t_d1QgAACAAJ

[113] G. C. Goodwin and K. S. Sin, *Adaptive filtering prediction and control*. Courier Corporation, 2014.

[114] H. John, *Holland. Adaptation in natural and artificial systems*. University of Michigan press Ann Arbor MI, 1975.

[115] K. Deb, *Multi-objective optimization using evolutionary algorithms*. John Wiley & Sons, 2001, vol. 16.

[116] A. E. Eiben and J. E. Smith, *Introduction to evolutionary computing*. Springer, 2015.

[117] K. S Jr, "Optimization by simulated annealing," *Science*, vol. 220, no. 4598, pp. 498–516, 1983.

[118] X.-S. Yang and S. Deb, "Cuckoo search via lévy flights," in *2009 World congress on nature & biologically inspired computing (NaBIC)*. Ieee, 2009, pp. 210–214.

[119] X.-S. Yang and A. Slowik, "Cuckoo search algorithm," in *Swarm Intelligence Algorithms*. CRC Press, 2020, pp. 109–120.

[120] K. R. Harrison, A. P. Engelbrecht, and B. M. Ombuki-Berman, "An adaptive particle swarm optimization algorithm based on optimal parameter regions," in *2017 IEEE symposium series on computational intelligence (SSCI)*. IEEE, 2017, pp. 1–8.

[121] J. Kennedy and R. Eberhart, "Particle swarm optimization," in *Proceedings of ICNN'95-international conference on neural networks*, vol. 4. ieee, 1995, pp. 1942–1948.

[122] X.-S. Yang, S. Deb, and S. Fong, "Accelerated particle swarm optimization and support vector machine for business optimization and applications," in *Networked Digital Technologies: Third International Conference, NDT 2011, Macau, China, July 11-13, 2011. Proceedings 3*. Springer, 2011, pp. 53–66.

[123] X.-S. Yang, "Firefly algorithms for multimodal optimization," in *International symposium on stochastic algorithms*. Springer, 2009, pp. 169–178.

[124] X.-S. Yang and A. Slowik, "Firefly algorithm," in *Swarm intelligence algorithms*. CRC Press, 2020, pp. 163–174.

[125] H. M. Paynter, "Analysis and design of engineering systems," *MIT press*, 1961.

[126] D. C. Karnopp, D. L. Margolis, and R. C. Rosenberg, *System dynamics: modeling, simulation, and control of mechatronic systems*. John Wiley & Sons, 2012.

[127] W. Borutzky, *Bond graph methodology: development and analysis of multidisciplinary dynamic system models*. Springer Science & Business Media, 2009.

[128] B. P. Zeigler, H. Praehofer, and T. G. Kim, *Theory of modeling and simulation*. Academic press, 2000.

[129] P. Gawthrop and L. Smith, *Metamodelling: For bond graphs and dynamic systems*. Prentice Hall International (UK) Ltd., 1996.

[130] J. E. Dennis Jr and R. B. Schnabel, *Numerical methods for unconstrained optimization and nonlinear equations*. SIAM, 1996.

[131] W. C. Davidon, "Variable metric method for minimization," *SIAM Journal on optimization*, vol. 1, no. 1, pp. 1–17, 1991.

[132] R. Fletcher, "A new approach to variable metric algorithms," *The computer journal*, vol. 13, no. 3, pp. 317–322, 1970.

[133] M. J. Powell, "A hybrid method for nonlinear equations," *Numerical methods for nonlinear algebraic equations*, pp. 87–161, 1970.

[134] C. G. Broyden, "The convergence of a class of double-rank minimization algorithms 1. general considerations," *IMA Journal of Applied Mathematics*, vol. 6, no. 1, pp. 76–90, 1970.

[135] D. Goldfarb, "A family of variable-metric methods derived by variational means," *Mathematics of computation*, vol. 24, no. 109, pp. 23–26, 1970.

[136] D. F. Shanno, "Conditioning of quasi-newton methods for function minimization," *Mathematics of computation*, vol. 24, no. 111, pp. 647–656, 1970.

Appendix A

Linear Active Disturbance Rejection Controller

In [72], it describes the liquid level control of a QTP using Active Disturbance Rejection (ADR) control technology which covers various aspects such as system modelling, controller design, simulation and experimental validation.

Linear ADR (LADR) controller is based on the fundamental principles of ADR controller which aims to estimate and compensate the disturbances in real time without demanding an accurate system model. In linear systems, the LADR controller utilises linearised models of the plant dynamics to design control strategies that mitigate the effects of disturbances and uncertainties. This typically consists of two main components: (i) an Extended State Observer (ESO) and (ii) a linear feedback controller. The closed loop representation of the plant with LADR controller is shown in Fig. A.1.

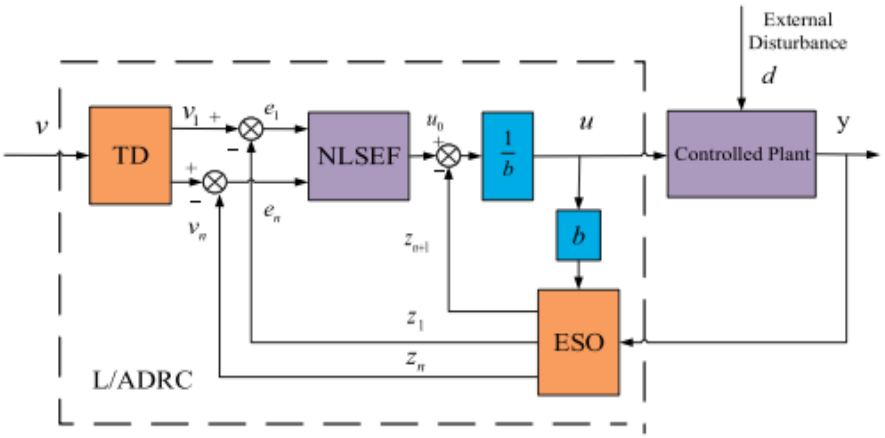

Figure A.1: Closed loop representation of LADR Controller with plant

Extended State Observer

ESO is responsible for estimating the system states and disturbances affecting the performance of the system. It provides real time estimates that the controller uses to generate control actions. The linear feedback controller computes the control signal based on the observed states and disturbances which aims to regulate the system behaviour with respect to the desired specifications. LADR controller design involves tuning the parameters of ESO and linear feedback controller. The observer gains are tuned to ensure accurate estimation of the system states and disturbances while the feedback gains are adjusted to achieve desired closed loop performance characteristics. The corresponding expressions are given below:

$$e_{12} = Z_1 - x_1 + Z_4 - x_4 \tag{A.1}$$
$$\dot{Z}_1 = Z_5 - \beta_{11} e_{12} + b_1 u_1 \tag{A.2}$$
$$\dot{Z}_4 = Z_7 - \beta_{41} e_{12} + b_4 u_1 \tag{A.3}$$
$$\dot{Z}_5 = -\beta_{12} e_{12} + b_4 u_1 \tag{A.4}$$
$$\dot{Z}_7 = -\beta 12 e_{12} \tag{A.5}$$

$$e_{22} = Z_2 - x_2 + Z_3 - x_3 \tag{A.6}$$
$$\dot{Z}_2 = Z_6 - \beta_{21} e_{22} + b_2 u_2 \tag{A.7}$$
$$\dot{Z}_3 = Z_8 - \beta_{31} e_{22} + b_3 u_2 \tag{A.8}$$
$$\dot{Z}_6 = -\beta_{22} e_{22} \tag{A.9}$$
$$\dot{Z}_8 = -\beta 32 e_{22} \tag{A.10}$$

Track Differentiator

LADR controller often incorporates a Track Differentiator (TD) as part of its ESO design. It estimates the derivative of the output signal which can be useful for disturbance estimation and compensation. By providing an estimate of the derivative, the TD enhances the performance of the ESO in estimating state variables and disturbances affecting the system performance. The TD design typically involves incorporating a high pass filter into the ESO structure. The high pass filter signal serves as an estimate of the derivative for the output signal.The ESO further uses this signal for disturbance estimation and compensation. The corresponding expressions are given below:

$$e_{11} = Z_{11} - x_{1d} + Z_{14} - x_{4d} \tag{A.11}$$

$$\dot{Z}_{11} = -r_1 e_{11} \tag{A.12}$$

$$\dot{Z}_{14} = -r_4 e_{11} \tag{A.13}$$

$$e_{21} = Z_{12} - x_{2d} + Z_{13} - x_{3d} \tag{A.14}$$

$$\dot{Z}_{12} = -r_2 e_{21} \tag{A.15}$$

$$\dot{Z}_{13} = -r_3 e_{21} \tag{A.16}$$

Nonlinear state error feedback control law

The nonlinear state error feedback control law refers to a control strategy incorporating nonlinear elements into the feedback loop to improve the controller performance which ensures robustness and disturbance rejection condition. By utilising nonlinearities in the control law, the controller can better handle uncertainties, disturbances and nonlinear dynamics present in the system. The design of the nonlinear state error feedback control law involves formulating a control law that incorporates nonlinear functions of the system states and control inputs. Nonlinear elements such as saturation functions, dead zones or nonlinear gains may be introduced into the control law to improve the controller's response. The corresponding expressions are given below:

$$e_{13} = Z_{11} - Z_1 + Z_{14} - Z_4 \tag{A.17}$$

$$u_{01} = \beta_{13} e_{13} + \beta 43 e_{13} \tag{A.18}$$

$$u_1 = u_{01} - \frac{Z_5}{b_1} - \frac{Z_7}{b_4} \tag{A.19}$$

$$e_{23} = Z_{12} - Z_2 + Z_{13} - Z_3 \tag{A.20}$$

$$u_{02} = \beta_{23} e_{23} + \beta 33 e_{23} \tag{A.21}$$

$$u_2 = u_{02} - \frac{Z_6}{b_2} - \frac{Z_8}{b_3} \tag{A.22}$$

List of Publications

Papers Published in Refereed International Journals

1. **R. S. Mohankumar**, N. Selvaganesan, M. Jayakumar and P. Sathishkumar. Heuristic algorithms based optimal tuning of FOLQI controller for quadruple tank process under disturbance conditions. Measurement and Control, SAGE Publications, Volume 57(2), 2023.

2. **R. S. Mohankumar**, N. Selvaganesan, M. Jayakumar and P. Sathishkumar. Centralised fractional order LQI controller design for quadruple tank process—An optimisation approach. Results in Control and Optimization, Elsevier Publications, Volume 10, p.100202, 2023.

Journal Paper under preparation

1. **R. S. Mohankumar**, N. Selvaganesan, M. Jayakumar and P. Sathishkumar. Feasibility study of Fractional order LQI controller in Bond Graph Domain.

.